SYNTHESIS AND KINETIC STUDY OF RHODIUM(I) COMPLEXES CONTAINING SUBSTITUTED CUPFERRATE LIGANDS

Fanuel Gebremichael Fessha

SYNTHESIS AND KINETIC STUDY OF RHODIUM(I) COMPLEXES CONTAINING SUBSTITUTED CUPFERRATE LIGANDS

A thesis submitted to meet the requirements for the degree of

Magister Scientiae

in the

Department of Chemistry
Faculty of Natural and Agricultural Sciences

at the

University of the Free State

by

Fanuel Gebremichael Fessha

Promoter

J.A.Venter

Co-promoter

Prof.W.Purcell

September 2005

ACKNOWLEDGEMENT

My utmost gratitude is to the Almighty God for giving me the strength, wisdom and courage to execute this dissertation.

This study was made possible only through the help, encouragement and cooperation of various individuals and institution to whom I am truly thankful.

I would like to thank my project promoter Mr. Johan Venter and co-promoter Prof. Walter Purcell for their wonderfully insightful comments and suggestions on reading material as I endeavoured to produce this report. Prof. Walter Purcell for his capable advice, criticism and appraisal of the draft manuscripts. His assistance, determination, guidance and analysis of my thesis throughout the research time.

My colleagues, in particular Wade Davis and Aurelien Auger, who played a vital role in making this study possible.

My sincere gratitude to the University of the Free State, department of chemistry for giving me the opportunity to pursue and complete my studies. I also would like to thank Prof. Basson for many functional and interesting discussions and his cordiality during my university days.

I also owe much more gratitude to my family for their unconditional support.

CONTENTS

Chapter Three

Synthesis and Characterisation of Ligands and Complexes

Chapter Four

Oxidative Addition of [Rh(CH_3cupf)(CO)(PX_3)] Complexes with Iodomethane

Chapter Five

Evaluation of the Study

LIST OF ABBREVIATIONS

acac	acetylacetone
AnMetha	4-methoxy-N-methylbenzothiohydroxamate
ba	benzylacetone
BTFA	benzolytrifluoroacetone
^{13}C-NMR	^{13}C nuclear magnetic resonance
cacsm	methyl(2-cyclohexylamino-1-cyclopentene-1-dithiocarboxylic acid
CH_3	methyl
CH_3cupf	methylcupferrate
Cod	1,5-cyclooctadiene
Cp	cyclopentadienyl
cupf	cupferrate
Cy	cyclohexyl
d	doublet
D	solvent donocity
dbm	dibenzoylmethane
DMAVK	dimethylaminovinylketone
DMF	N,N-dimethyl formamide
DMSO	dimethyl sulphoxide
Et	ethyl
^{1}HNMR	proton nuclear magnetic resonance
hfaa	hexafluoroacetlyacetone
hpt	1-hydoxy-2-piridinethione
L	ligand
L-L'-BID	mono anionic didentate ligand with donor atoms L and L'
M	molar

macsm	methyl(2-methylamino-1-cyclopentene-1-dithiocarboxylicacid)
MeO	methoxy
N,S-BID	monoanionic bidentate ligand with donor atoms N and S
nm	nanometer
NMR	nuclear magnetic resonance
NOS	nitrogenoxide synthase
O	ortho
OA	oxidative addition
ox	8-hydroxyquinoline
^{31}P-NMR	^{31}P nuclear magnetic resonance
p	para
PGM	platinum group metals
Ph	phenyl
pK_a	acid dissociative constant
ppm	parts per million
PX_3	tertiary phosphine
Py	pyridine
Quin	2-carboxylicquinoline
s	singlet or second
S	solvent
Sacac	thioacetylacetone
STE	structural trans effect
stsc	salicylaldehydethiosemicarbazone
T	temperature
TBP	trigonal bipyramidal
tfaa	1,1,1-trifluoro-2,4-pentanedione
tfba	trifluorobenzoylacetone
tfdmaa	1,1,1-trifluoro-5,5-dimethylpentanedione

TFHD	1,1,1-trifluoro-5-methylpentanedione
TFTMAA	1,1,1-triflouro-5,5,5-trimethylpentanedione
THF	tetrahydrofuran
Tol	tolyl
TS	transition state
UV/Visible	ultraviolet/visible spectroscopy
$\Delta H^{\#}$	activation enthalpy
$\Delta S^{\#}$	activation entropy
Å	angstrom
δ	chemical shift
ε	dielectric constant
θ	cone angle of tertiary phosphine
λ	wavelength
ν(CO)	infrared stretching frequency of carbonyl
π	pi
σ	sigma

LIST OF FIGURES

FIGURE

LIST OF SCHEMES

Scheme

LIST OF TABLES

TABLE

CHAPTER 1

INTRODUCTION AND AIMS OF STUDY

1.1 INTRODUCTION

NO releasing agents

Over the past ten years, nitrogen monoxide has been demonstrated to play a remarkable role in the biology of humans and animals. It has been shown that it can act as a neuronal mediator which is continuously synthesised by the endothelial nitric oxide synthase (NOS) and which is responsible for vasodilation. Its deficiency leads to hypertension (Alexandru *et al*, 1998:439). Relative large amounts of nitrogen monoxide are found in the brain, where it is produced by the neuronal NOS. Two of the constitutive NOS processes produce low amounts of NO, but much larger amounts are released by the third inducible process which is present in macrophages which plays a beneficial role in the killing of invading microorganisms (Alexandru *et al.*, 1998:439). When it is exposed to oxygen, the stable NO free radical reacts rapidly yielding the toxic NO_2 chemical (**Eq.1.1**). This reaction is much slower at very low concentrations of NO due to its second order [NO] dependence.

$$2NO + O_2 \rightarrow 2NO_2 \qquad \textbf{Eq.1.1}$$

For its bronchodilatory effect, NO can therefore be administered to newborn infants or patients with pulmonary problems. Admixed with air or oxygen, at NO concentrations of less than 100 ppm to prevent the formation of NO_2, it yields its medical benefits (Alexandru *et al.*, 1998:439). Nitrogen monoxide has been discovered to be a major signalling agent of profound importance throughout the animal kingdom (Williams, 1996:77). The major biological functions of NO include controlling blood pressure, smoothing muscle tone and platelet aggregation, assisting the immune system in destroying tumour cells and intracellular pathogens (virus, bacteria and parasites) and participating in neuronal synaptic transmission (Moncada *et al.*, 1991:109). Endogenous NO is generated from arginine by the catalytic activity of NO synthase (Ignarro and Murad, 1995:36). Exogenous production from NO releasing agents serves as a valuable tool in biological research for studying the functions of NO and offers a variety of pharmaceutical applications (Ignarro and Murad, 1995:36). Thus, the development of new substances and new approaches to the generation of NO is currently a challenging issue facing pharmaceutical and organic chemists. Several classes of NO releasing compounds are currently known and are given in **Figure 1.1** (Alexandru *et al.*, 1998:439).

Several books on NO have recently been published, and in 1992 the journal *Science* proclaimed NO as the molecule of the year (Vincent, 1995:193). This paper also describes cupferron and its derivatives (**Figure 1.2** and **1.3**), of which some are novel as possible donors of NO, which have been shown to generate NO under conditions of chemiluminiscence in the reaction with ozone and to cause muscular relaxation with tissues. Due to their ability

to act *in vivo* as NO donors, these compounds in addition to promoting vasodilation, may accelerate the healing of wounds and burns (Saavedra *et al*, 1992:6134).

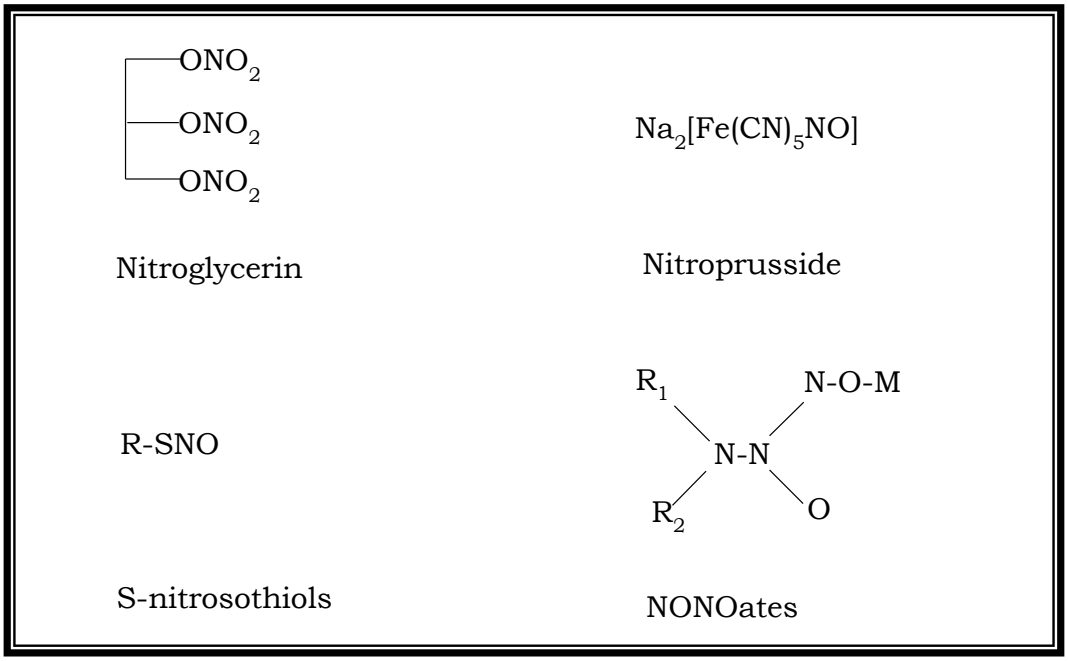

Figure1.1 Different NO releasing compounds

Different chemical reactions are utilised to generate nitrogen monoxide from the compounds indicated in **Figure 1.1**. *In vivo* generation of NO from organic nitrates (for example, nitroglycerine and isosorbide-dinitrate) is believed to occur through thiol-mediated, reductive metabolic pathways (Ignarro and Murad, 1995:36). *In vitro* generation can occur *via* spontaneous and non-spontaneous dissociation mechanisms from nucleophilic substances such as diazoniumdiolates, sodiumnitroprusside, S-nitrosothiols, sydnonimines and furoxanes (Saavedra *et al.*, 1992:6134)

The N-nitroso-N-oxyaryl-amine and N-nitroso-N-oxyalkyl (**Figure1.2**) functional groups that are needed for the generation of NO occur in a variety of natural and synthetic compounds (Kano and Anselme, 1993:9453).

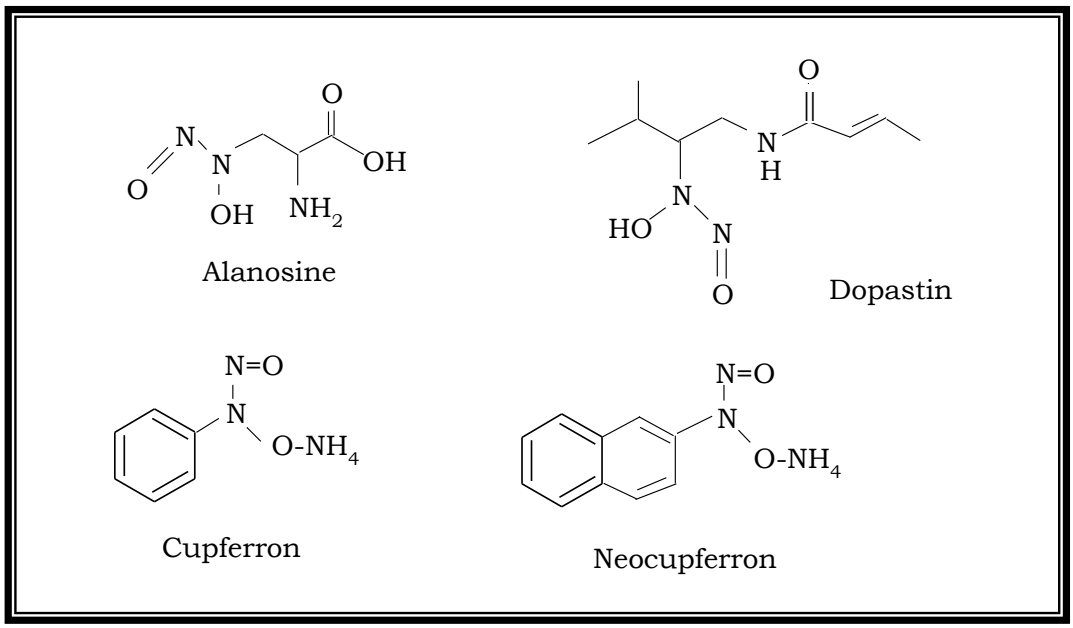

Figure 1.2 N-nitroso-N-oxyalkyl and N-nitro-N-oxyaryl amines

Alanosine and dopastin, a dopamine β-hydroxylase inhibitor, are natural products containing the N-nitroso-N-oxyalkylamine moiety (Andrea *et al*, 2000:405). The best known member of the synthetic N-nitroso-N-oxyarylamine family is cupferron (**Figure 1.3**, with X = H) which is commonly used on large scale in industry as a metal chelator and as polymerisation inhibitor (Alexandru *et al*, 1998:439).

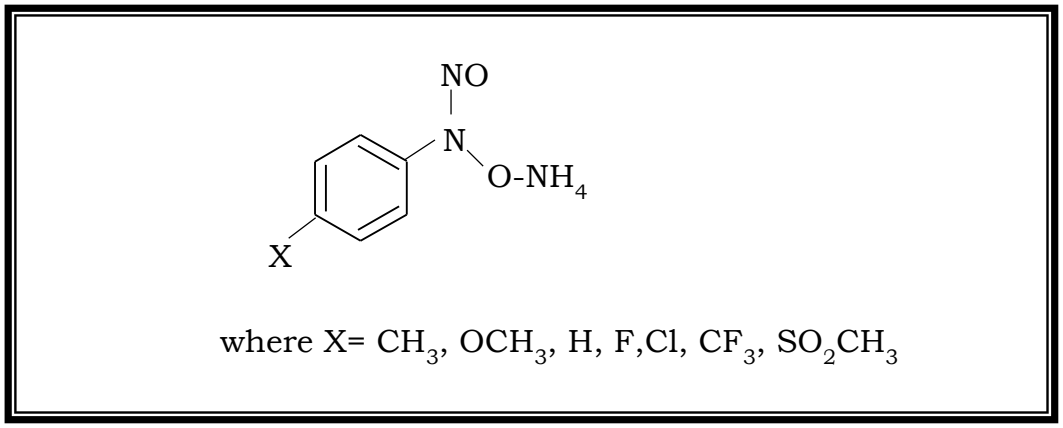

Figure 1.3 Cupferron and its derivatives

At room temperature, both in the solid state and in solution, cupferron is relatively stable, generating very little NO. Recently, Alexandru *et al*. (1998:439) found that *ortho*-substituted analogues of cupferron have faster decomposition rates than cupferron itself due to the *ortho* substitution, which prevents the NONO moiety from becoming inactive by decreasing the electron density around the NONO moiety. This causes an increase in its potential to be a good NO donor for both *in vitro* and *in vivo* assays. Another important property of these compounds is that it can undergo a one electron oxidation which results in the generation of nitrosobenzene.

Rhodium complexes

A considerable number of rhodium complexes have been investigated in terms of their antineoplastic activity since Giraldi and co-workers discovered the surprising antineoplastic activity of [Rh(acac)(cod)] (**Figure 1.4**) towards Ehrlich tumours in 1977

(Giraldi *et al*, 1977:2662). The high selectivity of this complex towards cancerous tissue, leading to considerably less histological damage to uninfected tissue, internal mucosa, spleen and kidneys, is according to Giraldi (Giraldi *et al*, 1977:2662) directly attributed to the lower reduction properties of cancerous tissue compared to healthy tissue. Giraldi also postulated a substantially lower rate of oxidation of the Rh(I) centre to the inactive octahedral Rh(III) complex in cancerous tissue compared to normal tissue. In addition, Giraldi stated that the relative lability of the acetylacetonato ligand also contributes to the antineoplastic action of this Rh(I) complex.

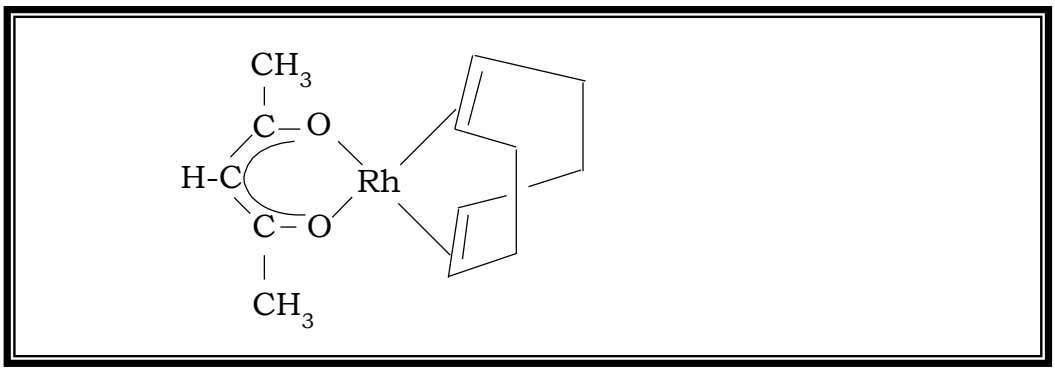

Figure 1.4 Structure of [Rh(acac)(cod)]

Rhodium and iridium were discovered independently in the same year and share many resemblances in their chemistry (Norman, 2004:1). Both metals exhibit extensive chemistry, principally in the +3 and +1 oxidation states with significant iridium chemistry in the +4 oxidation state. The rhodium(I) state has a d^8 electron configuration and its organometallic complexes usually form either four coordinate square planar or five coordinate trigonal

bipyramidal (TBP) structures. Two-electron oxidation to the octahedrally coordinated rhodium(III) state is usually facile through oxidative addition reactions (Dickson, 1985:1). These reactions for rhodium are reversible in many cases, unlike the corresponding iridium chemistry where oxidative addition usually occurs irreversibly. The reversibility of these reactions, connecting the Rh(I) and Rh(III) oxidation states, is responsible for many of the catalytic organic transformations which are encountered in organorhodium chemistry (Dickson, 1983:45) Rhodium is one of the rarest elements in the earth's crust and hence it is not economically viable to design industrial processes that do not allow for the complete recovery of the metal or its complexes after the useful life of the catalyst is over (Serpone and Jamieson, 1987:1097). In spite of its scarcity, rhodium complexes are still the most promising substances to be used as catalysts in industry provided they can be regenerated. In contrast to cobalt, which also belongs to the same group on the periodic table, only a few compounds of +2 oxidation state are known for rhodium and iridium (Huges, 1982:277).

The English scientist William Hyde Wollaston discovered rhodium in 1803. He dissolved impure platinum metal in aqua regia and found that on removal of the platinum and palladium a red solution remained from which he obtained the $Na_3[RhCl_6]$ salt. Upon reduction with hydrogen and washing with water, the metal was obtained. The rose-red colour (Greek; rhodon) of many rhodium salts gave the element its name. In the same year Smithson Tenant studied the black insoluble portion obtained from platinum ores after treatment with aqua regia. He found that, after fusion with soda and on extract with water, the black residue gave

a blue solution in hydrochloric acid that turned red when heated. The rhodium metal was obtained from the continuous heating of the red crystals.

Rhodium occurs in very low concentrations in the earth's crust, primarily as part of nickel or copper-nickel sulphide ores (Livingstone, 1973:1233). The extreme rarity of rhodium makes it economically impractical to recover from the sulphide ores. However, because it is closely linked to platinum, another constituent of the sulphide ores, it is recovered in small amounts. The production of rhodium is about 5% of that of platinum, corresponding to the relative abundance of the two metals in the ore (Griffith, 1967:589).

Rhodium, being part of the so-called platinum group metals (PGM), is currently isolated using the aqua regia refining process (Lanam and Zysk, 1982:228). The rocks containing the platinum group metals are first treated with aqua regia and the gold, platinum and palladium are dissolved whereas the rhodium, ruthenium, osmium, iridium and silver remain as an insoluble slag. Gold is separated by the precipitation of its salts and is then further purified. The mixture is then treated with ammonium chloride to precipitate ammonium chloroplatinate, leaving palladium in solution which is then treated with ammonia, hydrochloric acid and heated. Palladium diammine dichloride is thus precipitated. Fluxing materials, such as lead carbonate and carbon, are added to the slag which is then heated and poured into a mould. The slag and the lead are removed after solidification. It is then granulated and treated with nitric acid in order to dissolve the

precipitate and recover the rest of it. Sodium bisulphate is added to the insoluble material and heated to about 500 °C which converts rhodium to its sulphate form. It is then precipitated from a crude hydroxide form, which is then further dissolved in hydrochloric acid and the solution neutralised with sodium carbonate. After treatment with sodium nitrite a stable rhodium complex, $(NH_4)_3[(Rh(NO_2)_6]$, is formed. Rhodium metal is then produced in a series of steps starting with the addition of ammonium chloride. It is then treated with hydrochloric acid and passed through an ion exchange column, which separates ammonium and any base metals from the rhodium. The resulting solution is then boiled in the presence of formic acid and upon cooling in a hydrogen atmosphere, precipitates the rhodium.

The first compound containing a rhodium-carbon bond was synthesised by Manchot and Konig (1925:2173). They formulated the red volatile crystals which they obtained from treatment of $RhCl_3$ with CO, as the carbon monoxide complex of a rhodium oxychloride, $[Rh_2Cl_2O.3CO]$. In 1943, Hieber and Lagally (1943:96) correctly formulated this compound as the chloro bridged $[Rh_2Cl_2(CO)_4]$ dimer, and also described the synthesis of a number of other rhodium compounds, $[\{Rh(CO)_3\}n]$, later formulated as $[Rh_4(CO)_{12}]$, and $[Rh_4(CO)_{11}]$, and reformulated again as $[Rh_6(CO)_{16}]$. A decade later, stimulated by the discovery and structural characterisation of ferrocene, Cotton *et al* (1953:3586) reported the preparation and characterisation of the rhodicinium $[Rh(\eta\text{-}C_5H_5)_2]^+$ cation. In 1956, the first compound containing a rhodium-alkene bond was reported by Chatt and Venanzi (1956:852). They obtained the orange crystalline $[Rh(\eta\text{-}C_5H_5)(\eta^4\text{-}1,5\text{-cod})]$ compound. The same year also saw the first report of an

important class of carbonyl complexes, namely [*trans*-$RhCl(CO)L_2$] (L = tertiary phosphine or arsine), by Hieber and Heusinger (1956:678). Three years later, research groups of Fischer reported the discovery of the first rhodium compound containing a coordinated conjugated diene, namely [$Rh(\eta\text{-}C_5H_5)(\eta^4\text{-}C_5H_6)$] (Fisher *et al*, 1959;133). Another three years passed before the first rhodium complex containing a monoalkene ligand [$\{RhCl(\eta\text{-}C_2H_4)_2\}_2$] was isolated by Cramer (Cramer, 1962:722). This discovery was quickly followed in 1963 by a report of the first compound containing a rhodium-carbon σ-bond, when the five coordinate Rh(III) complex, [$RhBr(1\text{-naphthyl})_2L_2$], was synthesised by Chatt and Underhill (1963:2088).

1.2 RESEARCH REVIEW

Much of the impetus for the development of organometallic chemistry over the past years has been due to the ability of these complexes to catalyse various kinds of organic transformations (Douglas *et al*, 1983:405). Before 1938, when the oxo synthesis was discovered by Otto Roelen, homogeneous catalysis received only occasional mentioning in research articles (Cornils *et al*, 1994:2144). It was the work of Adkins and Krsek (1984:383) that confirmed oxo catalysts to be homogeneous in nature.

Homogeneous catalysis presents a far greater challenge than heterogeneous catalysis in the sense that there is a far better need to understand the catalytic cycles in the mechanisms of homogeneous catalysis with the possibility of influencing steric and electronic properties of these molecularly defined catalysts

(Cornils *et al.*, 1994:2144). It would be possible to tailor the chemical and structural properties of homogeneous catalysts to optimise its performance in the particular environment.

Most petrochemical processes make use of heterogeneous rather than homogeneous catalysts (Dickson, 1985:1). This is principally because heterogeneous catalysts are generally more stable at higher temperatures where these reactions are performed and are less troublesome to separate from the substrate phase. The major restriction of heterogeneous catalysts is however that they normally exhibit low selectivity, especially when stereochemistry is involved. Some of the best known catalytic processes involving organometallic compounds are shown in **Table 1.1**.

Table1.1 Catalytic processes involving organometallic compounds (Roelen, 1977:119)

Products	**Catalytic processes**
Hydrogenation of olefins	Wilkinson's catalyst
Hydroformylation of olefins	Oxo process
Oxidation of olefins	Wacker process
Polymerisation of propylene	Ziegler-Natta process
Olefin isomerisation	Nickel catalyst
Carbonylation of methanol	Monsanto process

The application of cobalt catalysts are mainly in the area of medium and long chain olefin production, and presently have reached a high standard due to the disintegration of $[HCo(CO)_4]$ after hydroformylation by altering the oxidation state of cobalt. This oxidation can be achieved by either hydrothermal treatment or by oxygen treatment in acidic medium, followed by regeneration of $[HCo(CO)_4]$. The disadvantages of using cobalt catalysts are that there is disintegration of the metal catalyst during distillation, with impurities causing side reactions, a low specific activity requires a large volume of reaction, and lastly hydrogenation of a considerable part of the olefin feedstock has to be tolerated.

The Monsanto acetic acid process is commercially an important process since it produces 50% of the annual world acetic acid capacity of 7 million metric tons (Guerra, 1994:368). The process involves carbonylation of methanol to yield acetic acid, as shown in **Figure 1.5**. The effect of the rhodium metal centre on the catalytic system is of prime importance, since the metal centre facilitates both the oxidative addition and reductive elimination steps as compared to that of the cobalt catalyst.

The key reaction in the Monsanto process is the facial oxidative addition of methyl iodide (step 1) to the square planar rhodium(I) metal centre to form the octahedral rhodium(III) species (**B**). Carbon monoxide insertion (step 2) into the *cis*-CH_3-Rh bond yields a five co-ordinated acyl intermediate (**C**), which undergoes carbon monoxide addition (step 3), followed by reductive elimination of the acetyl iodide (step 4) to yield the original rhodium (I) complex (**A**). Hydrolysis of the acetyl iodide by water in the aqueous-methanol

feed gives acetic acid and HI, and the latter reacts with methanol to regenerate methyl iodide and the cycle is complete. This mechanism was resolved after extensive research into the area and as recently as 1991 (Haynes *et al*, 1991:8567) the existence of the intermediates was confirmed in low concentrations using NMR technique.

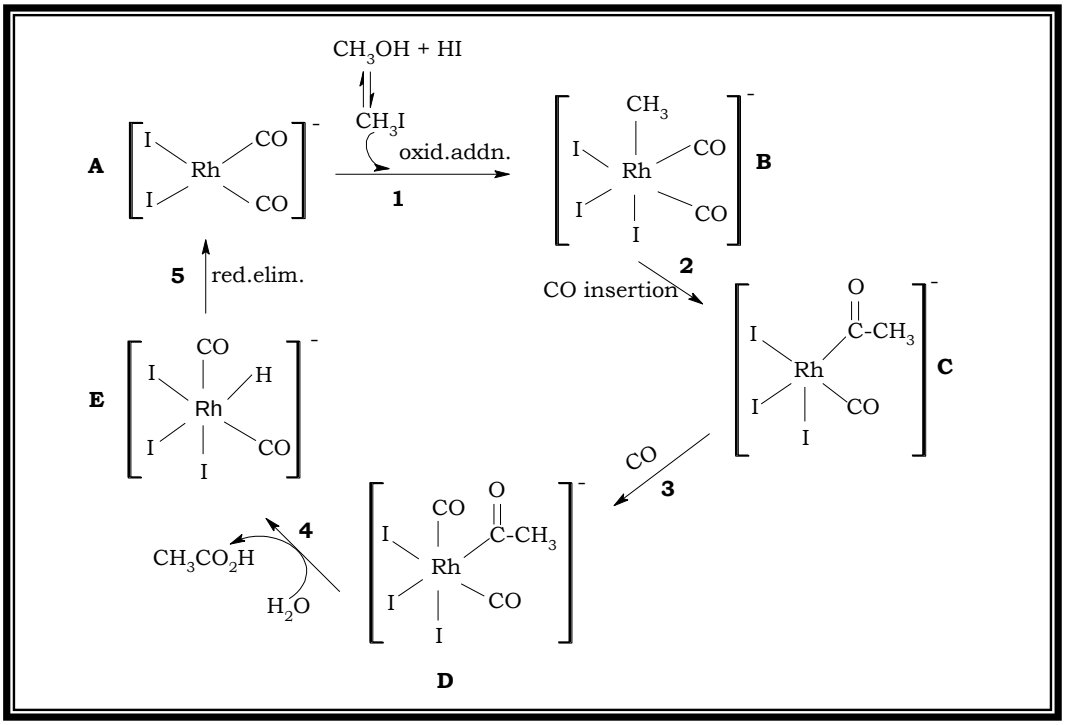

Figure 1.5 Monsanto process

Recently it has been found that methyl migration for the Cativa process can be accelerated by a factor of 10^4 with the addition of small amounts of methanol (Pearson *et al.*, 1995:1045). The iridium catalyst does not suffer from a slow rate-limiting step for oxidative addition of CH_3I with the catalytically active species. A higher stability and solubility are also obtained for the iridium

catalyst and productivity increases by 30% compared to that of the rhodium catalyst. These factors lead to the newly implemented Cativa process (**Figure 2.4**). The similarities between the two processes enable the Cativa process to be introduced into existing Monsanto plants with only minor conversions.

The importance of organometallic catalysts has brought about a great increase in research on catalysis and the mechanisms by which these processes take place. Some of the best known processes involving organometallic compounds are mentioned in **Table 1.1**. An important aspect worth mentioning is that each of the processes mentioned above represents to a greater or lesser extent several of the fundamental reactions that transition metal complexes undergo; reactions such as oxidative addition, substitution, insertion and reductive elimination which are discussed in detail in **Chapter 2**. Thus, a better understanding of catalytic cycles is primarily dependent on the study of these fundamental reactions of transition metal chemistry, and specifically for complexes that are closely related to those used in these processes.

The discovery of different catalyst systems gave rise for the intensive study of the substitution and oxidative addition reactions of square planar rhodium(I) complexes. Local researchers (Roodt and Steyn, 2000:1) have used this discovery to study different bidentate ligands with donor atoms varying from O-O-, O-S- to S-N-donor combinations to investigate their effect on the kinetic rate of substitution and oxidative addition. For example, two of the reaction steps in Monsanto catalytic process, *i.e.*, oxidative

addition and methyl migration, were studied for the reaction between square planar rhodium(I) complexes of the type [Rh(N,S-BID)(CO)(PPh_3)] and iodomethane (**Figure 1.6**).

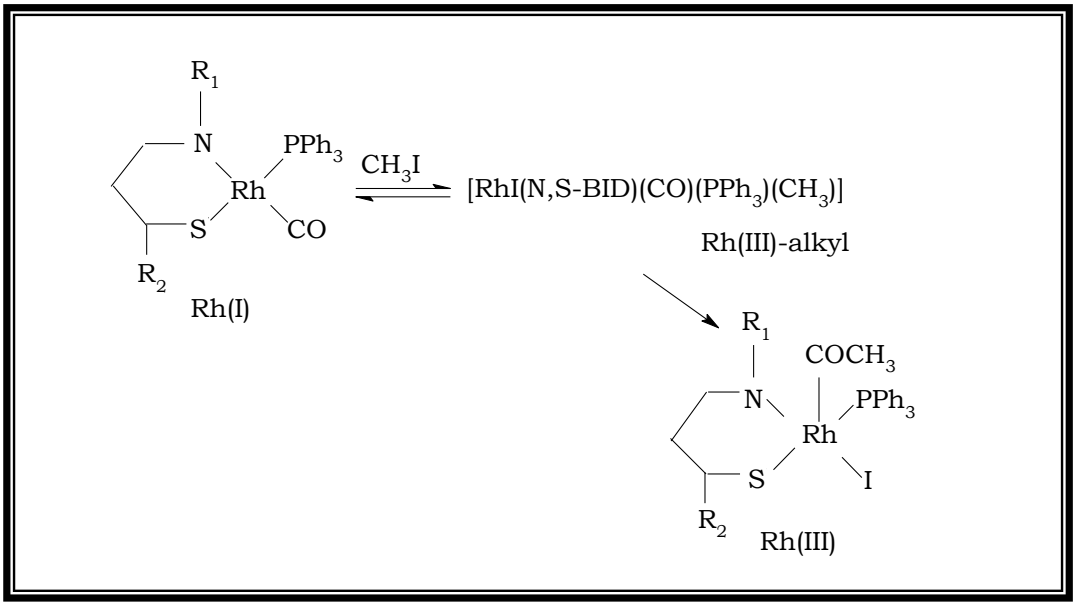

Figure 1.6 Reaction between complexes of the type [Rh(N,S-BID)(CO)(PPh_3)] and iodomethane

Local researchers (Roodt and Steyn, 2000:1) kinetically investigated the influence of the substituents R_1 and R_2 of the N,S-BID ligand on the reaction between iodomethane and [Rh(N,S-BID)(CO)(PPh_3) complexes for all the reaction steps that could be monitored (**Figure 1.7**). The electronic and steric influence of different tertiary phosphines on the reaction between [Rh(N,S-BID)(CO)(PPh_3)] and iodomethane were also kinetically investigated. Basson *et al.* (1984:167) have in recent years investigated the kinetics of the oxidative addition of iodomethane to complexes of the type [Rh(β-diketonato)(CO)(PX_3)], where X represents various alkyl and aryl groups. Temperature, pressure and solvent effects

were studied for a wide range of phosphines in order to gain information concerning the mechanistic nature of these reactions. Part of this study (Basson *et al*, 1987:31) was the isolation of different Rh(III)-alkyl complexes formed during the oxidative addition of rhodium(I) complexes of the type [Rh(cupf)(CO)(PX_3)] (where X represents *p*-Cl-Ph, Ph, *p*-MeO-Ph and Cy) with iodomethane. In the same study the activation entropy was determined for the reaction between [Rh(cupf)(CO)(PX_3)] and iodomethane in polar solvents such as acetone. The results indicated that an associative interaction of the solvent molecule with the alkyl complex takes place to form the activated complex. It has been also recognised that changing substituents on phosphorus ligands can cause marked changes in the behaviour of the free ligands and their corresponding transition metal complexes. The degree of accessibility is generally influenced by the bulkiness of the bonded ligands, for example PX_3. These steric properties of the ligand play an important role in some highly selective catalytic reactions like hydroformylation.

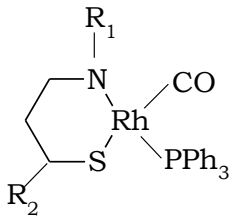

R_1	R_2
Me	Me
Cy	Me
H	Me
Me	H

Figure 1.7 Different substituents used in the complex of the type [Rh(N,S-BID)(CO)(PPh_3)]

Based on the results from previous studies **(Table 1.2)**, the following generalisations can be made:

Table 1.2: A summary of oxidative addition reactions of [Rh(LL'-BID)(CO)(PPh_3)] and [Rh(LL'-BID)(PX_3)] (Muller, 2000:6)

Complex	**Added molecule**	**LL'**
[Rh(LL')(CO)(PPh_3)]	CH_3I	acac, tfaa, hfaa, tfdmaa
[Rh(acac)(CO)(PX_3)]	CH_3I	
[Rh(Cupf)(CO)(PX_3)]	CH_3I	
[Rh(LL')($P(OPh)_3)_2$]	I_2	acac, ba, tfaa, hfaa, tfba
[Rh(LL')($P(OPh)_3)_2$]	CH_3I	acac, ba, dbm, tfaa, hfaa, tfba
[Rh(macsm)(CO)(PPh_3)]	CH_3I	
[Rh(LL')($P(OPh)_3)_2$]	$Hg(CN)_2$	acac, ba, dbm, tfaa, hfaa, tfba
[Rh(sacac)(CO)(PX_3)]	CH_3I	
[Rh(LL')(CO)(PX_3)]	CH_3I	hpt, AnMetha

i. The substitution of these complexes appears to proceed *via* a simple and straightforward associative mechanism.

ii. The first step of oxidative addition with CH_3I usually involves the formation of a rhodium(III) alkyl complex (**B**) followed by the formation of the rhodium(III) acyl complex (**C**) as shown in **Scheme 1.1**:

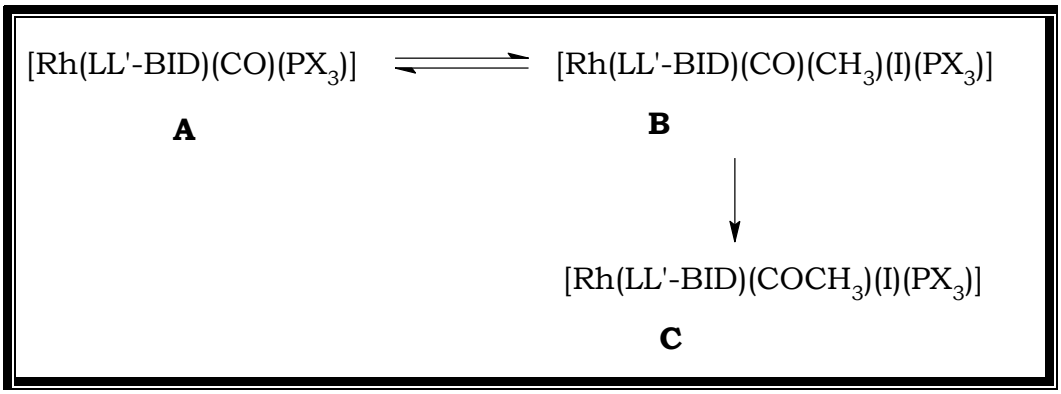

Scheme 1.1 Oxidative addition of [Rh(LL'-BID)(CO)(PX_3)] with iodomethane

The acyl formation (**C**) is one of the key steps in the Monsanto and Cativa processes.

iii. Electron withdrawing groups on the bidentate ligands (as in the case of [Rh(hfaa)(CO)(PPh_3)] have a remarkable effect on the rate of oxidative addition and that of the acyl formation. The reason for this is that electron density on the rhodium(I) centre is decreased by the substituents resulting in a weaker Lewis basicity of the rhodium(I) centre and thus slower reaction rates. A further decrease in the reactivity is observed when the bidentate ligand becomes more electron withdrawing.

iv. The different phosphines used also have a large effect on the rate of oxidative addition due to the difference in σ-donating capabilities as well as the steric hindrance, which can be expressed as the Tolman cone angle. It was found that a phosphine with a high σ-donating capability and small cone angle resulted in an

increase in the rate of oxidative addition and acyl formation. Tolman cone angles are further discussed in **Chapter 2**.

v. Different donor atoms not only have an influence on the rate of oxidative additions, but also on the composition of the final product. A rhodium(III) acyl complex was found for example in the case of [Rh(macsm)(CO)(PPh_3)] (donor atoms S,N) and a rhodium(III) alkyl complex was found in the case of the [Rh(cupf)(CO)(PPh_3)] (donor atoms O,O).

1.3 AIMS OF STUDY

Although acyl formation from the alkyl complexes has a very important role in catalytic industry, it is however troublesome from kinetic point of view. It sometimes happens that the reaction rate of oxidative addition and that of acyl formation are of the same magnitude. The reaction rates of these reactions cannot be studied independently since the resulting reaction is too complex. In addition, there may also exist two consecutive competing equilibria, one consisting of the formation of the alkyl derivative and its corresponding reverse reaction and the other reaction involve the CO insertion reaction to form the acyl complex with its reverse reaction. The main objectives of this study are as follows:

i. To synthesise the new bidentate ligand, CH_3cupf. Two different methods were used each following the general reaction mechanism given in **Scheme 1.2**.

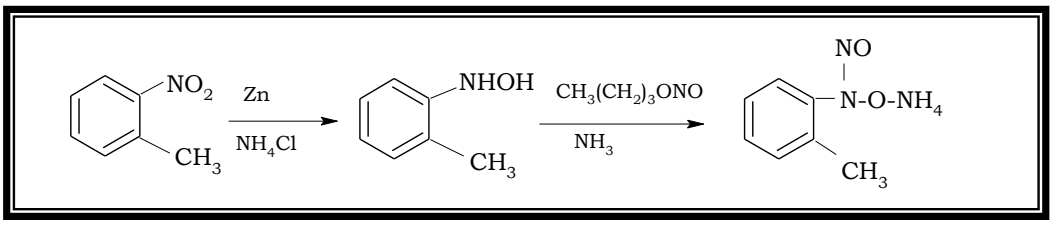

Scheme 1.2 General mechanism for the synthesis of CH_3cupf

ii. To characterise the ligand by means of NMR and IR techniques.

iii.To synthesise different Rh(I) complexes of the type [Rh(CH_3cupf)(CO)(PX_3)] and characterise each of the complexes by means of NMR and IR techniques.

iv. To study the reaction rates of oxidative addition of the complex of the type [Rh(CH_3cupf)(CO)(PPh_3)] with iodomethane using UV and IR spectroscopy in different solvents. Part of this study was also to investigate the electronic and steric influence of different tertiary phosphines on the reaction between CH_3I and the new Rh(I) complex.

v. To compare the results obtained from the oxidative addition of [Rh(CH_3cupf)(CO)(PX_3)] with iodomethane with other Rh(I) complexes of the type [Rh(LL'-BID)(CO)(PX_3)].

CHAPTER 2

THEORETICAL OVERVIEW

2.1 INTRODUCTION

Organometallic compounds are generally defined as compounds having at least one metal-carbon bond. However, some compounds that do not contain any metal-carbon bonds, such as hydrides and dinitrogen complexes are also considered to be members of this class due to the similarity of their chemistry with organometallic compounds (Sanshiro, 1997:2). Many types of organometallic compounds of transition metals have been isolated and have proven to be of interest not only as novel structures exemplifying novel bonding principles, but also as reagents, intermediates and catalysts in industrial processes (Sanshiro, 1997:2). The complexes provide interesting chemical entities such as hydride ions, carbanions, carbocations, carbenes and carbon free radicals. Before 1938, when the oxo synthesis was discovered by Otto Roelen, homogeneous catalysis was only mentioned occasionally in scientific literature (Cornils *et al.*, 1994:2144). It was the work of Adkins and Krsek (1984:383) as well as that of Berty and Marko (1953:177) that confirmed that the oxo catalyst was homogeneous in nature.

In depth studies done on all these organometallic complexes added new and important insight to the possible mechanisms of

industrial catalytic processes which also include transition metals, metal alloys and metal oxides.

Catalysts are divided into two groups, namely heterogeneous and homogeneous catalysts. The difference between the two types of catalysts is that heterogeneous catalysts are present in a different phase from that of reactants and products in the reaction they are catalysing, whereas homogeneous catalysts are in the same phase as the reactants and products (Richardson, 1989:217).

2.2 THE ROLE OF CATALYSIS

A large number of industrial chemical processes are based on the catalytic combination of small molecules such as NH_3, CO, H_2, H_2O and C_2H_4 to give larger molecules. These include the production of acrylonitrile, acetaldehyde, acetic acid and ethylene glycol from these rather small and simple molecules (Purcell and Kotz, 1977:700). There are four requirements for a successful catalytic process, namely

i. The reaction being catalysed must be thermodynamically favourable

ii. The reaction must proceed at a reasonable rate

iii. The catalyst must have an appropriate selectivity toward its desired product.

iv. The catalytic process should have a relatively long life-time to be economically viable.

Rhodium and cobalt complexes are the main contributors to the carbonylation of different products *via* catalytic processes. It can be seen from **Figure 2.1** that rhodium complexes tend to operate under milder conditions and are more selective towards product formation than that of cobalt complexes, which operate at higher concentrations and pressures to retain the catalytically active complex (Hermann and Cornils, 1997:1048).

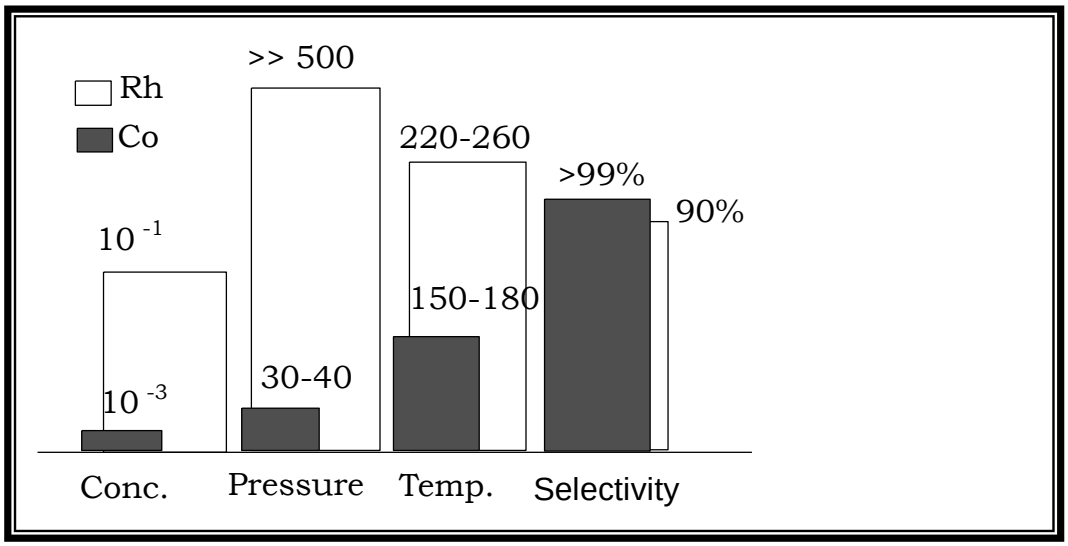

Figure 2.1 Rhodium *vs.* cobalt catalysis in the homogeneous carbonylation of methanol

Another aspect of importance in rhodium catalysis is the role that the metal complex plays in the catalytic cycle (Stille and Lau, 1977:434). This effect is best illustrated by the hydroformylation of propene with $[Rh(H)(CO)(PPh_3)_3]$ in the presence of an excess of

PPh_3 (**Figure 2.2**). A steady increase of the reaction rate as well as selectivity is observed (Olivier and Booth, 1970:245). The reaction peaks at a PPh_3:Rh ratio of approximately 5:1 after which any further addition of PPh_3 lowers the reaction rate.

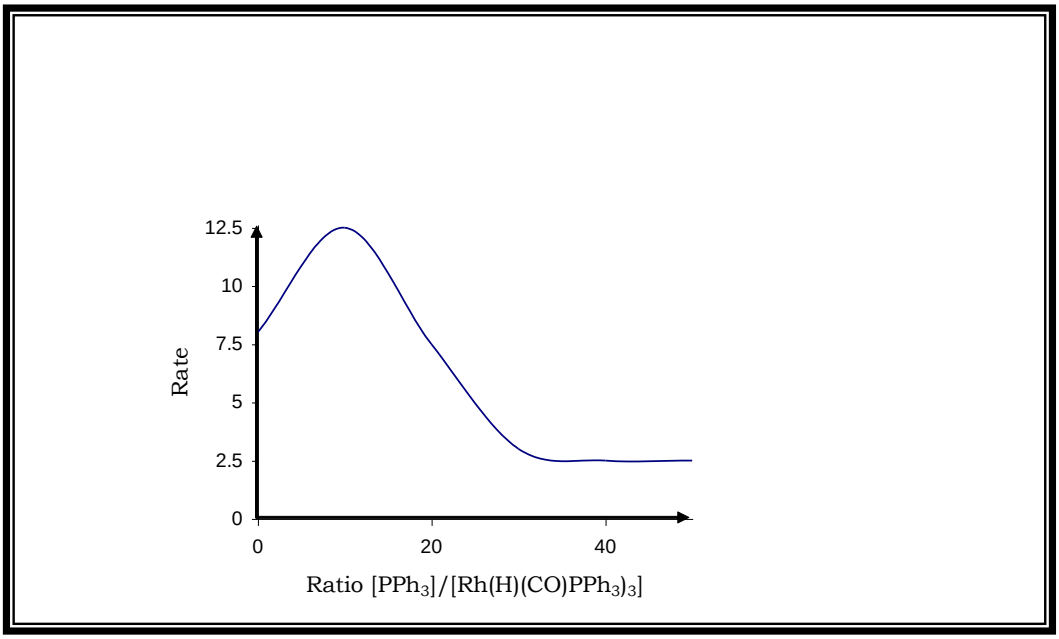

Figure 2.2 Dependence of reaction rate (gC_4H_8O)/min) on the PPh_3:Rh ratio

Parallel to the change of catalyst from Co to Rh in methanol carbonylation, the feedstock for the manufacturing of acetic acid was also changed from ethylene to methanol when Rh replaced Co as catalyst (**Figure 2.3**). The development began to steadily reduce the capacities of acetaldehyde, which previously had been made by the oxidation of ethylene. The big strides in the development of homogeneous catalysis were not only through changing the central metal atoms, but also through the changing of the ligands

surrounding the transition metal centres (Garlaschelli *et al.*, 1989:457).

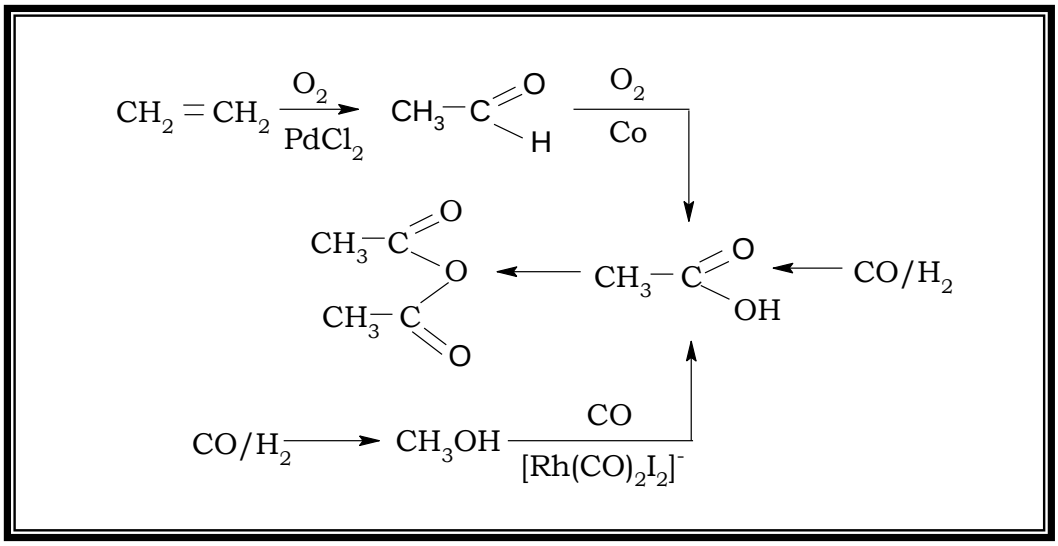

Figure 2.3 Alternative routes to acetic acid preparations (Cornils and Hermann, 2000:198)

Recently iridium replaced rhodium as the preferred catalyst in the production of acetic acid in the so-called Cativa process (**Figure 2.4**) where ligand modification played an important part in the successful implementation of the new process. It has been found that methyl migration in the Cativa process can be accelerated by a factor 10^4 with the addition of small amounts of methanol. A higher stability and solubility are also obtained for the iridium catalyst and productivity increases by 30% compared to that of the rhodium catalyst.

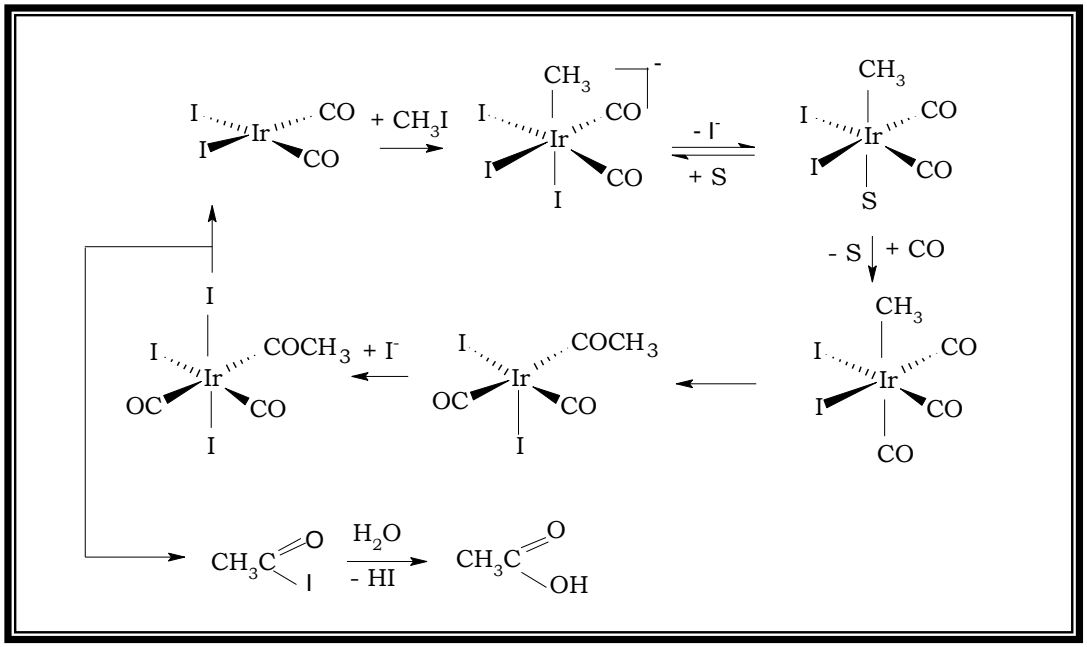

Figure 2.4 A schematic presentation of the Cativa catalytic process

In general, chemical reactions catalysed by transition metal complexes consist of a sequence of elementary reactions which include the following:

1. Olefin insertion
2. Carbonyl-insertion
3. Oxidative addition
4. Reductive elimination
5. *Cis*-migration
6. β-hydrogen elimination

Organometallic complexes which have the potential to act as catalysts should have the ability to participate in these reactions and be able to exert kinetic control. Oxidative addition, reductive elimination as well as carbonyl insertion reactions will be discussed in detail in the following paragraphs due to their importance in the catalytic processes as well as their relevance in this study.

2.3 OXIDATIVE ADDITION REACTIONS

2.3.1 INTRODUCTION

Oxidative addition reactions became well-known around the 1960's after Vaska's discovery that *trans*-[Ir(Cl)(CO)(PPh_3)$_2$] (Butler and Harrod, 1989:630) have the ability to bond with oxygen reversibly. These types of reactions, where transition metal complexes react with small molecules such as H_2, O_2, HCl and CH_3I, are described as oxidative addition reactions. An oxidative addition reaction (**Eq.2.1**) is one in which (usually) a neutral ligand adds to a metal centre and in doing so oxidises the metal, typically by 2e- (Bowser, 1993:549). The transferring of the two electrons from the metal to the incoming ligand breaks an existing bond in the ligand and form in the process two new anionic ligands. At least one of these new anionic ligands ends up bonded to the metal centre.

$$M^nL_4 + XY \rightleftharpoons M^{n+2}L_4XY$$

Eq.2.1

Oxidative addition reactions (**Figure 2.5**) have been observed with compounds containing metals such as rhodium, iridium, ruthenium, nickel, palladium and platinum.

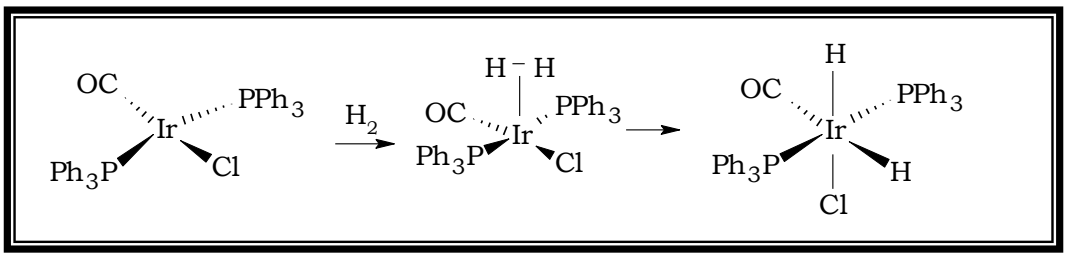

Figure 2.5 Typical example of an oxidative addition reaction (Cross, 1985:197)

There are three main classes of molecules (substrates) that can perform oxidative additions to metal centres: non-electrophilic, electrophilic and intact. Collman *et al.* (1987:279) classify these as Class A, B, and C substrates respectively.

Non-electrophilic or class A (Collman *et al.*, 1987:279): These molecules do not contain electronegative atoms and/or are not good oxidising agents. Aside from H_2, they are often considered to be "non-reactive" substrates. These molecules generally require the presence of an empty orbital on the metal centre in order for them to pre-coordinate prior to being activated for the oxidative addition reaction. Examples include H_2, C-H bonds, Si-H bonds, S-H bonds, B-H bonds, N-H bonds, S-S bonds and C-C bonds.

Electrophilic or class B (Collman *et al.*, 1987:279): These molecules do contain electronegative atoms and are good oxidising agents. They are often considered to be "reactive" substrates. These molecules do not require the presence of an empty orbital on the metal centre in order to perform the oxidative addition reaction. Examples include: X_2 (X = Cl, Br, I), R-X, Ar-X, H-X, O_2, etc. The most common substrates used here are R-X (alkyl halides), Ar-X (aryl halides), and H-X as shown in **Figure 2.6**.

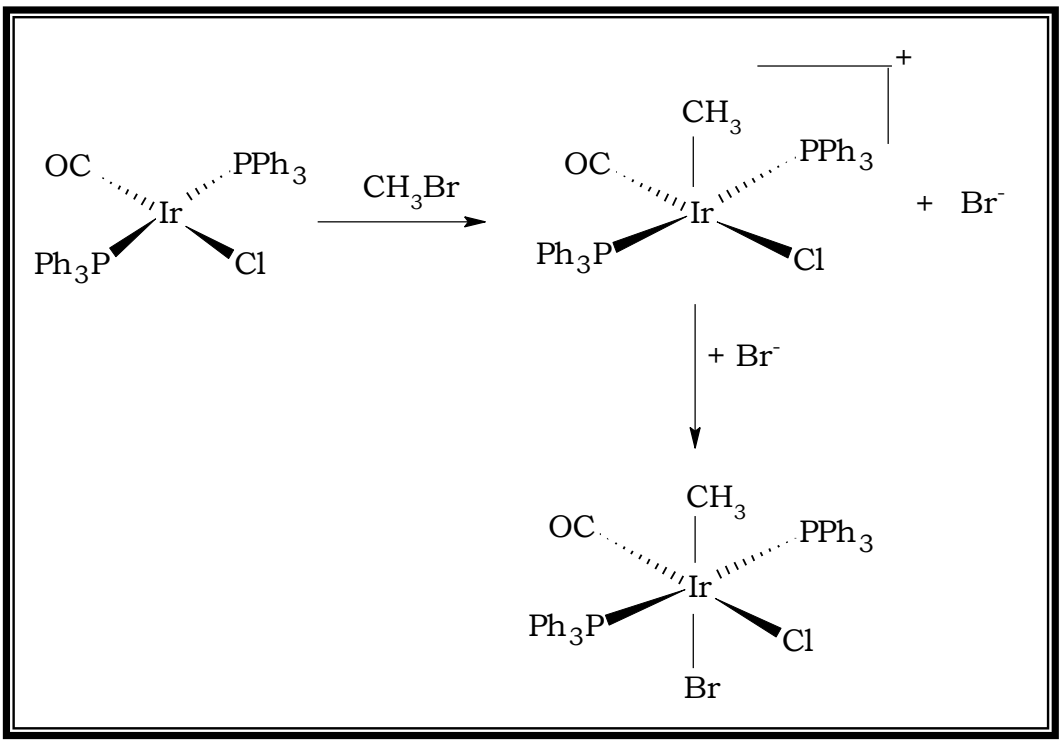

Figure 2.6 Oxidative addition of $[IrCl(CO)(PPh_3)_2]$ with CH_3Br

In **Figure 2.6** the C-Br bond is broken during the oxidative addition reaction generating new anionic ligands where the ligands usually end up coordinated to the metal to form an $18e^-$ complex.

"Intact" or class C (Collman *et al.*, 1987:279): These molecules may or may not contain electronegative atoms, but there need to be either a double or triple bond present in the molecule. Unlike most of the other substrate molecules that break a single bond to form two separate anionic ligands upon the oxidative addition, these ligands possessing double or triple bonds only allow for breaking of the σ-bond, leaving the π-bonds intact. The ligand receives two electrons from the metal and becomes a dianionic ligand.

A metal centre (**Figure 2.7**) with an empty orbital is needed in order to pre-coordinate the ligand before the oxidative addition occurs. The one notable exception to this is O_2, which can also act as an electrophilic (Class B) substrate. Typical "intact" ligands that can perform an oxidation addition without fragmenting apart are alkenes, alkynes and O_2.

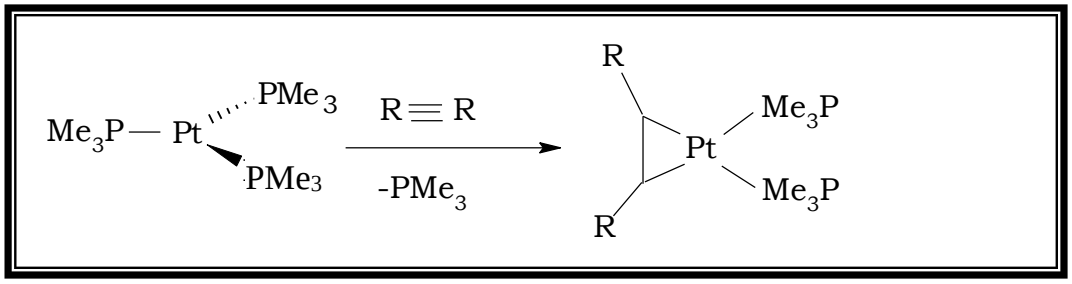

Figure 2.7 Oxidation of the Pt centre from Pt(0) d^{10} to Pt(+2) d^8

2.3.2 STEREOCHEMISTRY OF OXIDATION ADDITION

A large amount of the research on rhodium-phosphine catalysis has focused on the area of asymmetric synthesis (Dickson, 1985:1). This involves the transformation of a prochiral substrate into one predominant enantiomer. There are many applications for this in the pharmaceutical industry where often only enantiomer of a particular compound is biologically active. In order to keep the production of these compounds inexpensive, industry requires complexes that can control catalytic enantiomeric selectivity of an important synthetic step such as hydrogenation. In hydrogenation reactions the catalytic properties can be markedly affected by the nature of the ligands attached to the central metal atom (Bird, 1967:345). In particular, the presence of phosphines or arsines is likely to increase the effectiveness of a catalyst in relation to the transfer of hydride ions. There has been much interest in the stereochemistry and the mechanism of oxidative addition reactions of the Vaska compounds (Vaska, 1968:136), which has been closely scrutinised for clues to elucidate the reaction mechanism and geometry of the transition state (Rusina, 1965:295). Generally, non-polar substances such as H_2, O_2 and C_2H_4 add in a

cis-fashion (Vaska and Diluzzio, 1961:2784). An example is oxidative addition of H_2 to Vaska's complex, *trans*-[IrCl(CO)(PPh_3)$_2$] as shown in **Figure 2.8**.

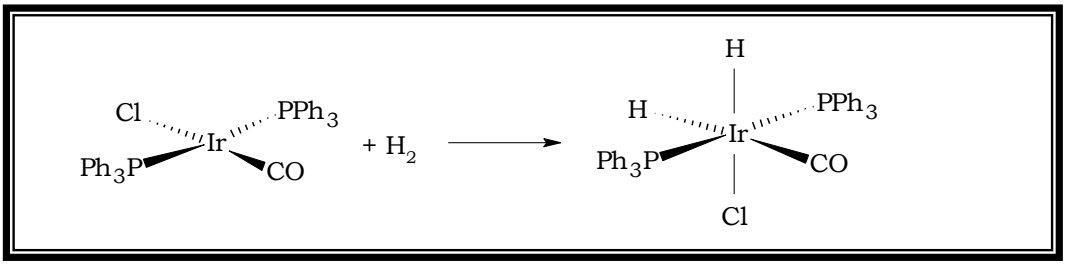

Figure 2.8. Oxidative addition of Vaska's complex with H_2 (Vaska and Diluzzio, 1961:2784)

Alkyl halide addition has been reported to yield both *cis* and *trans* products (La Planca and Ibers, 1966:405), but predominantly *trans*-isomer. An example of *cis*-addition has been found for the oxidative addition of [Rh(cupf)(CO)(PX_3)] (where PX_3 = PCy_3, P(*o*-Tolyl)$_3$, PPh_3, $PPh_2C_6F_5$ and P(*p*-ClC_6H_4)$_3$, and cupf = cupferrate ligand) with iodomethane which proceed *via* a three-centred transition state as shown in **Figure 2.9** (Basson *et al.*,1987:31).

In **Figure 2.9** the trigonal-bipyramidal (TBP) intermediate A isomerises to give the structure shown in B.

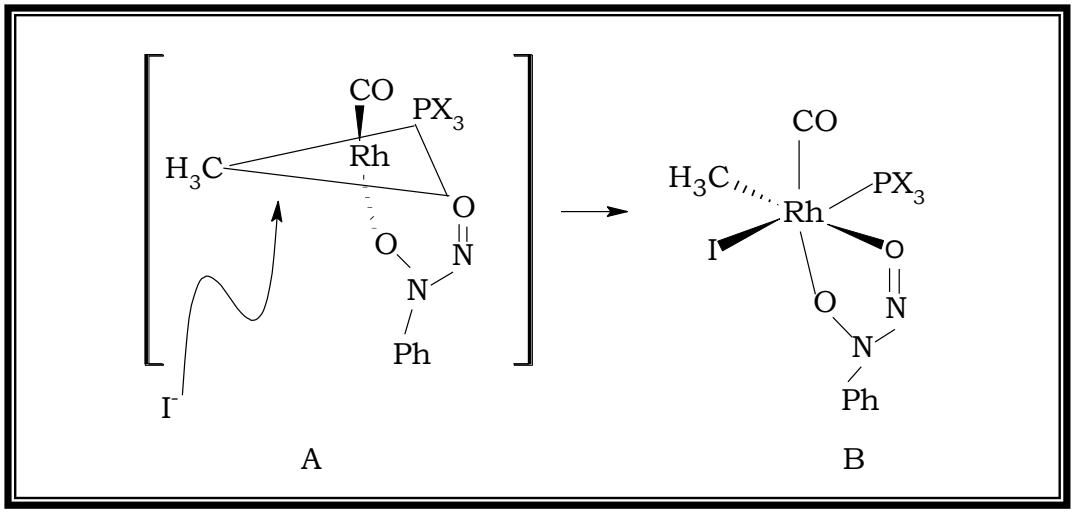

Figure 2.9 Oxidative addition of [Rh(cupf)(CO)(PX_3)] with CH_3I

An example of *trans*-addition is the oxidative addition of [Rh(tfba){$P(OPh)_3$}$_2$] with iodomethane (Van Zyl *et al.*, 1988:223) as shown in **Eq 2.1**.

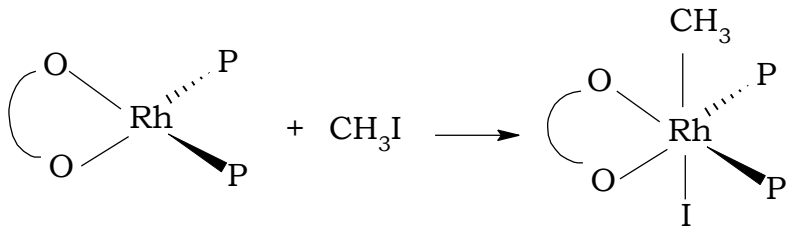

Eq.2.1

It is accepted that this reaction proceeds *via* a linear transition state. There are known examples where isomerisation of ionic intermediates takes place, yielding products in which the fragments of the addend molecule are *cis* to one another after

coordination of the anion. Thus a *cis*-product does not necessarily indicate a three-centre intermediate. Furthermore, the final oxidative addition product can also isomerise as was found in the case of *trans* oxidative addition product obtained from the addition of CH_3Cl to *trans*-[$IrBr(CO)(PPh_2Me)_2$] (Collman and Sears, 1968:27). On refluxing the resulting *trans*-product in a methanol/benzene mixture the *cis*-product was obtained. This suggests that the stereochemistry of oxidative addition of CH_3I results in a mixture of both the *cis* and *trans*-products (Blake and Kubota, 1970:989).

2.3.3 THE MECHANISM OF OXIDATIVE ADDITION

Information on the mechanism of oxidative addition can be found by studying the stereochemistry of the starting material as well as that of the final product. From this, possible postulations of intermediate products can be made. Unfortunately this can be complicated by the fact that ligand exchange and isomerisation can occur before isolation of the final product (Cross, 1985:197). Another way of obtaining more information on the mechanism is by investigating the regiochemistry of the newly bonded carbon atom to the metal. By determining the configuration on the carbon atom before and after oxidative addition, a possible transition state can be postulated to describe the mechanism.

The four most commonly proposed mechanisms include the concerted three-centre mechanism, the S_N2 two-step mechanism, free radical mechanism and ionic mechanism. These mechanisms are briefly reviewed below and discussed individually.

2.3.3.1 The Concerted Three-Centre Mechanism

This mechanism is mainly active during oxidative addition of non-polar molecules like H_2 and I_2 in non-polar reaction solvents (Thompson and Sears, 1977:769). The mechanism involves the interaction of the filled d_{xz} or d_{yz} metal orbital with the empty anti-bonding orbital of the addendum molecule (Cross, 1985:197). In addition to the above mentioned interaction, the overlapping of the filled σ-orbital of the addendum with an empty metal orbital resulting in electron flow to the metal also plays an important role in this mechanism. The formation of a three-centred transition state proposed for this type of reaction is given in **Figure 2.10**.

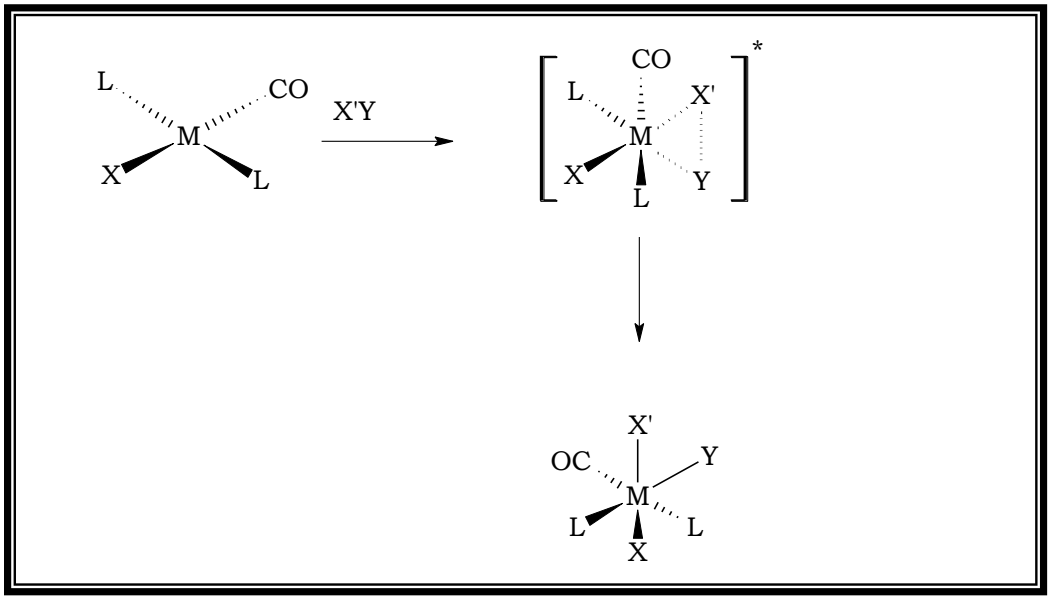

Figure 2.10 Oxidative addition *via* the concerted three-centre Mechanism

The main driving force being the simultaneous formation of a M-X and M-Y bond, leading to the final dissociation of the X-Y bond.

The oxidative addition of H_2 to the square planar d^8 *trans*-$[IrX(CO)L_2]$ complex (X = halide and L = tertiary phosphine) proceeds along one of the two ligand axes, X-Ir-CO or L-Ir-L, leading to formation of one of the two possible adducts (Deutsch and Eisenberg, 1988:1147).

2.3.3.2 The S_N2 Two-Step Mechanism

The S_N2 mechanism is associated with the addition of dipolar molecules (methyl-, allyl-, benzyl halides, *etc.*) to the metal centre. Unlike the concerted mechanism, where nucleophilic attack of the added molecule takes place on the metal, the S_N2 mechanism involves nucleophilic attack by the metal on the α-carbon of the added molecule (Griffin *et al.*, 1995:3029).

The S_N2 mechanism, as in the case of the concerted type mechanism, is second order in nature, and can be accelerated by the use of polar solvents. The S_N2 mechanism normally has large negative entropy values which are usually dependent on the solvent polarity. All this is consistent with a well-oriented, polar transition state, similar to what is seen for S_N2 reactions in organic chemistry. These observations lead to a proposed mechanism for oxidative addition where the metal can participate in the nucleophilic displacement of the halide of the addendum molecule *via* an attack of the metal on the α-carbon in the initial step, followed by either a two-centre or three-centre transition state (Cross, 1985:197).

It is important to note that oxidative addition reactions that proceed along an S_N2 type mechanism (**Figure 2.11**) usually result in the *trans*-product (Thompson and Sears, 1977:769), unlike the one step concerted mechanism where the *cis* configuration is dominant. However isomerisation may also lead to the formation of the *cis*-product (Blake and Kubota, 1970:989).

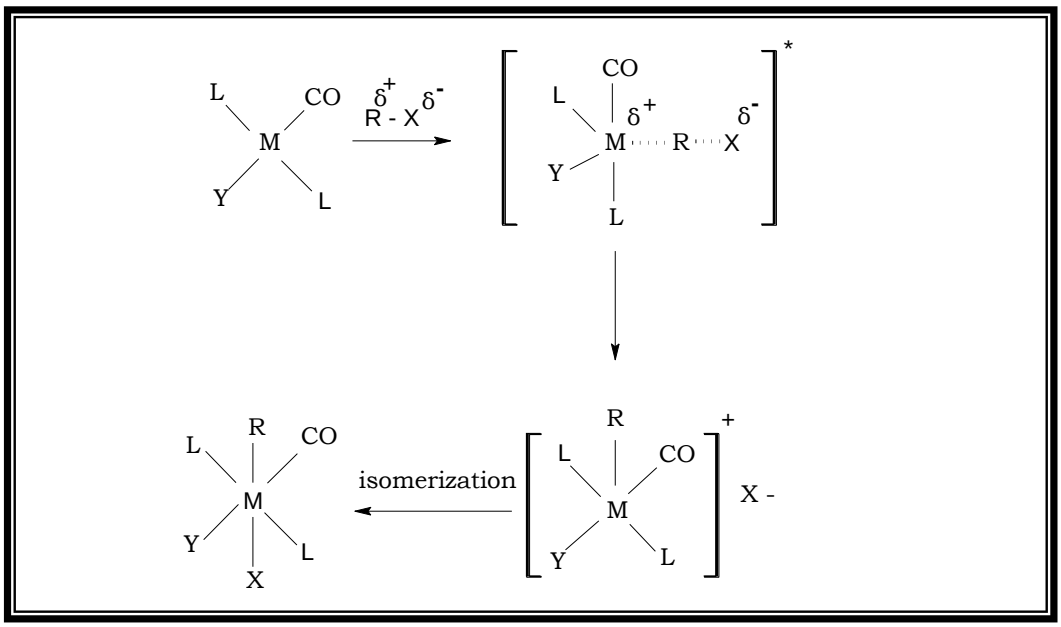

Figure 2.11 Oxidative additions *via* the S_N2 mechanism

2.3.3.3 Free Radical Mechanism

A few oxidative addition reactions proceed *via* a free radical mechanism. There are two main mechanisms of importance to the d^8 square planar complexes (Nylom and Vrieze, 1965:5337) which are i) the radical chain reaction and ii) the inner-sphere electron transfer mechanism.

The radical chain reaction

Alkyl, aryl and vinyl halides can undergo oxidative addition to Vaska type complexes *via* a radical chain mechanism (Parshall and Ittel, 1992:346). A proposed radical chain mechanism is shown in **Scheme 2.1**, where M = *trans*-[MX(CO)L_2].

Initiation:

$[M^{I}] + Q^{\cdot} \longrightarrow [M^{II}] - Q^{\cdot}$

$[M^{II}] - Q^{\cdot} + R\text{-}X \longrightarrow R\text{-}[M^{III}]\text{-}Q + R^{\cdot}$

Propagation:

$[M^{I}] + R^{\cdot} \longrightarrow R - [M^{II}]^{\cdot}$

$R - [M^{II}]^{\cdot} + R - X \longrightarrow R - [M^{III}] - X + R^{\cdot}$

Termination:

Two radicals $\longrightarrow$ non-radical products

Scheme 2.1 The free radical chain mechanism, where $Q^{\cdot}$ represents any trace of radicals

In the initiation step the first radical $R^{\cdot}$**,** in the chain is created while the propagation step is a succession of elementary reactions in which the radical, which is produced in the reaction, is

consumed in the next step. This step is fundamental in the formation of the required products. The termination step involves the dimerisation, disproportionation, oxidation or reduction of the radicals involved in the rate-determining step to form the stable final products.

The inner-sphere mechanism (Purcell and Kotz, 1980:392)

This free radical mechanism is represented in **Scheme 2.2** below

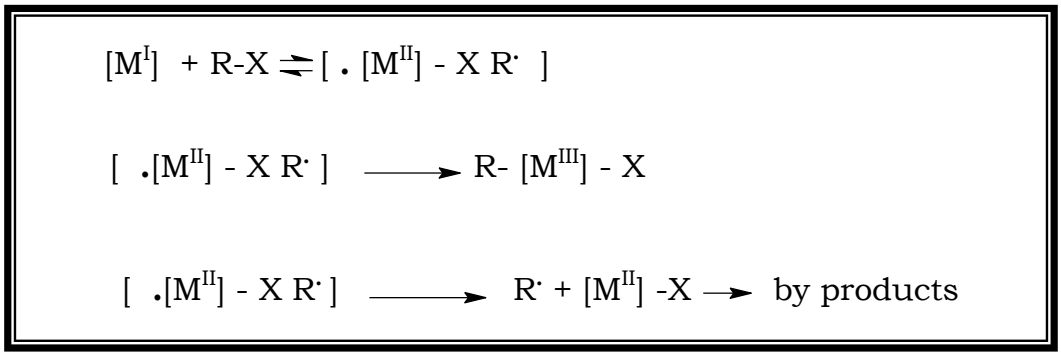

Scheme 2.2 The inner-sphere mechanism

In this mechanism the organic halide first coordinates to the metal centre then electron transfer takes place subsequently forming a radical pair consisting of the group R and the metal halide. Combination of this radical pair gives the final oxidative product, but the escape of the free radicals may lead to the formation of by-products as shown in **Scheme 2.2**.

2.3.3.4 The Ionic Mechanism

This mechanism is one of the least well-known mechanisms and is normally favoured by polar reaction medium which would allow the two reagents HCl or HBr to be dissociated and react with the metal complex. Protonation of a square planar complex, like *trans*-$[MX(CO)L_2]$ produces a five-coordinate intermediate, $[HMX(CO)L_2]$ which then proceeds to the formation of the final products.

2.3.4 FACTORS INFLUENCING THE RATE OF OXIDATIVE ADDITION

Different experiments are required to deduce the specific mechanism of activation for the oxidative addition reactions. It is not a simple case of applying certain rules to kinetic or to structural results obtained, and then arriving at an answer indicating whether the mechanistic route is concerted, ionic or free radical. The uses of stereochemistry of the final oxidative products have been discussed previously as well as the problems encountered with it. It is still however necessary to evaluate the effects that factors such as different solvent, the ligands bonded to the transition metal complex and the characteristic of the central metal atom have on the oxidative addition reactions.

2.3.4.1 The Metal Center

One way of visualising oxidative addition reactions is to consider the metal as acting as a nucleophile. Anything that affects the

nucleophilicity of the metal therefore influences the course of the reaction. The general tendency for d^8 metals to undergo oxidative addition is represented in **Figure 2.12** (Laplanca and Ibers, 1966:405).

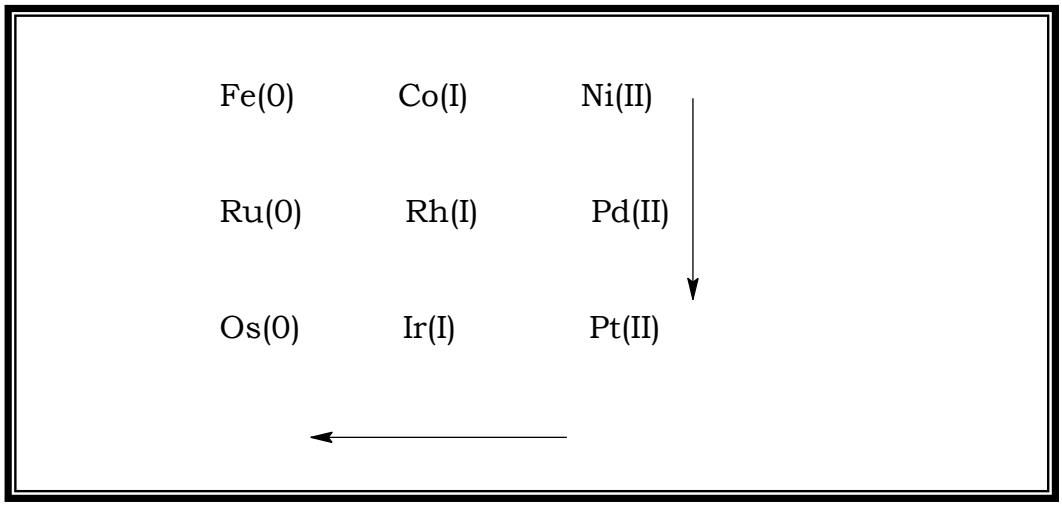

Figure 2.12 Ability of a d^8 metal to undergo oxidative addition. The arrows indicate increasing reactivity towards oxidative addition.

The general requirements for a metal to undergo oxidative addition are as follows:

i. The availability of non-bonding electron density in the metal

ii. The availability of two vacant coordination positions on the metal to form the two new bonds

iii. The ability to form a product with an oxidation state two units

higher than that of the starting material

Generally this series can be used as an estimate when different metals are used for oxidative addition.

2.3.4.2 The Bonded Ligands

It is evident from previous discussions that the metal centre is not the only factor that influences oxidative addition reaction rates. Ligands surrounding the metal centre may cause the rate of oxidative addition to increase if they are good electron donors, or decrease, depending on the ligand's inherent characteristics. There are two main aspects involved in the bonding of ligands to transition metals, namely electronic and steric properties, which have a dramatic influence on the properties of the metal complex (Tolman, 1970:2953). It has for example been recognised that changing substituents on tertiary phosphine ligands can result in marked changes in the behaviour of the free ligands as well as their transition metal complexes (Tolman, 1977:313). Both the electronic and steric influences of ligands are to be considered when the transition metal complex undergoes oxidative addition. Increasing the electron donating ability of the coordinated ligand, as measured by its Brönsted basicity (Ugo *et al.*, 1972:7364), increases the relative rate of oxidative addition. However, increasing the steric hinderance of the coordinated ligand as measured by the Tolman cone angle decreases the relative rate of oxidative addition (**Figure 2.13**).

Electronic effect

The σ- and π-bonding properties of bonded ligands largely influence the electron density and thus the nucleophilicity of the metal centre. Ligands with good σ-donating properties generally enhance oxidative addition rates while good π-accepting ligands inhibit reactivity (Bonder *et al.*, 1980:1971). As mentioned earlier, there is a good correlation between the basicity of the metal complex and the tendency of such complex to undergo oxidative addition reactions. The parameter used to indicate the Lewis basicity of tertiary phosphines is the pK_a value that is a measure of the Brönsted basicity.

Phosphine ligands containing substituents with increasing electron-donating capability are given in **Table 2.1**. An increase in the σ-donating ability of tertiary phosphines should be considered in conjunction with the effect that electron-donating groups would have on the π-back bonding capability of the phosphine. This is especially true when tertiary phosphines are bonded to transition metal complexes. The electron donor-acceptor capacities of these ligands will determine the electron density on the metal and this will have a substantial effect on the other ligands bonded to the metal centre.

Table 2.1 The rate of oxidative addition of $PhCH_2Cl$ to tertiary phosphines, the pK_a values (Wilkinson, 1987:458) and the Tolman electronic parameter values (Tolman, 1970:2953) for tertiary phosphines

Tertiary phosphines	**$10^4k/M^{-1}s^{-1}$**	**pK_a**	**$\nu(CO)/cm^{-1}$**
PCy_3		9.65	2056.4
$P(p\text{-}C_6H_4OCH_3)_3$	3.3	4.57	2066.1
$P(p\text{-}C_6H_4CH_3)_3$		3.84	2066.7
PPh_3	12	2.73	2068.9
$P(p\text{-}C_6H_4F)_3$		1.97	2071.3
$P(p\text{-}C_6H_4Cl)_3$	0.2	1.03	2072.8

From **Table 2.1** it is clear that as the electron donating capability of the substituent on the tertiary phosphines increases (from top to bottom), the CO stretching frequencies decreases. This means that as the electron density on the metal is decreased, less electron density is accepted by the CO moiety *via* π-back bonding into the π*-orbitals, resulting in decrease in M-CO bond strength and a resulting increase in ν(CO). However, electron withdrawing substituents will decrease the σ-donating ability of the tertiary phosphine, implicating less electron density on the metal centre available for the π-back bonding to the carbonyl which will also lead to an increase in ν(CO). It is important to note that a coordinated tertiary phosphine that has good π-acceptor capability, like $P(p\text{-}C_6H_4Cl)_3$, will remove electron density from the metal centre with greater ease than one like PPh_3, which has a weaker π-acceptor capability but a better σ-donor ability (Tolman, 1970:2953).

According to the trend in ν(CO) values the π-accepting tendencies of phosphorus ligands can be placed in the following order:

PF_3 > PCl_3> $P(OAr)_3$ > $P(OR)_3$ > $P(Ar)_3$ > $PR(Ar)_2$ > PR_2AR > PR_3

An excellent example of the electronic effect of the different phosphine ligands is illustrated in **Table 2.2**, giving the rate of oxidative addition of [Rh(acac)(CO)(PX_3)] with iodomethane (PX= P(*p*-PhCl)$_3$, PPh_3, P(*p*-PhOMe)$_3$) (Basson *et al*, 1986:35).

Table2.2 Experimental data for the oxidative addition of [Rh(acac)(CO)(PX_3)] with iodomethane

PX_3	**$k_1\times 10^3/M^{-1}S^{-1}$**	**K/M^{-1}**	**$\nu(CO)/cm^{-1}$**
P(*p*-PhCl)$_3$	3.46(9)	4.0(2)	2064
PPh_3	23(3)	9(1)	2060
P(*p*-PhOMe)$_3$)	138(3)	16(2)	2056

The kinetic results shown in **Table 2.2** indicate that the increase in the rate constants can be correlated to the phosphine's σ-donating capabilities. This correlation can be seen from the ν(CO) values, which are an indication of the electronic influence of the different phosphines. These phosphines in **Table 2.2** are iso-steric with a cone angle of 145°, thus no difference in the steric influence on the rate for these phosphine ligands are expected. The rate of oxidative addition was found to increase in accordance with the

increased electron donating ability of the tertiary phosphines in the following order:

$$P(p\text{-}PhCl)_3 < PPh_3 < P(p\text{-}PhOMe)_3$$

It can be seen that the increase of electron density on the central metal atom renders it a strong nucleophile, thus enhancing the rate of oxidative addition (Ugo *et al.*, 1972:7364).

Steric effects

The steric bulk of the ligand bonded to the metal complex is also a highly important factor in determining the influence that the ligand has on the reactivity of the organometallic compound. The cone angle, shown in **Figure 2.13** (Tolman, 1977:313), is frequently used as an index of the steric bulk of phosphorus ligands. The cone angle, θ, is estimated by assuming an average M-P bond distance of 2.28 Å and maximum occupation of Van der Waal's sphere of the substituents on the phosphorous atom. The model of Tolman assumes that the phosphines are tetrahedrally surrounded with substituents and that free rotation is possible at all times around the bond axis.

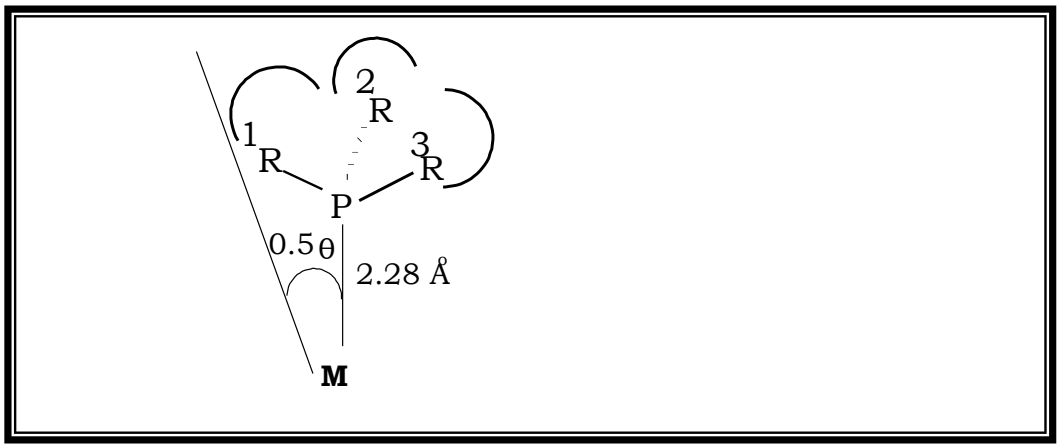

Figure 2.13 Representation for the calculation of the cone angles in symmetrical phosphines.

An excellent example of the influence of the steric parameter were done by Hart-Davis and Graham (1970:2658) in the reaction between [(η^5-C_5H_5)Co(CO)L] and CH_3I, (L = PPh_3, $PMePh_2$ and PMe_2Ph). The increase in the reaction rates from PPh_3 with a Tolman cone angle of 145˚ to PMe_2Ph with a Tolman cone angle of 122˚ can only be explained by the difference in steric bulkiness of the phosphine ligands.

2.3.4.3 The Addend molecules

The added molecule also has an influence on the mechanism, the stereochemistry as well as the nature of the oxidative addition products. According to Collman and Hegedus (1980:345) a distinction between three classes of addend molecules can be made:

i. Polar electrophiles like halogen acids (HX), alkylation reagents

(RX, RCN, HgX_2, etc.)

ii. Unsaturated reagents like O_2, S_2, RC=CR, etc.

iii. Non-polar addenda like H_2, R-H, RSH, etc.

Addend molecules of class i generally proceed along a polar, S_N2 two-step mechanism or free radical mechanism. The products of these reactions can either be *cis* or *trans*, but in the case of alkyl halides it is generally found to be the *trans*-isomer as the final product (Purcell and Kotz, 1977:700). The reactivity of the alkyl substituent of the alkyl halides can be arranged as follows (Collman and Maclaury, 1974:3019):

$$CH_3 > CH_3CH_2 > \text{secondary} > \text{cyclohexyl}$$

The order of the halogen reactivity was found to be as follows (Stille and Lau, 1977:434):

$$I^- > Br^- > Cl^-$$

The unsaturated reagents in class ii retain at least one bond in the addendum molecule. In this case only the *cis* -product is possible. The non-polar addenda of class iii react only with coordinative unsaturated complexes in a concerted three-centre mechanism, and only *cis*-addition takes place. If *trans*-addition is found,

isomerisation of the original *cis*-product most probably occurred in the final step.

2.3.4.4 The Reaction Medium

Protic solvents like H_2O, CH_3OH, HF etc. are capable of strong hydrogen bond formation while dipolar aprotic solvents like acetone, acetonitrile and dimethylformamide, though very polar, are much less capable of hydrogen bond formation. This classification has lead to the conclusion that hydrogen bonds may be an important interaction in determining the solvent effect on reaction rates of oxidative addition. Basson *et al* (1987:31) observed a marked effect of solvent polarity and donocity on the rate of oxidation addition reaction of [Rh(cupf)(CO)(PPh_3)] with iodomethane. The solvents in which the reaction was carried out ranged from acetone to toluene. The use of solvents with low polarity, such as toluene and chlorobenzene, resulted in small forward rate constants compared to the rate found for the same reaction followed in polar solvents, which indicate that a highly polar solvent increases the rate of oxidative addition.

The solvents used for these kinds of reactions can also influence the mechanism of the oxidative addition reaction. Solvent molecules can act as ligands that can coordinate to the square-planar complexes to form five-coordinate complexes. These complexes then have a greater susceptibility to electrophilic attack which means a faster rate of oxidative addition (Blake and Kubota, 1970:989).

2.3.4.5 The Effect of Solvent

The polarity of the solvent in which the reaction is carried out also influences the rate of the reaction. The reaction investigated by Basson *et al* (1987:31) is a good example which clearly demonstrates the solvent effect on the oxidative addition reaction as shown in **Figure 2.14**.

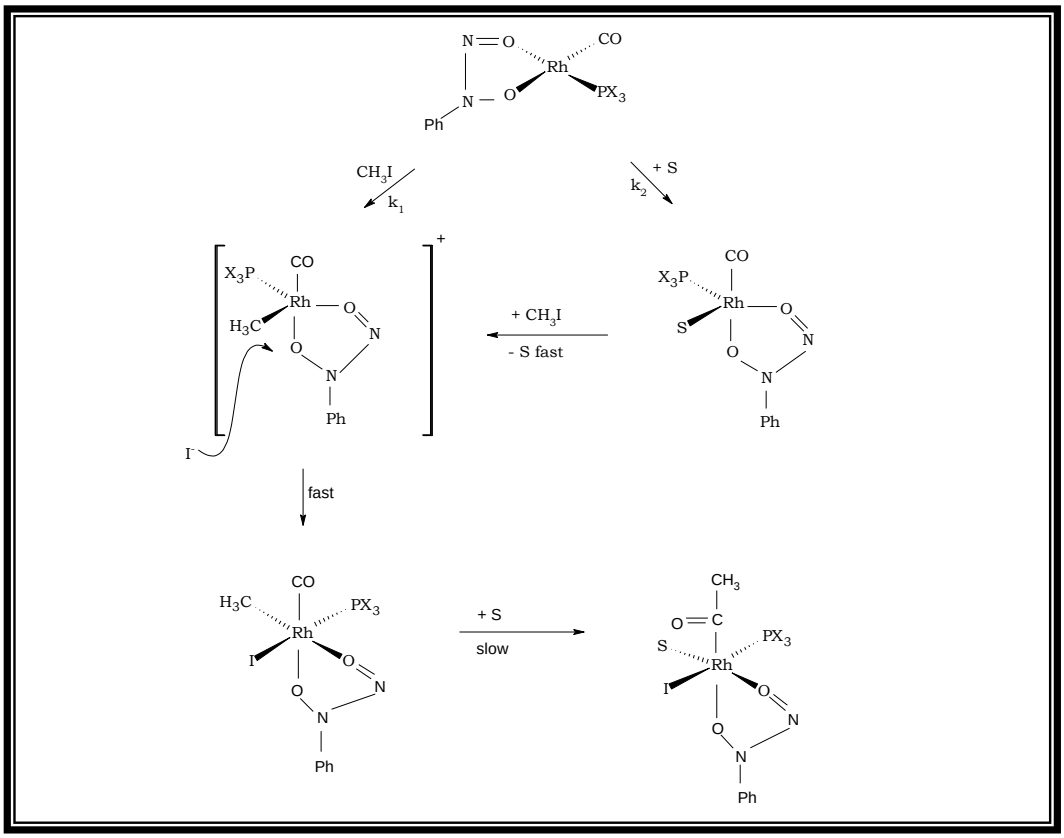

Figure 2.14. The reaction scheme for the oxidative addition of [Rh(cupf)(CO)(PX_3)] with CH_3I

In their research they postulated a mechanism with two parallel pathways, a direct k_1 path involving the oxidative addition of the

metal complex with iodomethane as well as the k_2 solvent catalysed route with the initial reaction between a solvent molecule and the metal complex followed by the oxidative addition reaction. Changes in the rates of the competing pathways were noticed as the polarity of the solvent changes. The rate of oxidative addition along the k_1-path changes with a factor 840 as the polarity of the solvent increases from benzene to acetonitrile. Highly polar solvents favoured the solvent route (k_2-path) since a factor 4667 increase was found in the k_2-path, while only a factor of 840 increase was noticed for the k_1-path.

2.4 REDUCTIVE ELIMINATION

2.4.1 INTRODUCTION

A reductive elimination reaction is the reverse of an oxidative addition reaction (Vallarino, 1957:2287). In this reaction bond formation between two cisoidal anionic ligands (**Figure 2.15**) on a metal centre takes place (Deutsch and Eisenberg, 1988:1147). Each anionic ligand donates an electron to the metal centre (in the case of a monometallic complex) to reduce the metal centre by two electrons. In the subsequent step the newly formed chemical entity is released from the metal centre leaving the metal coordinatively unsaturated.

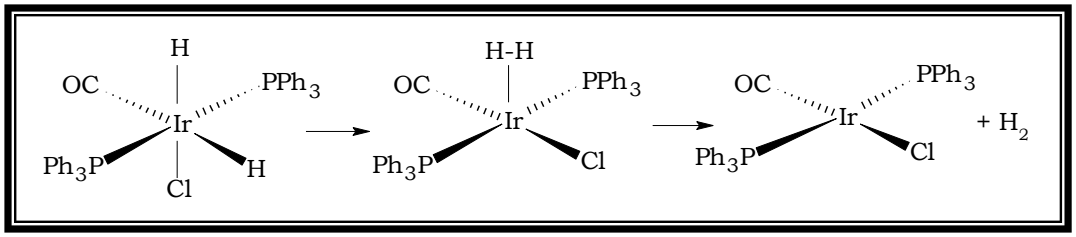

Figure 2.15 Reductive elimination (Cross, 1985:197)

Since electron-rich metal complexes favour oxidative addition, the reverse is true for reductive elimination. Reductive elimination involves the reduction of the metal centre by the two anionic fragments that are usually more electronegative than the metal centre. These reactions are therefore favoured by metal centres which are electron deficient. Electron deficiency can be accomplished by electron-withdrawing ligands, cationic charge(s), and/or coordinative unsaturated metal complexes.

2.4.2 MECHANISMS OF REDUCTIVE ELIMINATION

Four common reductive elimination reactions are shown in **Scheme 2.3**, where R is an alkyl or aryl group.

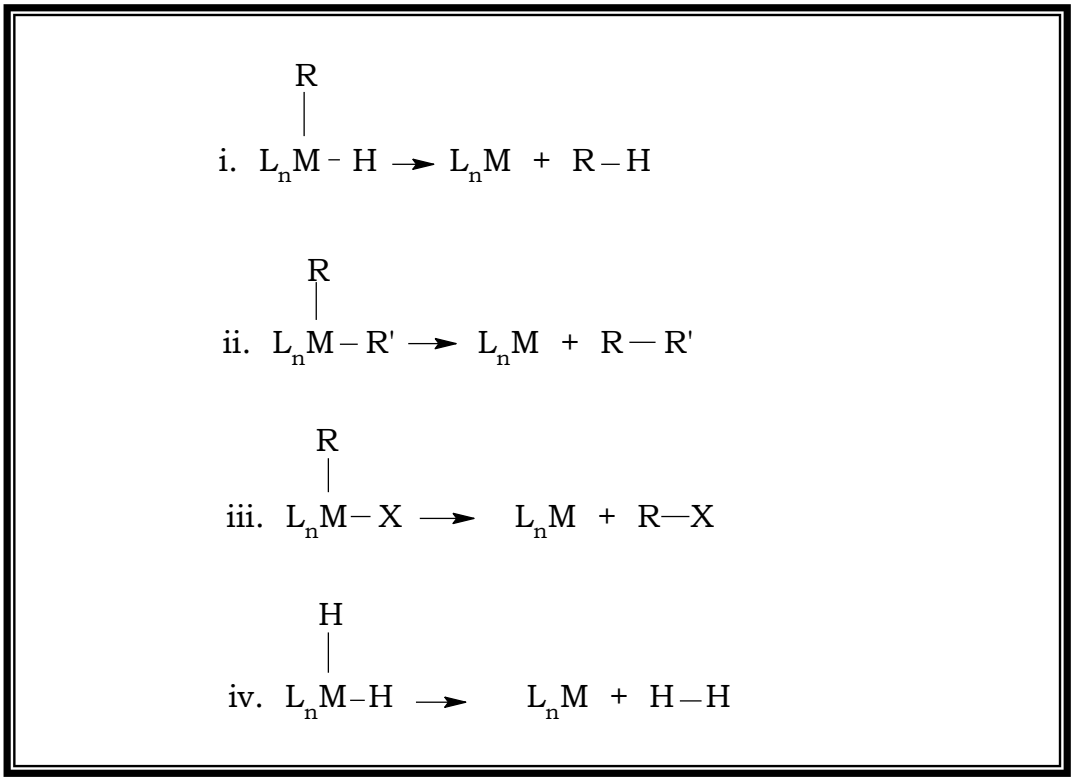

Scheme 2.3 Common reductive elimination mechanisms

The R-H elimination step in (i) represents the C-H bond formation which is an important step for many catalytic cycles. This type of elimination is usually very facile and often occurs rapidly and under mild conditions. The R-R' elimination step in (ii) represents C-C bond formation which is of fundamental importance to organic synthesis, while the reductive elimination of organohalides in (iii) frequently occurs as the last step of a sequence of reactions. Finally, the reductive elimination of molecular hydrogen in (iv) is observed for mono-, di- and polynuclear complexes. Either thermal or photochemical activation can initiate the loss of H_2.

Reductive elimination reactions are as mechanistically diverse as oxidative addition reactions (Deutsch and Eisenberg, 1988:1147). The most common types of reductive elimination reactions include intramolecular, mononuclear or 1,1-reductive eliminations and intermolecular, dinuclear or 1,2-reductive eliminations. Intra and intermolecular processes are distinguished by using isotopically labelled ligands and by observing the absence or the presence of crossover products. The absence of crossover implies intermolecular reductive elimination while the presence of crossover indicates that intramolecular reductive elimination occurred.

2.4.3 FACTORS INFLUENCING REDUCTIVE ELIMINATION

The following factors affect reductive elimination (Deutsch and Eisenberg, 1988:1147):

i. A *cis*-orientation between the two ligands being eliminated.

ii. The presence of bulky ancillary ligands is also vital, which contributes a thermodynamic driving force towards the elimination process. A metal complex should also be able to undergo a change of two units upon elimination, affording a product with considerable less intramolecular steric repulsion.

iii. The relatively high formal charge on the metal atom.

iv. The possible formation of an electronically stable product (L_nM).

The electronic stability of a complex L_nM usually depends on the electronic properties of the ligands, the coordination number as well as the geometry of the complex and the d electronic configuration of the metal ion. An example of a reductive elimination reaction is illustrated by square planar d^8 Pd(II) complexes (Deutsch and Eisenberg, 1988:1147). These organopalladium complexes undergo 1,1-reductive elimination with retention of configuration at the carbon bound to palladium; indicating the absence of a free-radical mechanism in these reactions. A concerted, thermal, 1,1-reductive elimination from a *cis*-square planar d^8 complex is formed.

2.5 CARBONYL INSERTION REACTIONS

In transition metal chemistry, CO insertion reactions may generally be defined as the insertion of CO between the metal and ligand R to form the acyl species as shown in **Eq.2.2** (Atwood, 1985: 113).

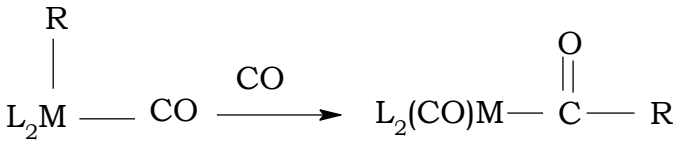

Eq.2.2

The transition state for CO insertion may be represented by a three-centre transition state as shown in **Figure 2.16**.

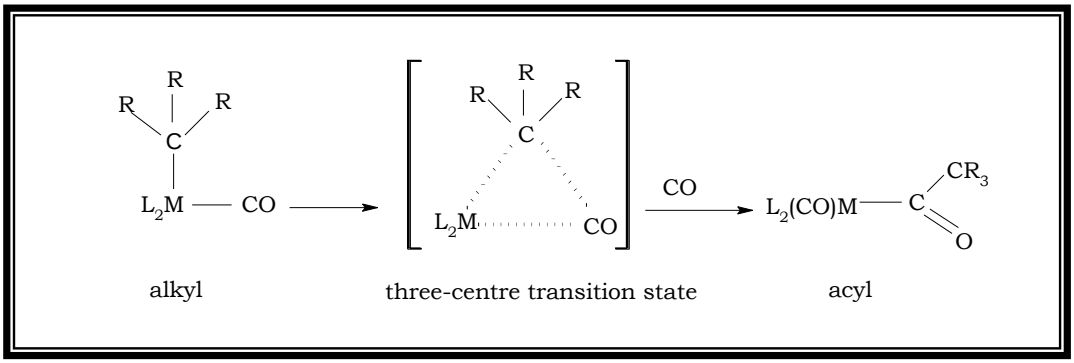

Figure 2.16 The transition state for CO insertion

An important aspect to take into account is the fact that the conversion of the alkyl to acyl species (**Figure 2.16**) for various transition metal complexes is also affected by the addition of ligands other than CO, such as tertiary phosphines, arsines, stibines and iodides. Carbonyl insertion (not indicating any specific mechanism) can proceed with or without external addition of another ligand. Reactions where no formal incoming ligand is involved in the CO insertion reaction follows a mechanism such as that in **Scheme 2.4** where k_2 represents the acyl formation step (Basson *et al.*, 1986:35).

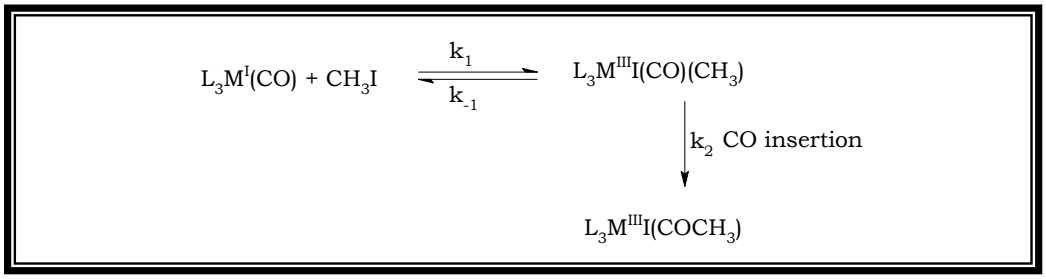

Scheme 2.4 Carbonyl insertion proceeding without a formal incoming ligand

Research has shown that solvents can play an important role in carbonyl insertion reactions. This was illustrated with the isolation of Rh(III) alkyl complexes after the oxidative addition of rhodium(I) complexes (**Eq 2.3**) of the type [Rh(cupf)(CO)(PR_3)] (R = *p*-Cl-Ph, Ph, *p*-MeO-Ph, Cy) (Basson *et al*, 1987:31) with iodomethane. This made it possible to selectively study the carbonyl insertion reactions that these alkyl complexes undergo, without interference from any initial oxidative addition steps:

$$[Rh(cupf)(CO)(CH_3)(PX_3)I] \underset{}{\overset{+ S}{\rightleftharpoons}} [Rh(cupf)(COCH_3)(PX_3)I]$$

(alkyl) (acyl)

Eq.2.3

The isolated alkyl complex such as [RhI(cupf)(CO)(CH_3)(PR_3)] was dissolved in pure solvents with different polarity and donocity properties. The results obtained from this study clearly showed a substantial increase in oxidative addition for a solvent such as acetonitrile compared to that of benzene.

2.5.1 FACTORS INFLUENCING CARBONYL INSERTION

2.5.1.1 Solvent Effects

CO insertion reactions are fairly dependent on solvent effects, which in some cases are quite large (Webb *et al*, 1986:345). Calderazzo and Cotton (1962:30) observed enhanced rates in polar, donating solvents, which they attributed to variations in the dielectric constant of the solvent. Two explanations were given for these observations:

i. Stabilisation of the transition state by solvation (especially when polar solvents are used)

ii. Direct attack of solvent (solvent with high donocity) at the metal centre which increases the electron density on the metal centre. Subsequently this leads to a decrease in M-R bond strength and in the process increases the migratory ability of the coordinated R group to the carbonyl.

Rate data can be interpreted when there are changes in kinetic order encountered, as for example, when alkyl complexes are treated with nucleophiles in various solvents. Butler *et al* (1967:2074) found that the rate of CO insertion of $[CpMo(CO)_3CH_3]$ is a linear function of $[PPh_3]$ in benzene but is independent of the amount of phosphine present in THF. In chloroform, both of these

types of behaviour are exhibited simultaneously by $[CpMo(CO)_3C_5H_5]$ (Craig and Green *et al.*, 1968:1978).

$$[Cp(CO)_3Mo(CH_3)] + PMePh_2 \xrightarrow{k} [Cp(CO)_2Mo(PMePh_2)COCH_3]$$

Eq.2.4

An example of the solvent effects on CO insertion for **Eq.2.4** is illustrated in **Table 2.3** where the solvents vary in donocity but not in their dielectric constant properties. In **Table 2.3** it is shown that despite the higher Lewis basicity of 2,5-Me_2THF (compared to THF), the conversion to the acyl species still proceeded more rapidly in THF. This observation was explained in terms of the larger steric demand of 2,5-Me_2THF in an associative step. The steric hindrance of the solvent thus leads to retardation in the formation of the solvent coordination intermediate, prior to the migration of the methyl group.

Table 2.3 Rate of CO insertion of **Eq 2.4** showing solvent dependence (Reichardt, 1979:186)

solvent	**10^4k,$M^{-1}s^{-1}$**
THF	1.73
3-MeTHF	1.86
2-MeTHF	1.95
2,5-Me_2THF	1.67

.

2.5.1.2 Ligand Effects

The effect of different ligands on the rate of carbonyl insertion was investigated by Anderson and Cross (1984:67) for the complex [PtCl(CO)Ph($PMePh_2$)] with Ph (which is *trans* to $PMePh_2$) as a migrating group (**Figure 2.17**). They found that phosphines with better electron donating properties favoured the formation of the halogen bridged acyl dimer.

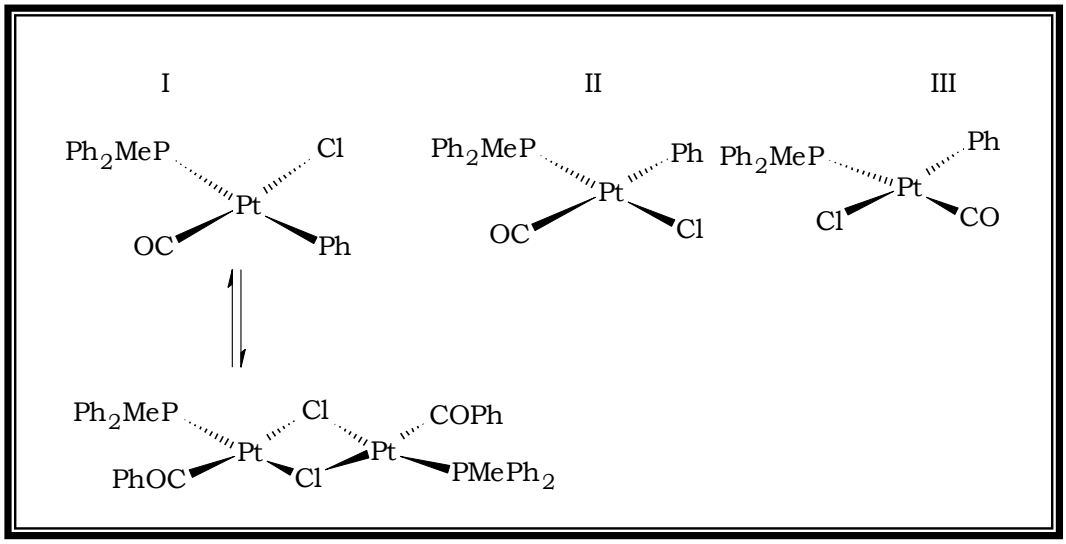

Figure 2.17 Selected formation of acyl complex in different isomers of [Pt(Cl(CO)Ph($PMePh_2$)] (Anderson and Cross, 1984:67)

In isomer (II) the migrating group (Ph) and CO are *trans* to one another making methyl migration impossible, since a *cis* configuration is needed. In isomer (III) the phenyl group is *trans* to Cl and is thus not labilised.

CHAPTER 3

SYNTHESIS AND CHARACTERISATION OF LIGANDS AND COMPLEXES

3.1 INTRODUCTION

The synthesis of rhodium organometallic complexes is covered in a large number of articles (Basson *et al*, 1984:167 and Basson *et al*, 1986:35). Many of these references involve the synthesis of [Rh(LL'-BID)(CO)(PPh_3)] (Basson *et al*, 1984:167) (where LL'-BID = monocharged bidentate ligands containing different donor atoms L and L') and other relevant complexes. These complexes were synthesised to study the electronic and steric influence of the different bidentate (LL') and monodentate ligands on the rate of substitution and oxidative addition reactions, as well as to evaluate the complexes as possible catalysts in organic synthesis. One of the complexes that were synthesised for this purpose and yielded surprising results was that of the [Rh(cupf)(CO)(PPh_3)] complex (Basson *et al*, 1987:31). Results obtained from this study indicated that this complex has the tendency to form a very stable 5-coordinated complex as was illustrated by the characterisation of [Rh(cupf)(CO)(PPh_3)$_2$].

Previously it was found that the addition of an excess of phosphine and phosphite ligand in cases such as [Rh(LL'-BID)(CO)(PX_3)] resulted in the substitution of the carbonyl ligand resulting in formation of the square planar [Rh(LL'-BID)(PX_3)$_2$) complexes such as [Rh(acac)(P(OPh_3))$_2$] (Leipoldt *et al*, 1984:L31) and [Rh(Tfaa)(P(OPh)$_3$)$_2$] (Van Zyl *et al.*, 1985:L1). The oxidative addition reaction between [Rh(cupf)(CO)(PPh_3)] and CH_3I also clearly indicated the participation of the five-coordinated complex, [Rh(cupf)(CO)(PPh_3)(S)] in the reaction process, confirming the formation of an important five-coordinated species for this reaction. Another interesting result from this study was the formation of a *cis*-[Rh(cupf)(CO)(PPh_3)(CH_3)(I)] complex compared to the *trans* final product for a large number of those complexes such as [Rh(ox)(CO)(PPh_3)(CH_3)(I)] (Van Aswegen *et al.*, 1991:369) and [Rh(dmavk)(CO)(PPh_3)(CH_3)(I)] (Damoense *et al.*, 1995:6).

This chapter deals firstly with the synthesis and characterisation of a new cupferron derivative ligand, CH_3cupf. It also illustrates the synthesis and identification of a number of new rhodium-cupferrate complexes and the oxidative addition of these complexes. The rhodium complexes were synthesised according to the well-known method shown in **Scheme 3.1**, which will be described in more detail in **Section 3.9**.

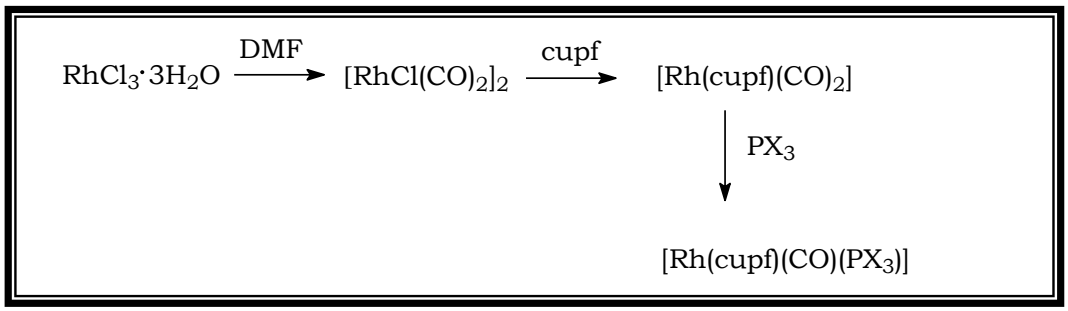

Scheme 3.1 Synthesis of [Rh(cupf)(CO)(PX_3)] complex (Goswami and Singh, 1980:83)

3.2 INSTRUMENTS AND CHEMICALS

Chemicals from Merck, Next Chimica and Aldrich were used without further purification. Organic solvents used were distilled prior to use and water was double distilled. Ammonia gas was used with extreme precautions in a hood. It is very poisonous by inhalation and ingestion and is also an irritant to the eyes and mucous membranes. Rhodium(III) trichloride (Next Chimica), 2-nitrotoluene (Merck), butyl nitrile (Merck), triphenyphosphine (Merck) and methyl iodide (Merck) were also used without further purification. Solid infrared spectra were collected in the range of 2300-550 cm^{-1}, and liquid infrared in the range 2100-1600 cm^{-1} using a Digilab Merlin 3.0 Spectrophotometer equipped with a temperature cell regulator (accurate within 0.3 ˚C). UV/Visible spectra were collected on a Varian Carey 50 double beam spectrophotometer equipped with temperature cell regulator (accurate within 0.1 ˚C). The ^{1}H-NMR spectra were obtained with a Bruker 300 MHz Spectrophotometer. All chemical shifts are

reported in parts ppm with (m) = multiplet, (t) = triplet, (d) = doublet and (s) = singlet.

3.3 SYNTHESIS OF THE CUPFERRATE LIGAND, CH_3cupf

It has already been mentioned in **Chapter 1** that cupferron is relatively stable at room temperature, both in solid and solution states, generating very little NO. N-nitroso-N-oxybenzenamine ammonium salts with -OMe, -Me, -H, -F, -Cl, -CF_3 and –SO_2Me substituents (**Figure 3.1**) at the *para* position of the phenyl ring constitute a new class of nitric oxide releasing compounds (Alexandru *et al.*, 1998:439). These compounds release NO *via* spontaneous dissociation during one electron oxidation. Electron withdrawing groups can increase the oxidation potential and make NO release easier. Recently, Alexandru *et al.* (1998:439) found that *ortho* substituted derivatives of cupferron are good NO donors both *in vitro* and *in vivo* positions.

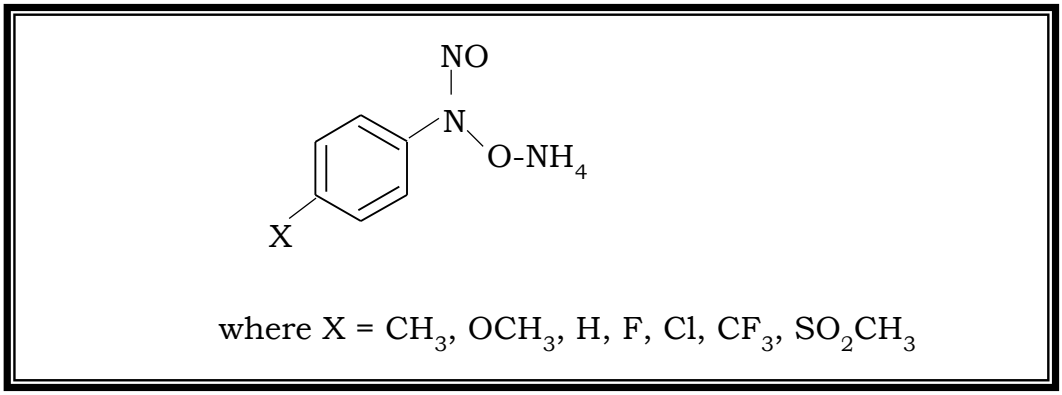

Figure 3.1 Cupferron derivatives

Several methods have been published for the preparation of N-nitroso-N-phenylhydroxylamine, its derivatives and its salts. In this case two of the methods have been attempted (**Scheme 3.2**) due to the fact that the first method did not give satisfactory results.

3.3.1 ATTEMPTED SYNTHESIS (Vogel, 1989:955)

Ammonium chloride solution (0.200 mol, 11.0 g), 2-nitrotoluene (0.100 mol, 13.7 g) and 500 ml of double distilled water was added to a 500 ml volumetric flask, equipped with a thermometer and mechanical stirrer. The mixture was vigorously stirred and zinc powder (0.200 mol, 13.1 g) was added in portions to the solution during the course of 20 minutes. The rate of addition was controlled to try and maintain the reaction temperature at 60-65 ºC, which proved to be difficult (**Section 3.9**). Stirring was continued for a further 15 minutes by which time the reduction was completed as indicated by a drop in reaction temperature. The hot mixture was filtered and washed with 50 ml hot water. The solution was then saturated with 75 g of sodium chloride and cooled on an ice bath for 2 hours. Pale yellow crystals were expected to crystallise, but no product was obtained after cooling the solution.

3.3.2 METHOD TWO (Alexandru *et al.* 1998:439)

A solution containing 2-nitrotoluene (0.200 mol, 27.4 g) ammonium chloride (0.400mol, 22.0 g) and 500 ml double-distilled

water was mechanically stirred. The temperature was then raised to 60-70 °C and zinc powder (0.400 mol, 26.2 g) was added gradually with vigorous mechanical stirring so as to maintain the temperature around 70 °C. The reaction was monitored with thin layer chromatography (TLC) using benzene:acetone (80:20%) mixture. The plate was examined under ultraviolet light every one hour and spots were identified by comparison of their positions with those of the starting material. At the end two spots were clearly identified indicative of the starting material that has been changed to product. The mixture was then cooled to 35 °C and suction-filtered. The solid residue was thoroughly washed with four 60 ml portions of diethyl ether. The ether portion was saved and used for extracting the required product. The combined extracts were dried over sodium sulphate at a temperature of 0 °C using an ice-salt bath. A vigorous stream of gaseous ammonia was bubbled into the ether solution for 5-10 minutes. A slight excess of n-butyl nitrite (0.300 mol, 30.8 g) was added in small portions for approximately 15 minutes while maintaining the temperature at 0 °C and the flow of ammonia gas. The brownish-yellow product was precipitated and collected after been kept at 0 °C for at least 2 hours. It was repeatedly washed with diethyl ether and dried at room temperature.

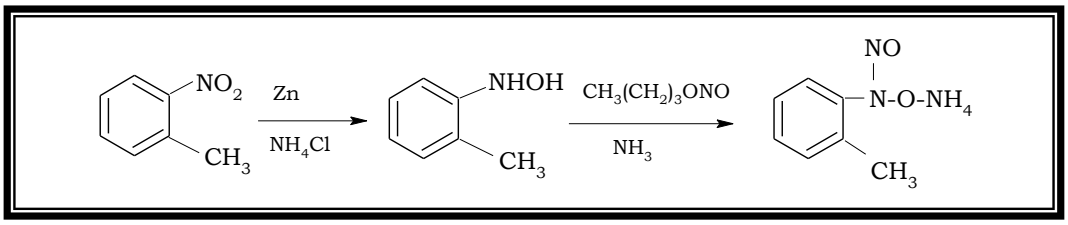

Scheme 3.2 Reaction procedure for the synthesis of CH_3cupf

Yield: 66%

^{1}H-NMR in DMSO: δ 7.3 (4H, d, ar,), δ 2.2 (3H, s, CH_3), (**Figure 3.2**)

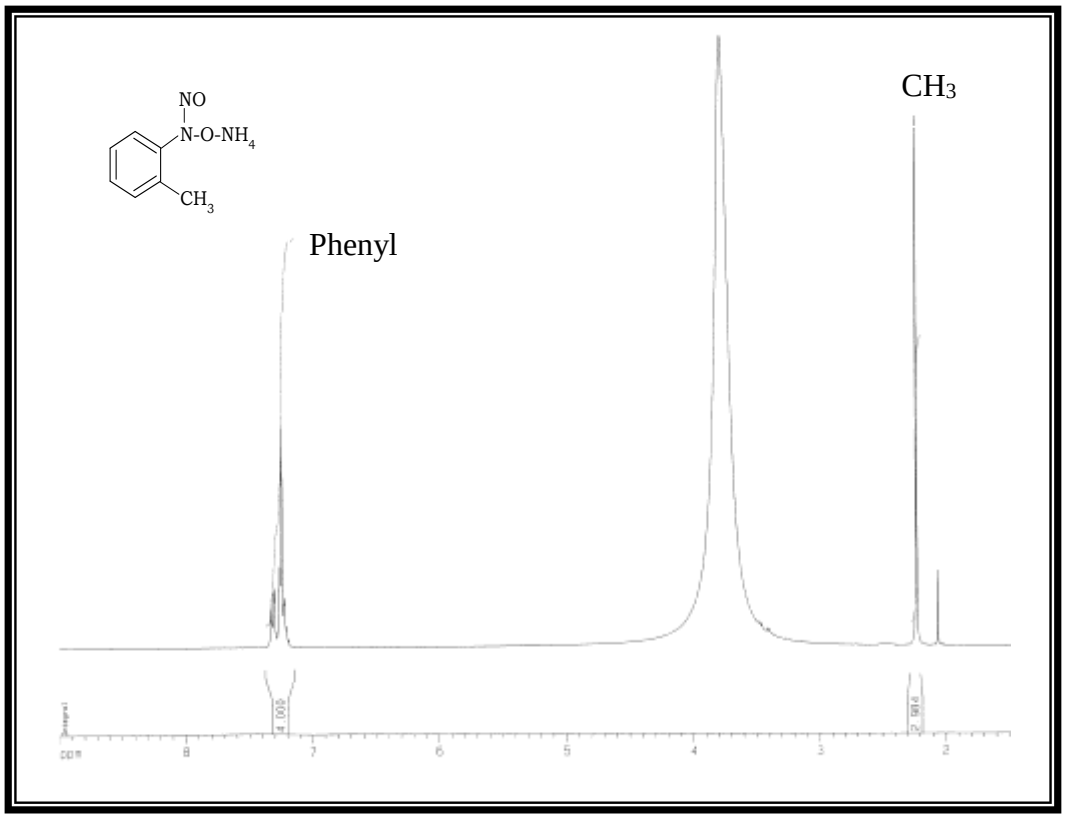

Figure 3.2 ^{1}H NMR spectrum of the CH_3cupf ligand

3.4 SYNTHESIS OF [Rh(CH_3cupf)$(CO)_2$] (Goswani and Singh, 1980:83)

$RhCl_3 \cdot 3H_2O$ (0.300 g, 1.12 mmol) was dissolved in 25 ml DMF. The solution was refluxed for approximately 20 minutes during which time the solution changed colour to give the light orange indicating the presence of the ($[RhCl(CO)_2]_2$) complex. The solution was

allowed to cool to room temperature and poured into a small beaker. Portions of the cupferrate (0.190 g, 1.26 mmol) were added with continuous stirring. Ice water was then added drop wise while the solution was continuously stirred with a glass rod. The brown [Rh(CH_3cupf)($CO)_2$] complex precipitated from the solution.

Yield: 72%

^{1}H-NMR in acetone : δ 7.6 (5H, m), δ 2.3 (3H, s) (**Figure 3.3**)

IR: ν(CO) = 2063, 2087 cm^{-1} (**Figure 3.4**)

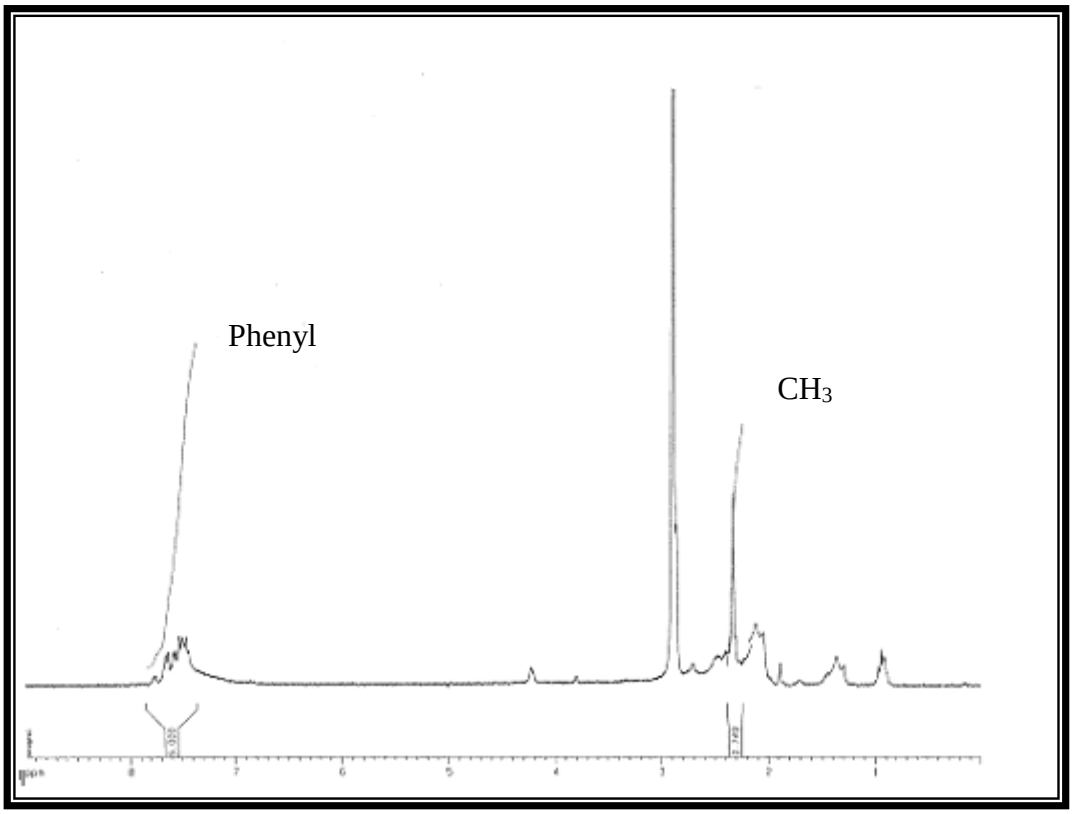

Figure 3.3 ^{1}H NMR spectrum of [Rh(CH_3cupf)($CO)_2$]

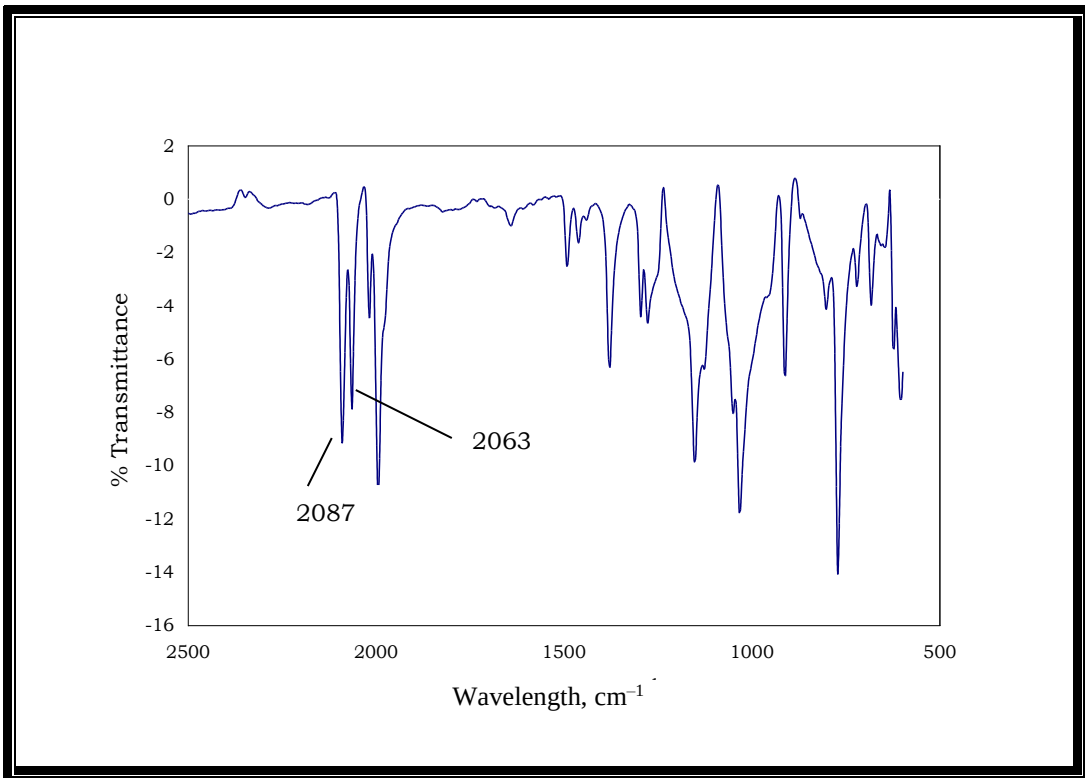

Figure 3.4 IR spectrum of [Rh(CH_3cupf)($CO)_2$]

3.5 SYNTHESIS OF [Rh(CH_3cupf)(CO)(PPh_3)]

[Rh(CH_3cupf)($CO)_2$] (0.252 g, 0.814 mmol) was dissolved in 15 ml acetone. Small portions of PPh_3 (0.235 g, 0.895 mmol) were added to the acetone solution with continuous stirring. Ice water was added drop wise while the solution was continuously stirred using a glass rod. A yellow product precipitated from the solution. The solution was stirred for another 30 minutes, filtered and then dried at room temperature.

Yield: 57%

^{1}H-NMR in acetone: δ 7.5 (m, 20H), δ 2.1 (s, 3H) (**Figure 3.5**)

IR: ν(CO)= 1982 cm $^{-1}$ (**Figure 3.6**)

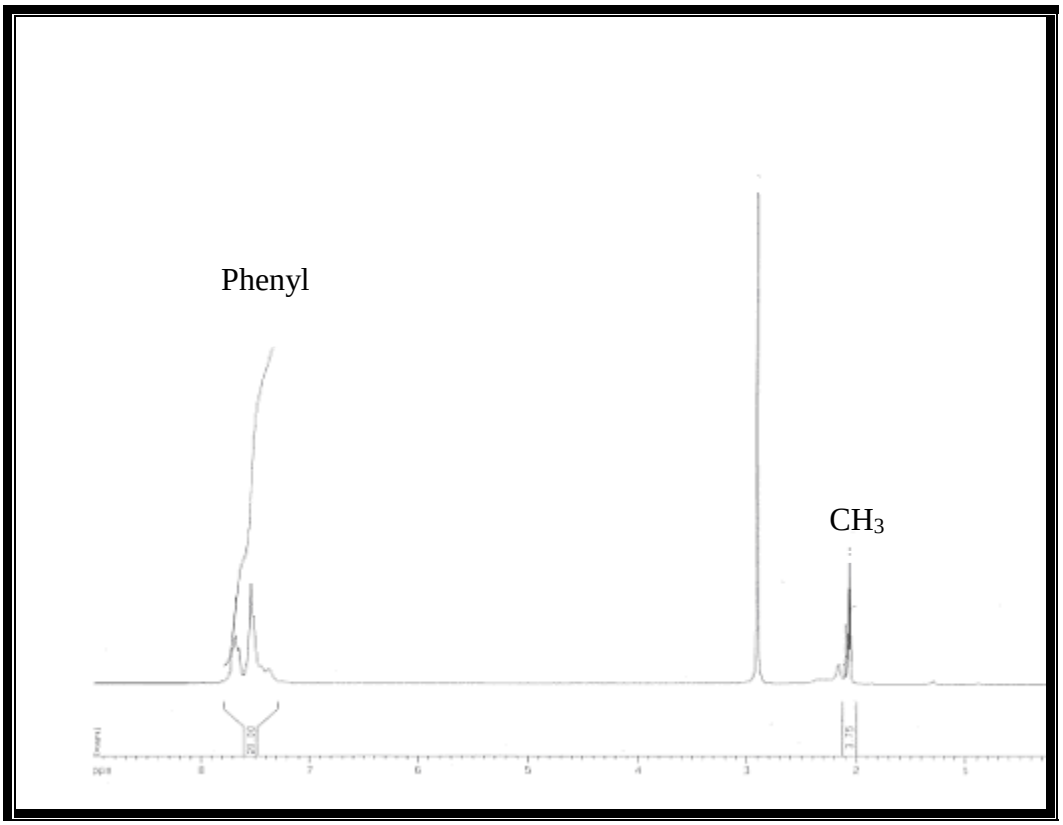

Figure 3.5 ^{1}H NMR spectrum of [Rh(CH_3cupf)(CO)(PPh_3)]

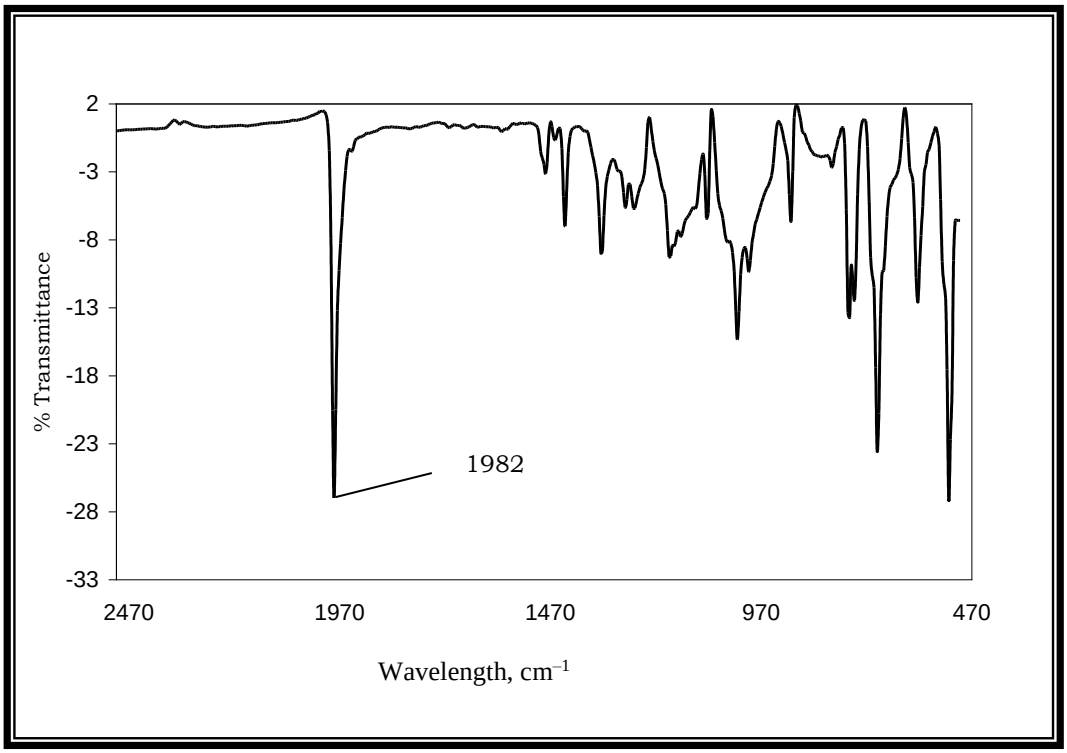

Figure 3.6 IR spectrum of [Rh(CH_3cupf)(CO)(PPh_3)]

3.6 SYNTHESIS OF [Rh(CH_3cupf)(CO)(P(*p*-$MeOC_6H_4$)$_3$)]

[Rh(CH_3cupf)$(CO)_2$] (0.148 g, 0.478 mmol) was dissolved in 15 ml acetone. Small portions of P(*p*-$MeOC_6H_4$)$_3$ (0.185 g, 0.526 mmol) were added to the acetone solution with continuous stirring. Ice water was added drop wise while the solution was continuously stirred using a glass rod. A yellow product precipitated from the solution. The solution was stirred for another 30 minutes, filtered and then dried.

Yield: 36%

^{1}H-NMR in acetone: δ 7.2 (m, 8H), δ 7.6 (m, 8H), δ 3.6 (s, 9H), δ 2.2 (s, 3H) (**Figure 3.7**)

IR: ν(CO)= 1965 cm $^{-1}$(**Figure 3.8**)

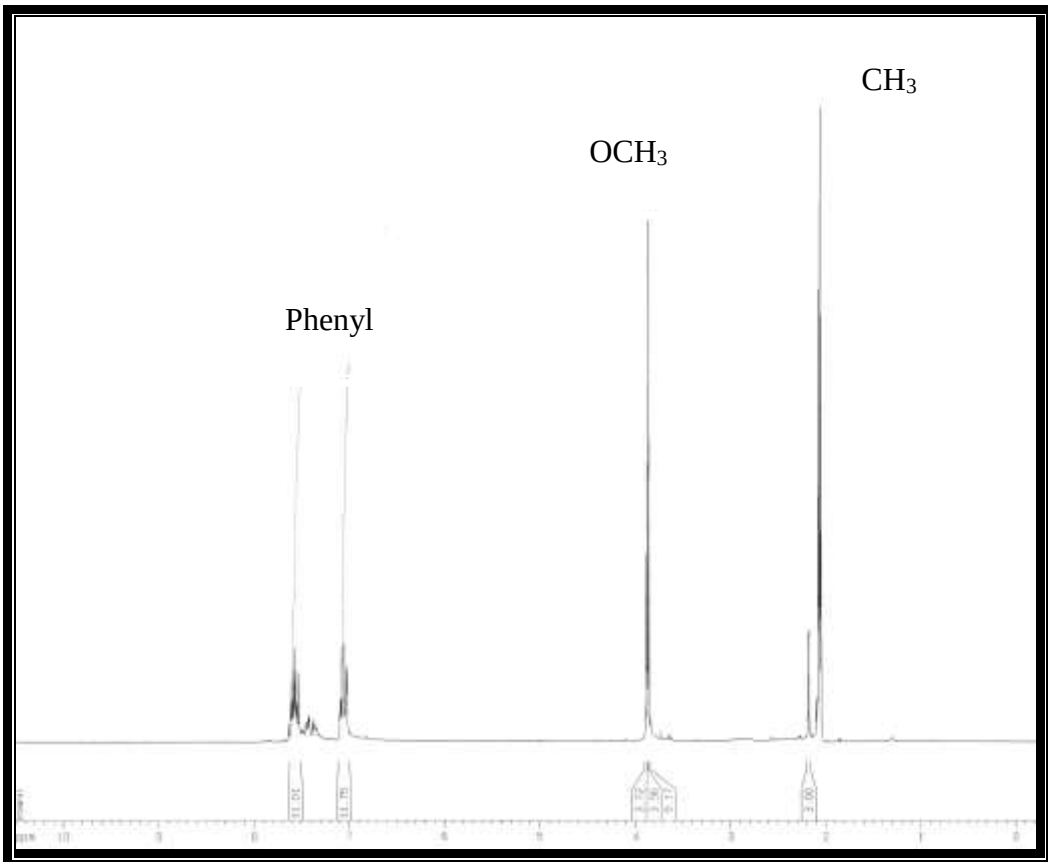

Figure 3.7 ^{1}H NMR spectrum of [Rh(CH_3cupf)(CO)(P(*p*-$MeOC_6H_4$)$_3$)]

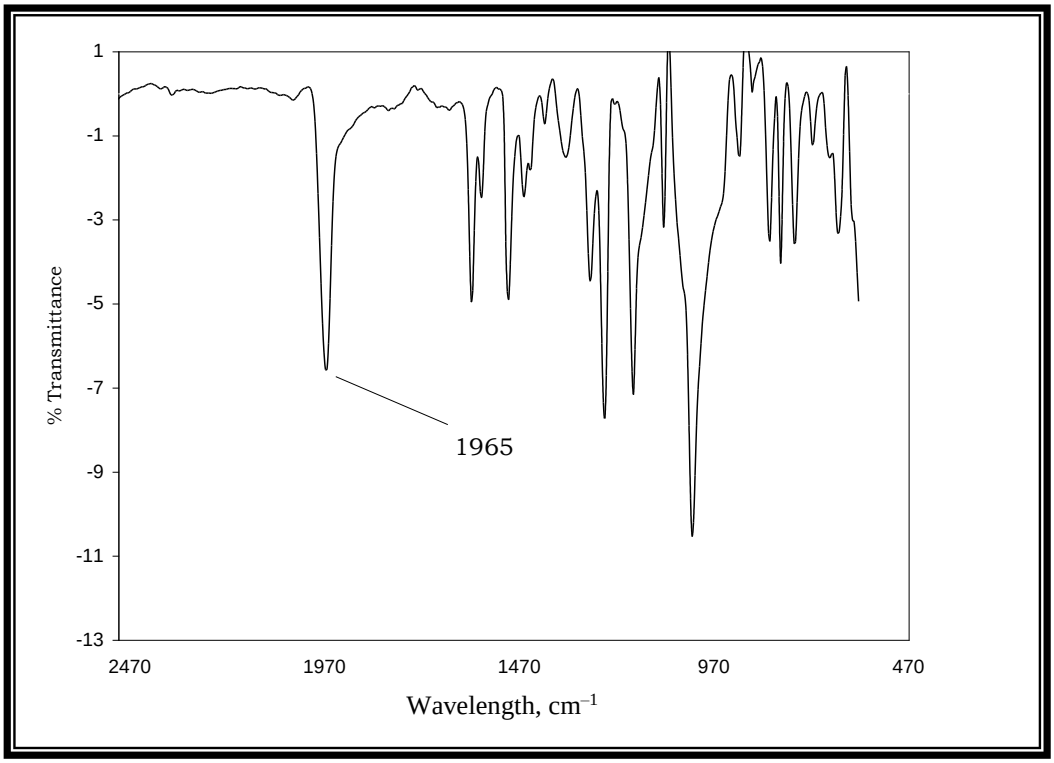

Figure 3.8 IR spectrum of [Rh(CH_3cupf)(CO)(P(*p*-$MeOC_6H_4)_3$]

3.7 SYNTHESIS OF [Rh(CH_3cupf)(CO)[(P(*o*-Tol)$_3$]

[Rh(CH_3cupf)$(CO)_2$] (0.233 g, 0.750 mmol) was dissolved in 15 ml acetone. Small portions of P(*o*-Tol)$_3$ (0.251 g, 0.826 mmol) were added to the acetone solution with continuous stirring. Ice water was added drop wise while the solution was continuously stirred using a glass rod. A yellow product precipitated from the solution. The solution was stirred further for 30 minutes, filtered and then dried.

Yield: 57%

^{1}H-NMR in acetone: δ 7.3 (m, 8H), δ 7.4 (m, 4H), δ 7.9 (m, 4H), δ 2.4 (m, 12H) (**Figure 3.9**)

IR: ν(CO)= 1970 cm $^{-1}$(**Figure 3.10**)

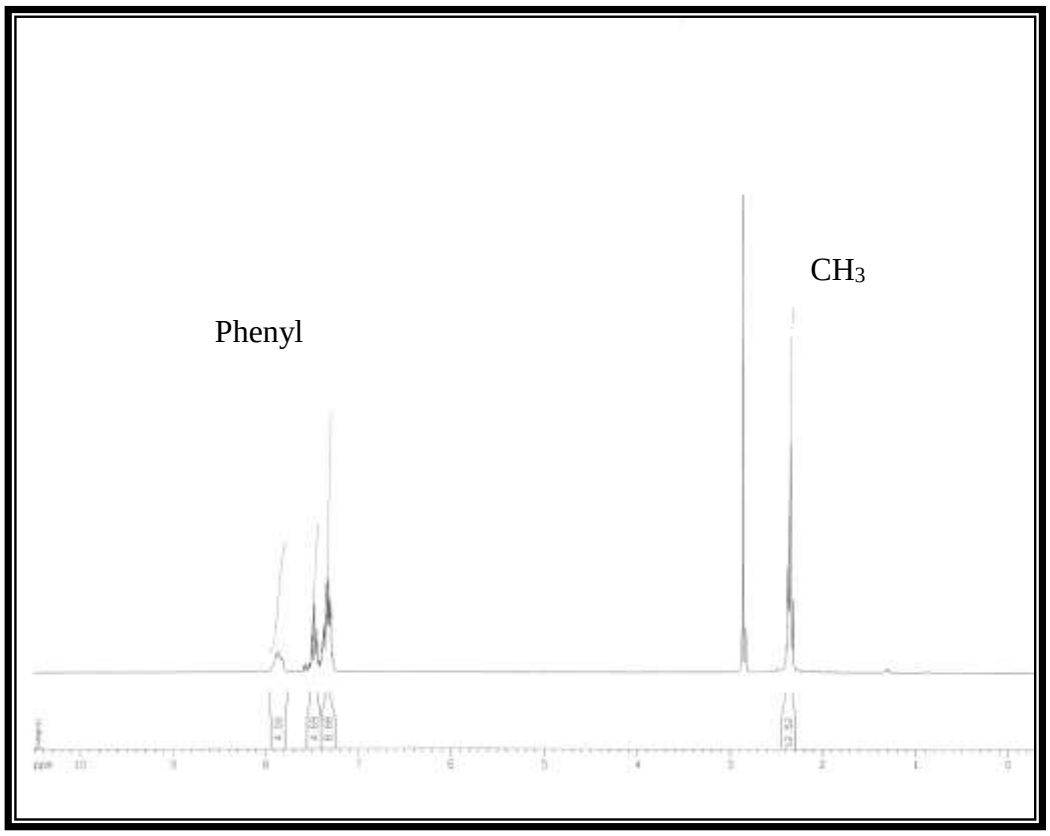

Figure 3.9 ^{1}H NMR spectrum of [Rh(CH_3cupf)(CO)(P(*o*-Tol)$_3$)]

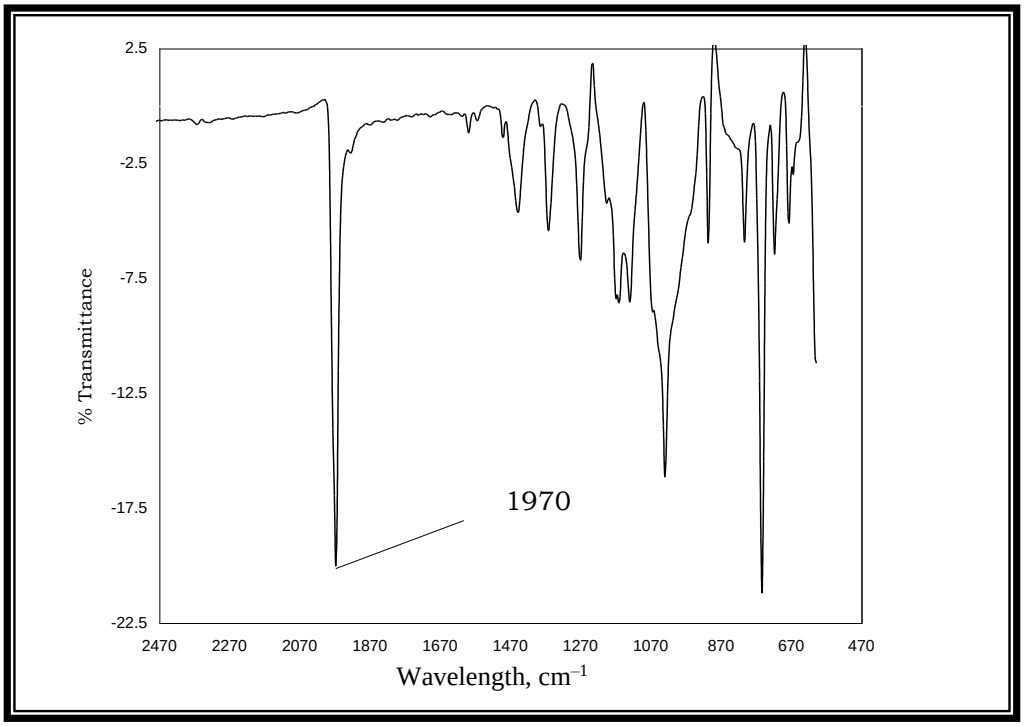

Figure 3.10 IR spectrum of [Rh(CH_3cupf)(CO)(P(*o*-Tol)$_3$]

3.8 SYNTHESIS OF [Rh(CH_3cupf)(CO)(P(*p*-Tol)$_3$]

[Rh(CH_3cupf)$(CO)_2$] (0.118 g, 0.379 mmol) was dissolved in 15 ml acetone. Small portions of P(*p*-Tol)$_3$(0.127 g, 0.417 mmol) were added to the acetone solution with continuous stirring. Ice water was added drop wise while the solution was continuously stirred using a glass rod. A yellow product precipitated from the solution. The solution was stirred further for 30 minutes, filtered and then dried.

Yield: 32%

H-NMR: δ 7.3 (m, 8H), δ 7.5 (m, 8H), δ 2.4 (s, 3H), (**Figure 3.11**)

IR: ν(CO)= 1969 cm^{-1} (**Figure 3.12**)

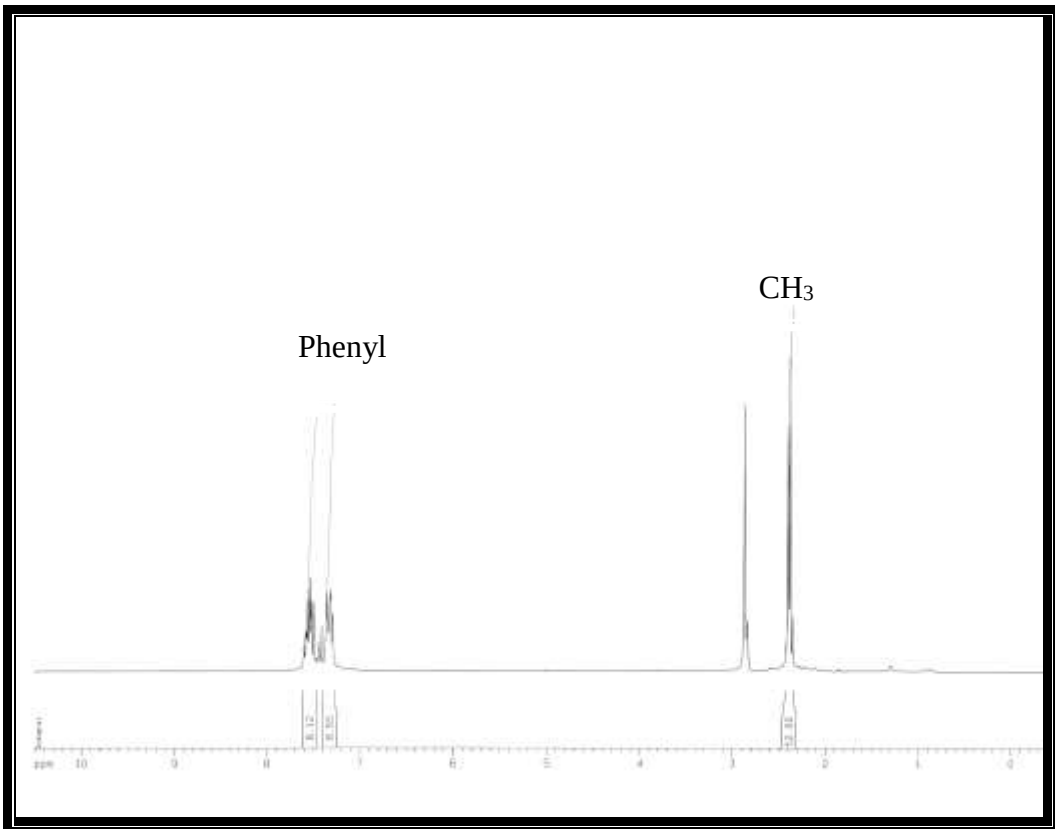

Figure 3.11 ^{1}H NMR spectrum of [Rh(CH_3cupf)(CO)(P(*p*-Tol)$_3$]

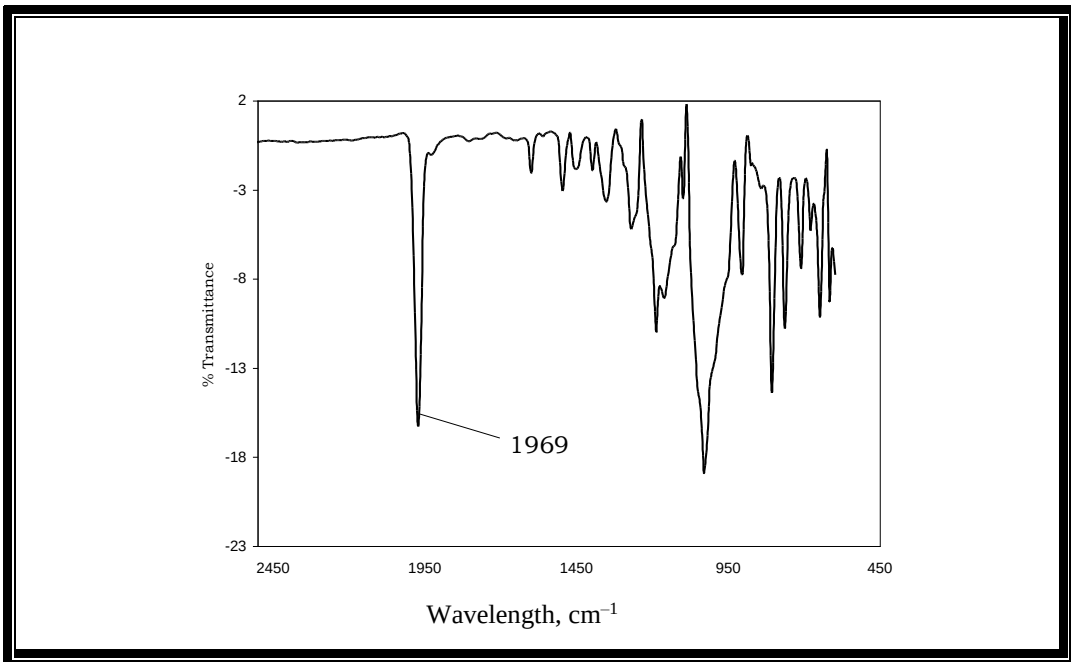

Figure 3.12 IR spectrum of [Rh(CH_3cupf)(CO)(P(*p*-Tol)$_3$]

3.9 SYNTHESIS OF [Rh(CH_3cupf)(CO)(PCy_3)]

[Rh(CH_3cupf)$(CO)_2$] (0.201 g, 0.648 mmol) was dissolved in 15 ml acetone. Small portions of PCy_3 (0.200 g, 0.713 mmol) were added to the acetone solution with continuous stirring. Ice water was added drop wise while the solution was continuously stirred using a glass rod. A brown-yellowish product precipitated from the solution. The solution was stirred further for 30 minutes, filtered and then dried.

Yield: 53%

H-NMR: δ 7.5 (m, 4H), δ 2.3 (s, 3H), δ 1.3 (m, 10H), δ 1.7 (d, 16H), δ 2.1 (s, 4H) (**Figure 3.13**)

IR: ν(CO)= 1956 cm^{-1}(**Figure 3.14**)

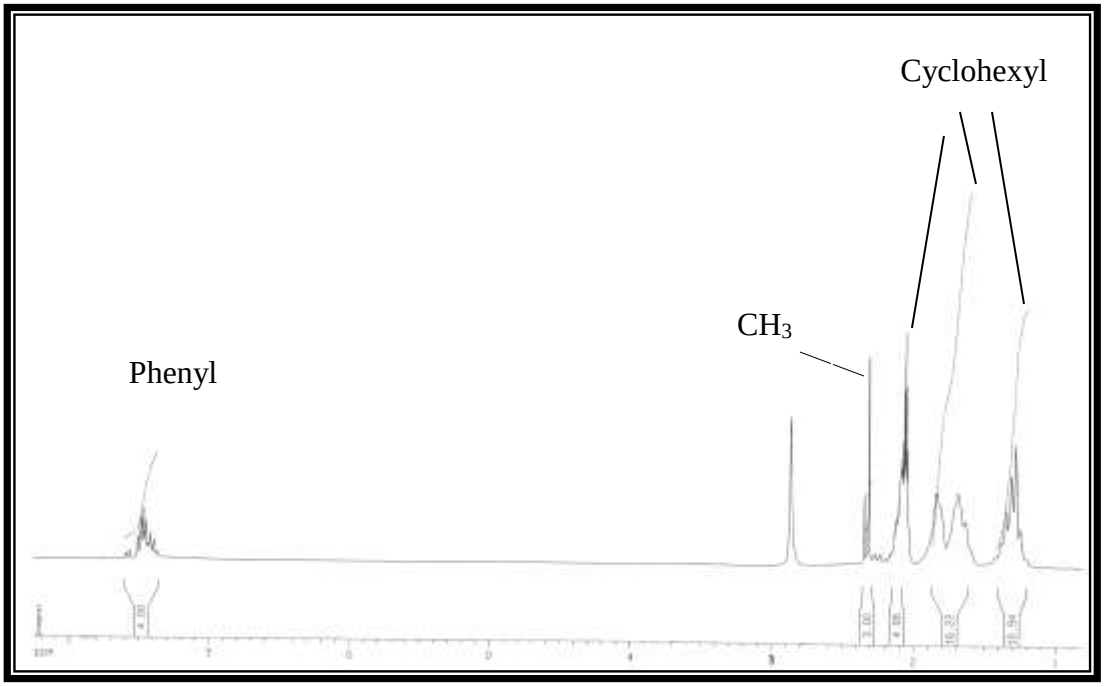

Figure 3.13 ^{1}H NMR spectrum of [Rh(CH_3cupf)(CO)(PCy_3)]

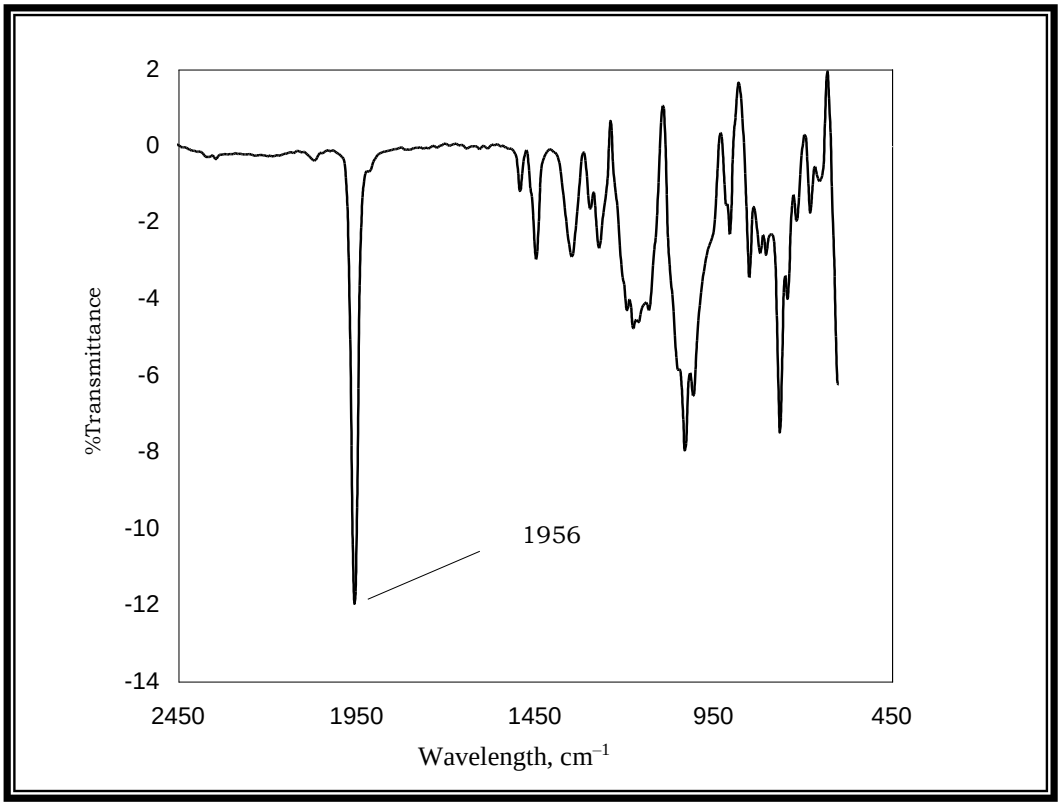

Figure 3.14 IR spectrum of [Rh(CH_3cupf)(CO)(PCy_3)]

To check the presence of [Rh(CH_3cupf)($COCH_3$)(PPh_3)I] in a solution, IR measurement was done on the reaction between [Rh(CH_3cupf)(CO)(PPh_3)] and excess amount of iodomethane. The result is shown in **Figure 3.15**.

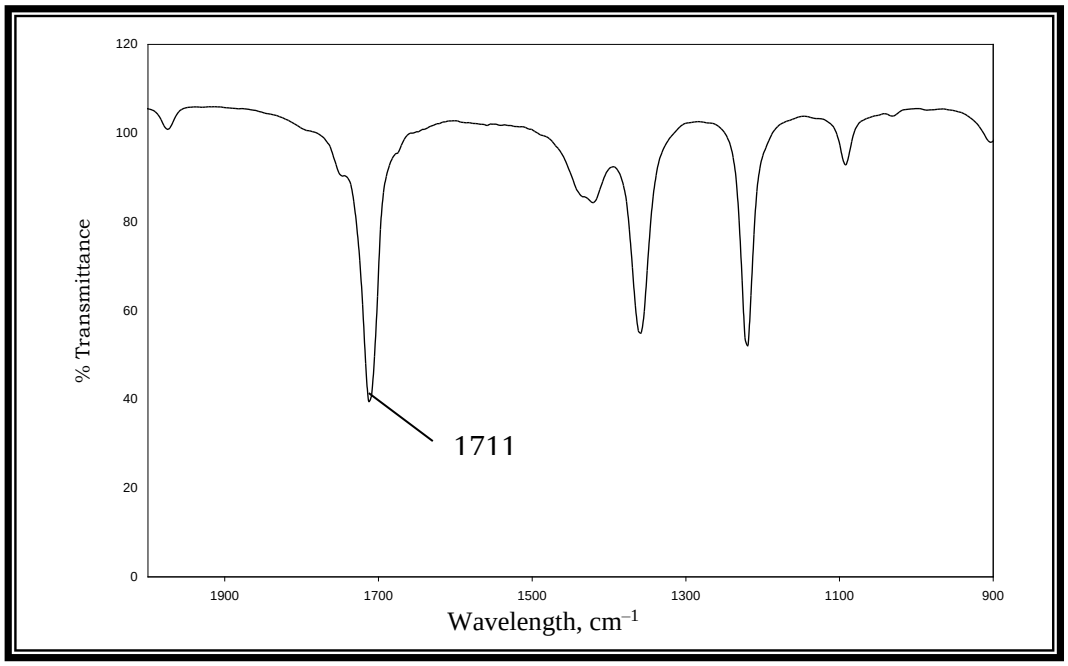

Figure 3.15 IR spectrum of [Rh(CH_3cupf)($COCH_3$)(PPh_3)I]

3.10 DISCUSSION

One of the main aims of this study was to synthesis the methyl substituted cupferron, CH_3cupf. For this synthesis two different methods were employed. The first method required, as a first step, the synthesis of the 2-methyl phenylhydroxylamine and in the next step, the formation of the methylcupferrate ligand. The synthesis

of the ligand using the first method proved to be less successful due to a number of experimental difficulties.

The first drawback of this synthesis is that during the synthesis the temperature of the mixture never reached 60-65 °C. At 50-55 °C, the maximum temperature obtained during the process, the yield was about 17%, which was too low to yield a substantial amount of the final product.

The biggest disadvantage of this method is that the pale yellow crystals of phenylhydroxylamine decompose rapidly upon storage and they need to be used immediately after synthesised.

The second method is a much more simplified version of the first method and saved a great deal of time and effort. This method is a well-known procedure for the synthesis of cupferron and its different derivatives without requiring of the synthesis of phenylhydroxylamine as an intermediate product. The final product was identified using ^{1}H-NMR (**Figure 3.2**). The phenyl protons (aromatic hydrogens) resonate as a doublet at δ 7.3 ppm. The singlet at δ 2.2 ppm was assigned to methyl protons. This method is also very applicable for most of the nitro derivatives that have a melting point above 85 °C or a very low solubility in water.

N-hydroxy-N-nitrosamines such as cupferron and its derivatives are usually prepared by the nitrosation of the corresponding N-

hydroxyamines. Hydroxyamines are readily obtained from the reduction of the corresponding nitrobenzenes. **Scheme 3.2** in **Section 3.4** illustrates the typical reactions involved in the synthesis of the methylcupferrate ligand. It is a general procedure for the synthesis of cupferron and its derivatives.

The initial step in the preparation of the rhodium complexes involve the reduction of Rh(III) to the Rh(I) with DMF. In this process the $[RhCl(CO)_2]_2$ dimer complex is formed *in situ*.

$$RhCl_3 \cdot 3H_2O \longrightarrow [Rh(CO)Cl_2]_2 + COCl_2 + H_2O$$

Eq.3.1

The next step involve the addition of the cupferrate ligand which reacts with the dimer complex to yield $[Rh(CH_3cupf)(CO)_2]$ (**Eq.3.2**).

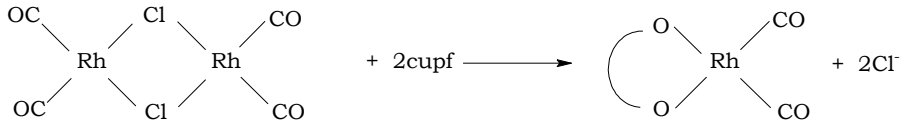

Eq.3.2

The final step in the synthetic process involves the substitution of one of the carbonyl groups with the addition of a phosphine ligand.

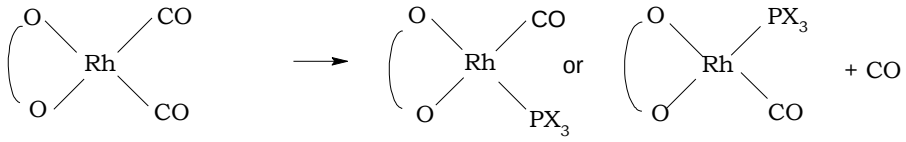

Eq.3.3

The IR spectrum of [Rh(CH_3cupf)$(CO)_2$] clearly shows two prominent ν(CO) stretching frequencies at 2063 and 2087 cm^{-1} (**Figure 3.4**). Fessahaye (2004) confirmed the formation of the dicarbonyl [Rh(cupf)$(CO)_2$] complex observing CO stretching frequencies for two peaks at 2009 and 2087 cm^{-1}. In contrast only one ν(CO) stretching frequency was obtained for all the monocarbonyl complexes confirming the substitution of one of the carbonyl ligands with addition of phosphine (**Figure 3.6, 3.8, 3.10, 3.12 and 3.14**). The [Rh(CH_3cupf)(CO)(PPh_3)] complex has a ν(CO) at 1982 cm^{-1} while [Rh(CH_3cupf)(CO)(P(*p*-Tol)$_3$)] has a ν(CO) at 1970 cm^{-1}. **Figure 3.15** also confirms the formation of an acyl peak at 1711 cm^{-1}. A summary of the physical data of all the [Rh(CH_3cupf)(CO)(PX_3)] complexes is given in **Table 3.1**.

Table 3.1 Summary of the physical data of the different [Rh(CH_3cupf)(CO)(PX_3)] complexes prepared in this study

complex	**ν(CO) /cm^{-1}**	**pK_a**	**chemical shifts (Ph protons)/ ppm**	**chemical shifts(Me protons)/ ppm**	**Figure**
A	1982	2.73	7.5	2.1	**3.5**
B	1970		7.3 and 7.5	2.4	**3.11**
C	1965	3.08	7.3, 7.4 and 7.9	2.4	**3.9**
D	1964	4.57	7.5	2.2, 3.6(MeO protons)	**3.7**
E	1954	9.65	7.5(Ph), 1.3, 1.7 and 1.2 (cyclohexyl protons)	2.3	**3.13**

Where A = [Rh(CH_3cupf)(CO)(PPh_3)]

B = [Rh(CH_3cupf)(CO)(P(*p*-Tol)$_3$)]

C = [Rh(CH_3cupf)(CO)(P(*o*-Tol)$_3$)]

D = [Rh(CH_3cupf)(CO)(P(*p*-MeOPh_3))]

E = [Rh(CH_3cupf)(CO)(PCy_3)]

The pK_a values of the phosphines are frequently used as an index of basicity and are proportional to the electron donating ability of the phosphine. According to **Table 3.1**, pK_a values for the different phosphine ligands increase from PPh_3 to PCy_3 which indicates that there is an increase in electron donating capability (strong basicity) of the substituent on the tertiary phosphine from PPh_3 to PCy_3. This implies that the phosphine ligand with better electron donating abilities, illustrated by higher pK_a values, increase the electron density on the metal centre. The metal centre subsequently reduces the electron density with π-back donation

via the π*-orbitals of the carbonyl ligand. The resulting effect is an increase in the M-CO bond order and a decrease in the CO bond order, as indicated by the lower ν(CO) stretching frequencies. However, electron withdrawing substituents will also decrease the σ-donating ability of the tertiary phosphine, implicating less electron density on the metal centre available for π-back bonding to the carbonyl which also lead to an increase in ν(CO). Hence the following decreasing order in ν(CO) was observed for the different phosphine ligands used in this study:

$$PPh_3 > P(p\text{-}Toly)_3 > P(o\text{-}Toly) > P(p\text{-}MeOC_6H_4)_3 > P(Cy_3)$$

The results obtained from the synthesis and characterisation of these new complexes from this study can be compared with the results obtained by Basson *et al* (1987:31). The [Rh(cupf)(CO)(P(*o*-Tol)$_3$)] has a ν(CO) at 1971 cm^{-1} while [Rh(CH_3cupf)(CO)(P(*o*-Tol)$_3$)] has a ν(CO) at 1965 cm^{-1}. **Table 3.2** shows IR values for some of the [Rh(cupf)(CO)(PX_3)] complexes.

Table 3.2 Summary of carbonyl stretching frequencies for some of the [Rh(LL)(CO)(PX_3)] complexes.

Complex	**ν(CO)/cm^{-1}**	
	cupf (Basson *et al*, 1987:31)	CH_3cupf
[Rh(LL')(CO)(PPh_3)]	1982	1982
[Rh(LL')(CO)(P(*o*-Tol)$_3$)]	1971	1965
[Rh(LL')(CO)(P(*p*-MeOPh)$_3$)]	1971	1964
[Rh(LL')(CO)($AsPh_3$)]	1978	1976

The sensitivity of the ν(CO) for changes in the complex environment is clearly illustrated by the comparison of the data obtained from these studies (see **Table 3.2**). The addition of the methyl group to the cupferron ligand lowers in general the ν(CO) for the different complexes. The shifting of the ν(CO) for [Rh(cupf)(CO)(P(*o*-Tol)$_3$)] from 1971 cm^{-1} to 1965 cm^{-1} for [Rh(CH_3cupf)(CO)(P(*o*-Tol)$_3$)] can be attributed to the fact that the methyl substituent on the phenyl ring is capable of donating electrons better than the phenyl ring in cupferron which results in an increase in π-back donation from the rhodium metal to carbonyl group. This in turn increases the M-C bond and decreases the CO bond which is responsible for the decrease in ν(CO).

The square planar [Rh(LL'-BID)(CO)(PPh_3)] complexes (LL' = monoanionic bidentate ligand with different donor atoms L and L')

are formed by substituting one CO ligand in the parent [Rh(LL'-BID)$(CO)_2$] complexes. In general, replacement of one CO ligand from the parent complex may lead to the formation of two isomeric monocarbonyl complexes (Trzeciak and Ziolkowski, 1985:15). If the difference in the donor/acceptor properties of the donor atoms L and L' is large enough (e.g. N and O atoms), NMR studies of reaction mixtures revealed high selectivity of the carbonyl group replacement (Roodt and Steyn, 2000:1). If the donor capabilities of L and L' are similar, isomers in **Figure 3.16** are formed in comparable ratios (Roodt and Steyn, 2000:1).

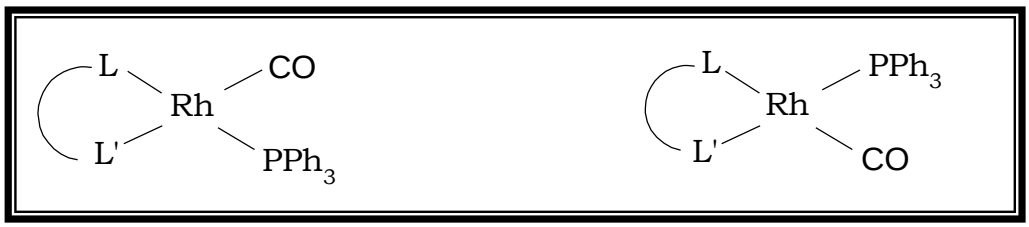

Figure 3.16 Possible isomer formations during the substitution reaction between [Rh(LL')$(CO)_2$] and PPh_3

The fact that only one CO group of the parent complex [Rh(cupf)$(CO)_2$] could be replaced by PPh_3, makes it possible to compare the relative *trans*-influence of the cupferrate oxygen atoms with those results of similar formulated complexes, [Rh(LL')(CO)(PPh_3)] (LL' = ligands such as β-ketones) (Basson *et al.*, 1986:L45). The order of *trans*-influence according to Rh-P bond distance in the above complexes, was found to be S > N > O. The fact that the CO group *trans* to nitroso group in [Rh(cupf)$(CO)_2$] was substituted by PPh_3 (Basson *et al.*, 1986:L45), shows that the

nitroso oxygen atom of the cupferrate ligand has the greater *trans*-influence. This also implies that the oxygen atom nearest to the phenyl ring is more electron deficient, thus exerts a smaller *trans* influence compared to the other oxygen atom. A Similar argument will also apply to the [Rh(CH_3cupf)(CO)(PPh_3)] complex. It is anticipated that the methyl group present in the CH_3cupf ligand would not alter the *trans*-influence significantly, resulting in a comparable *trans*-influence to that of the cupferrate ligand.

Comparing the cupferrate and methylcupferrate ligands for possible steric differences, the methyl group in CH_3cupf may increase the steric properties of the new ligand which can influence the substitution pattern of the phosphine ligand. For example, the unexpected substitution pattern observed for the [Rh(macsm)(CO)(PPh_3)] and [Rh(cacsm)(CO)(PPh_3)] complexes (CO group *trans* to the nitrogen atom being substituted) was attributed to the much larger steric demand of methyl and cyclohexyl groups on the nitrogen atom in the macsm and cacsm ligands (Roodt and Steyn, 2000:1). It was concluded that the substitution mode observed was sterically controlled rather than electronically controlled. Substitution patterns obtained which are also contrary to that expected with regard to the *trans*-effect were found in [Rh(TFHD)(CO)(PPh_3)] (Steynberg *et al.*, 1987:33), [Rh(TFDMAA)(CO)(PPh_3)] (Leipoldt *et al.*, 1983:85) and [Rh(TFTMAA)(CO)(PPh_3)] (Leipoldt *et al.*, 1986:L3) complexes (**Figure 3.17**).

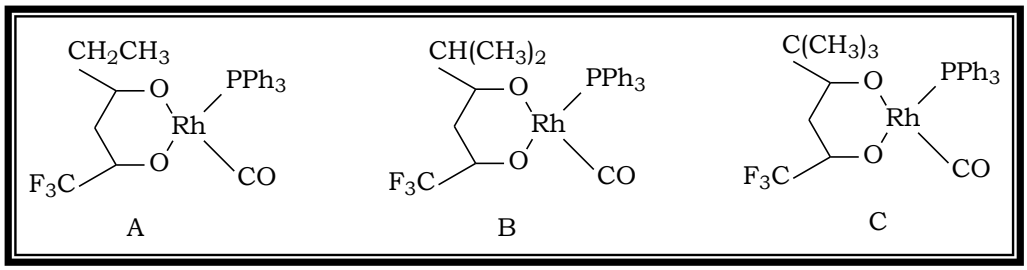

Figure 3.17 [Rh(TFHD)(CO)(PPh_3)], [Rh(TFDMAA)(CO)(PPh_3)] and [Rh(TFTMAA)(CO)(PPh_3)] complexes

A possible explanation for this observation is based on the steric implications of the bonded ligands in the transition state (TS) during the substitution process. The kinetic study of substitution reactions of this type of square planar complexes with 1,5-cyclooctadiene indicated an associative mechanism (Basson *et al.*, 1982:113). Such associative square planar substitution reactions are believed to proceed *via* a trigonal bipyramidal transition state. According to this postulate the entering ligand (PPh_3), the leaving group (CO) and the group *trans* to the leaving group (oxygen) occupy the trigonal plane of the trigonal bipyramid, while the other two ligands remain in the apical positions. This means that if the normal isomers were to be formed for the respective complexes (A), (B) and (C) (**Figure 3.17**), the oxygen nearest to the more bulky group (compared to the CF_3 group) that is (-CH_2CH_3), (-$CH(CH_3)_2$ and (-$C(CH_3)_3$) will have to be in the trigonal plane of the trigonal bipyramid. Since the steric hindrance between the bulky group and PPh_3 in the trigonal plane will render the intermediate relatively unstable, it is unlikely that the so called normal isomer will be formed and hence the unexpected isomer was isolated.

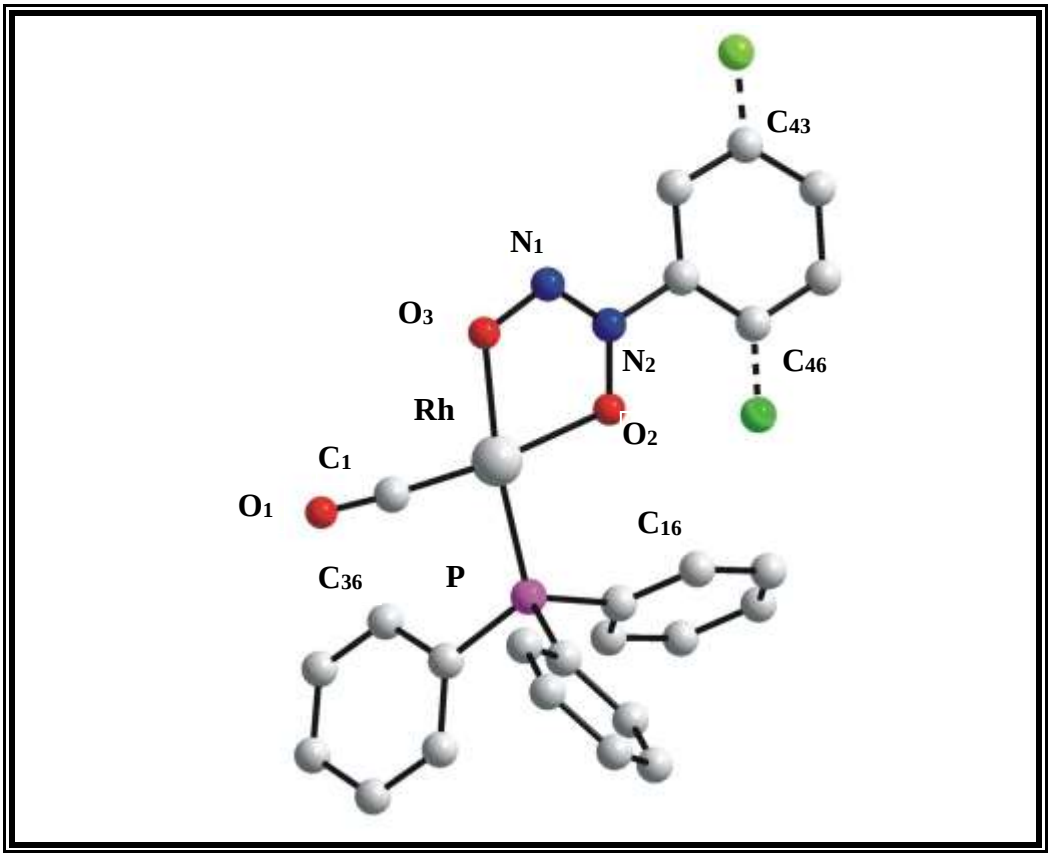

Figure 3.18 Expected arrangement of atoms in [Rh(CH_3cupf)(CO)(PPh_3)]

It is expected that [Rh(CH_3cupf)(CO)(PPh_3)] complex will have a similar geometric arrangement as that of [Rh(cupf)(CO)(PPh_3)] (Basson *et al.*, 1986:L45). The methyl group could be bonded to two possible phenyl carbons in the cupferrate ligand namely, C_{46} and C_{43}. Very little repulsion will exist between the cupferrate and the PPh_3 ligand if the methyl group is bonded to C_{43}. However, if the methyl group is bonded to C_{46} steric interaction may become a reality. The distance between C_{46} and C_{16} is approximately 4.0Å in [Rh(cupf)(CO)(PPh_3)] complex and with the presence of a carbon as well as the hydrogens of the methyl and phenyl groups in the cupferrate ring, the distance is likely to decrease with possible

interaction between them. However, due to the possible free rotation of the cupferrate phenyl group around the N_2-C_{41} bond axis as well as the rotation around the Rh-P bond, it is anticipated that the molecule would be able to relieve any steric strain by rotation. It is therefore anticipated that the -CH_3 group of CH_3cupf increases the bulkiness as compared to –H of the cupferron ligand and the three dimensional structure of the complex assumes the one given in **Figure 3.18**.

CHAPTER 4

OXIDATIVE ADDITION OF [Rh(CH$_3$cupf)(CO)(PX$_3$)] COMPLEXES WITH IODOMETHANE

4.1 INTRODUCTION

Oxidative addition of organic molecules to unsaturated transition metal complexes is a fundamental process in organometallic chemistry and plays a key role in many important catalytic reactions. An important example is the reaction between *cis*-$[Rh(CO)_2I_2]^-$ and iodomethane, the rate-determining step in the industrial carbonylation of methanol to acetic acid (Haynes *et al.*, 1993:4093). It is widely accepted that for simple substrates such as CH_3I, addition occurs *via* the reaction presented in **Scheme 4.1** (Hickey and Maitlis, 1984:1609).

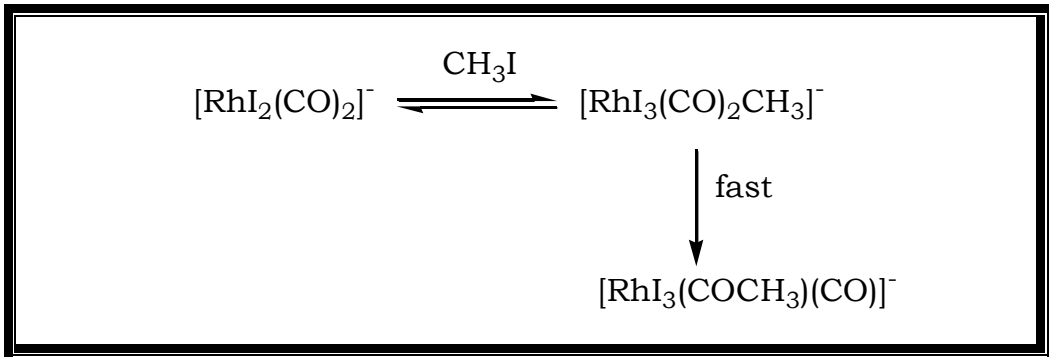

Scheme 4.1 Oxidative addition of $[Rh(CO)_2I_2]^-$ with iodomethane

Kinetic studies of oxidative addition reactions conducted locally in recent years mainly focused upon the manipulation of the reactivity of the Rh(I) centre in the [Rh(LL'-BID)(CO)(PX_3)] type of complexes (where LL'-BID = monocharged bidentate ligands containing different donor atoms L and L'). Since these complexes invariably contained at least one carbonyl ligand, it was found that most of the oxidative addition reactions were complicated by alkyl-acyl conversion reactions. Characterisation of the final products (alkyl *vs.* acyl) and an understanding of the factors influencing these conversion reactions were thus of primary importance. The geometry of the final product of these reactions varied. The oxidative addition of [Rh(ox)(CO)(PPh_3)] with iodomethane yielded the corresponding alkyl complex [RhI(ox)(CO)(CH_3)(PPh_3)] (Van Aswegen, 1991:369), with the fragments of iodomethane (CH_3 and I) *trans* to one another. The [Rh(cupf)(CO)(PPh_3)] complex however, gave the corresponding *cis* [Rh(cupf)(CO)(CH_3)(I)(PPh_3)] alkyl complex (Basson *et al.*, 1987:31). Acyl complexes such as [RhI(Sacac)($COCH_3$)(PPh_3)] were claimed to have been observed as final products when the bidentate ligand contained a sulphur atom as a donor atom (Roodt and Steyn, 2000:1)). A study of the solvent and pressure dependence of iodomethane oxidative addition to the [Rh(Sacac)(CO)(PPh_3)] complex (Van Eldik, 1991:2207) resulted in the presentation of the mechanism being a two step process (**Scheme 4.2**): (i) the oxidative addition step and (ii) the subsequent conversion of the alkyl complex to the corresponding acyl species.

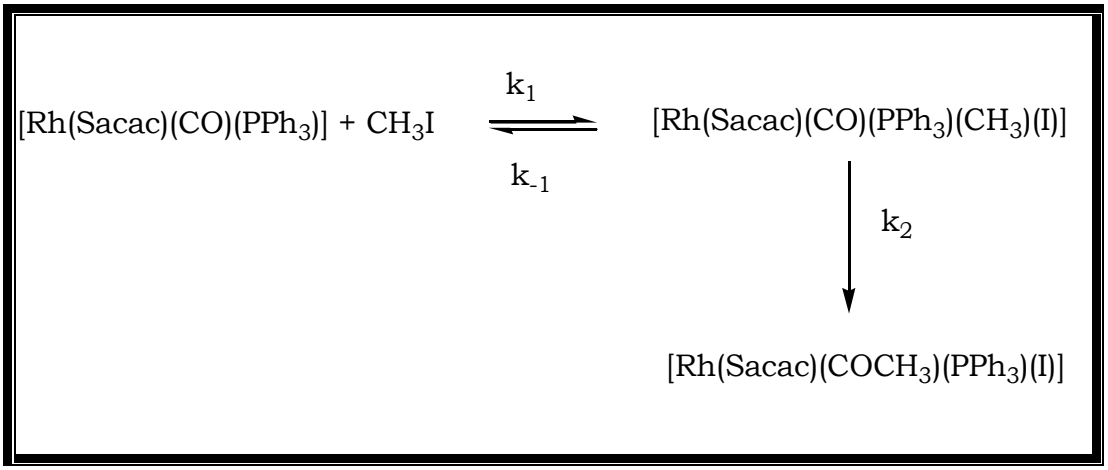

Scheme 4.2 Mechanistic representation for oxidative addition of [Rh(Sacac)(CO)(PPh_3)] with iodomethane

With regard to the solvent path of the mechanism in **Scheme 4.3** it may be stated that in the case of the reaction between [Rh(cupf)(CO)(PPh_3)] and iodomethane substantial solvent interaction was observed (Basson *et al.*,1987:31) but no such pathways have been presented in related studies of oxidative addition of other [Rh(LL'-BID)(CO)(PX_3)] complexes with iodomethane such as [Rh(macsm)(CO)(PPh_3)] and [Rh(acac)(CO)(PPh_3)].

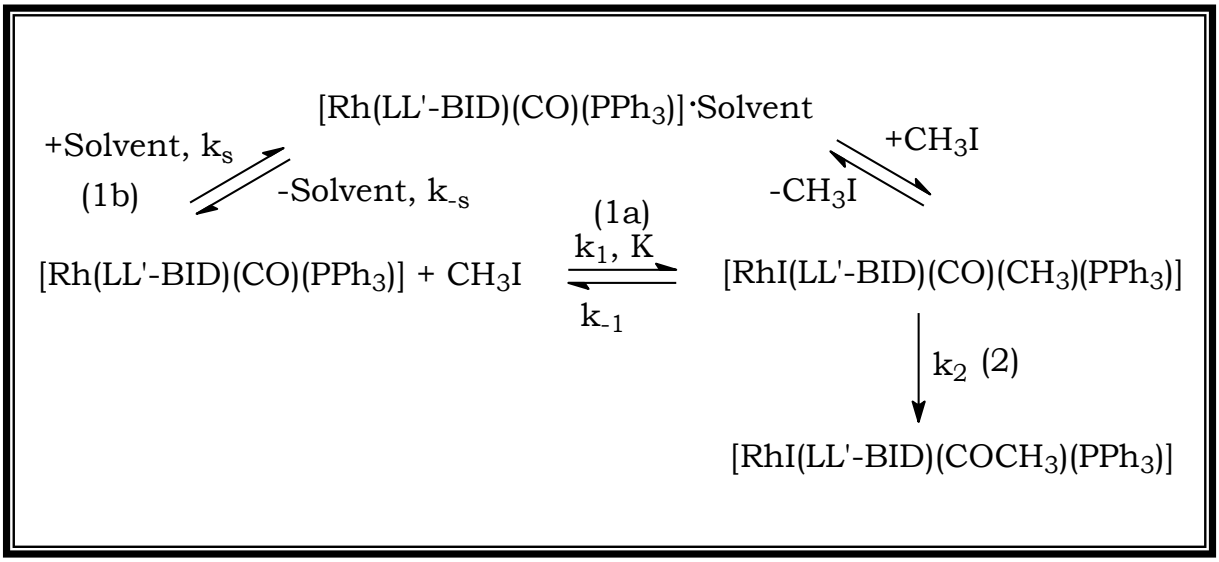

Scheme 4.3 Mechanism of oxidative addition and subsequent acyl formation (Roodt and Steyn, 2000:1)

The solvent pathway was however studied in a number of other cases. Rhodium (I) complexes such as [Rh(cupf)(CO)(PX_3)] (where PX_3 = PCy_3, P(*o*-Tol)$_3$, PPh_3, $PPh_2C_6F_5$, P(*p*-ClC_6H_4)$_3$ and P(*p*-$MeOC_6H_4$)$_3$) react with iodomethane to form Rh(III) alkyl compounds. The reaction was studied in solvents such as benzene, ethylacetate, acetone, acetonitrile, methanol and dimethylsulphoxide having different polarities and donocities. It was found that the reactions proceed through two competing rate determining steps, one of which is first-order in [CH_3I] and the other involving solvent participation before the final product is formed.

The results of the solvent effect in the oxidative addition of [Rh(cupf)(CO)(PPh_3)] with iodomethane is one of the first examples containing a solvent-catalysed pathway. The aim of this research is to study the reaction rates of oxidative addition of the newly

synthesised [Rh(CH_3cupf)(CO)(PX_3)] complexes with iodomethane using UV and IR spectroscopy in different solvents and compare the results with other rhodium complexes. Part of this study was also to investigate the electronic and steric influence of different tertiary phosphines on the reaction between the new Rh(I) complex and iodomethane.

4.2 EXPERIMENTAL

General considerations: unless otherwise stated, all chemicals were of reagent grade and all measurements were carried out in air. The preparation and characterisation of complexes are described in **Chapter 3**. Iodomethane used in this study was purchased from Merck and was stabilised with silver foil to prevent its decomposition to iodine. Iodomethane is highly volatile and the solutions were prepared in fume hood and used immediately after preparation.

Kinetic Measurements: A Cary 50 double-beam spectrophotometer was initially used to verify the stability of the [Rh(CH_3cupf)(CO)(PX_3)] complexes in different solvents. Suitable wavelengths were consequently selected to study the reaction between Rh(CH_3cupf)(CO)(PX_3)] complexes and iodomethane in the different solvents used (**Table 4.1**).

Table 4.1 Summary of the physical conditions of the reaction between [Rh(CH_3cupf)(CO)(PX_3)] and iodomethane

Complex	**Solvent**	**Temperature /K**
[Rh(CH_3cupf)(CO)(PPh_3)]	acetone	290.5, 298.0, 302.5 and 313.3
	chloroform	298.0
	acetonitrile	298.0
	ethylacetate	298.0
	methanol	298.0
	benzene	298.0
[Rh(CH_3cupf)(CO)(P(*p*-$MeOC_6H_4$)$_3$)]	acetone	298.0
[Rh(CH_3cupf)(CO)(PCy_3)]	acetone	298.0
[Rh(CH_3cupf)(CO)(P(*o*-Toly)$_3$)]	acetone	298.0
[Rh(CH_3cupf)(CO)(P(*p*-Toly)$_3$)]	acetone	298.0

Typical complex concentrations were 1.7×10^{-4} M for UV/Visible and 0.02 M for IR kinetic measurements. Iodomethane concentrations were varied between 0.2 and 1 M. Solid infrared spectra were collected in the range of 2300-550 cm^{-1} and liquid infrared in the range 2100-1600 cm^{-1} using a Digilab Merlin 3.0 spectrophotometer equipped with a temperature cell regulator (accurate within 0.3 ˚C). UV/Visible spectra were collected on a Varian Cary 50 double-beam spectrophotometer equipped with temperature cell regulator (accurate within 0.1 ˚C). The mathematical calculations of the kinetic investigations were done on desktop computer using the Scientist (Micromath, 1990) programme. In the case of acetone the reaction was also

performed at four different temperatures to determine the activation parameters using **Eq 4.1**. Some of the reactions were performed using both the IR and UV/Visible spectrophotometer to correlate the different reactions with all the physical changes during the reactions.

$$\ln(k/T) = \ln(k_b/h) + (\Delta S^{\#}/R) - (\Delta H^{\#}/RT) \qquad \textbf{Eq.4.1}$$

4.3 RESULTS

4.3.1 STABILITY OF THE COMPLEX IN DIFFERENT SOLVENTS

The stability of the complex in different solvents was verified by dissolving [Rh(CH_3cupf)(CO)(PPh_3)] in different solvents which included acetone, chloroform, acetonitrile, ethylacetate methanol and benzene. The solutions were monitored under UV/Visible spectroscopy for a number of hours and the results are given in **Figure 4.1**. No significant amount of decomposition took place under the selected experimental conditions.

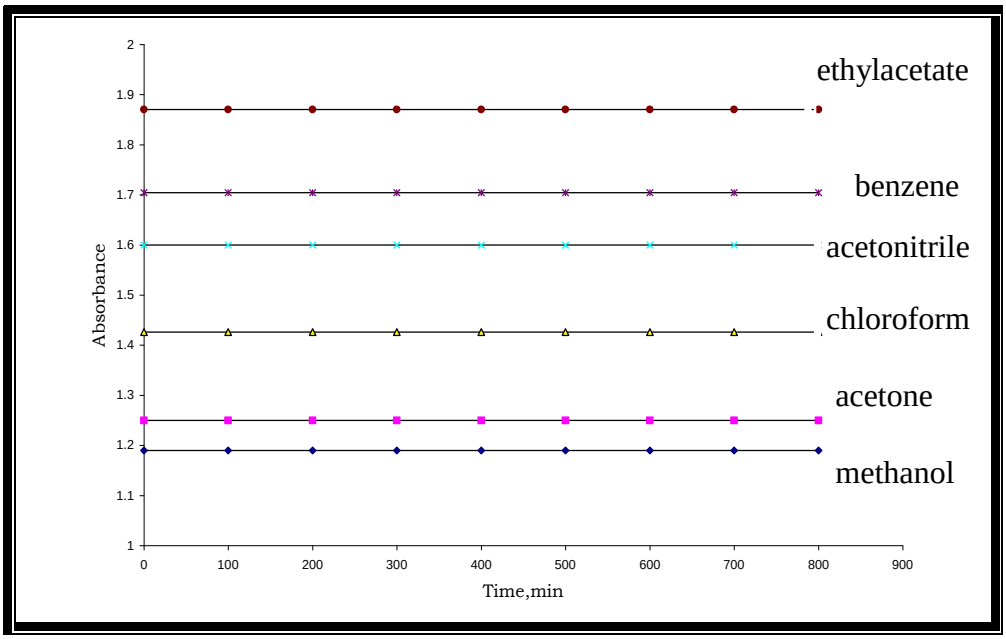

Figure 4.1 Stability of [Rh(CH_3cupf)(CO)(PPh_3)] in different solvents.

4.3.2 WAVELENGTH SELECTION FOR THE DIFFERENT REACTIONS

The reaction between [Rh(CH_3cupf)(CO)(PX_3)] and iodomethane gave a broad absorption maximum in the 340-450 nm region and all kinetic measurements were done at a particular maximum absorption which is given in **Table 4.2**.

Table 4.2 Absorption maxima used to investigate the kinetics in UV spectroscopy

Complex	**λ_{max}/nm**	**Results**
[Rh(CH_3cupf)(CO)(PPh_3)]	380	**Fig 4.2**
Rh(CH_3cupf)(CO)(P(*p*-$MeOC_6H_4$)$_3$]	375	**Fig 4.3**
[Rh(CH_3cupf)(CO)(P(*p*-Tolyl)$_3$]	377	**Fig 4.4**
[Rh(CH_3cupf)(CO)(PCy_3)]	400	**Fig 4.5**
[Rh(CH_3cupf)(CO)(P(*o*-Tolyl)$_3$]	380	**Fig 4.6**

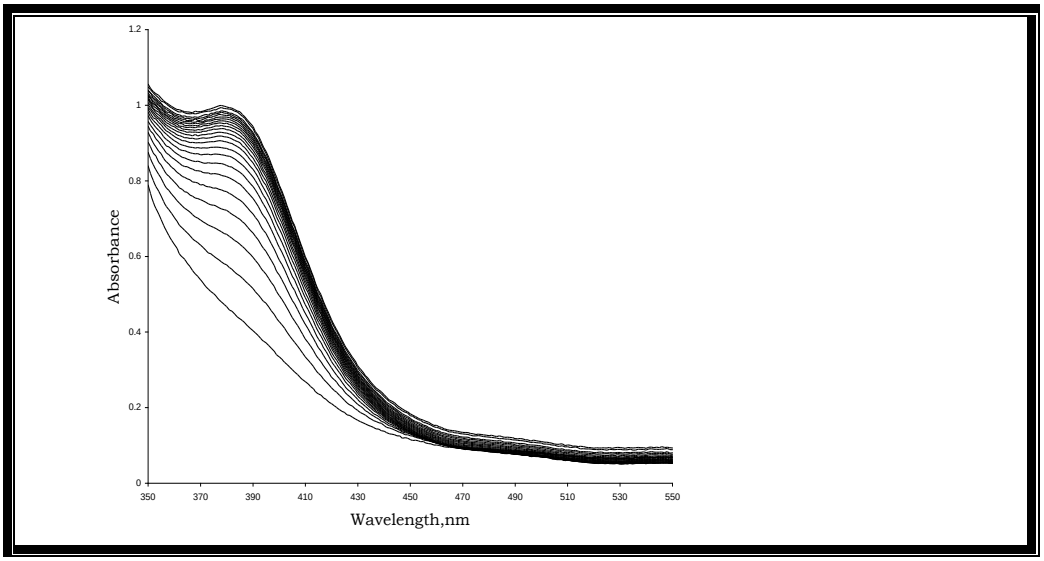

Figure 4.2: Visible spectra (4 min interval) for the reaction between [Rh(CH_3cupf)(CO)(PPh_3)] and iodomethane in acetone at 25.0 °C, [Rh]= 1.7 $\times 10^{-4}$ M, [CH_3I]= 0.5 M

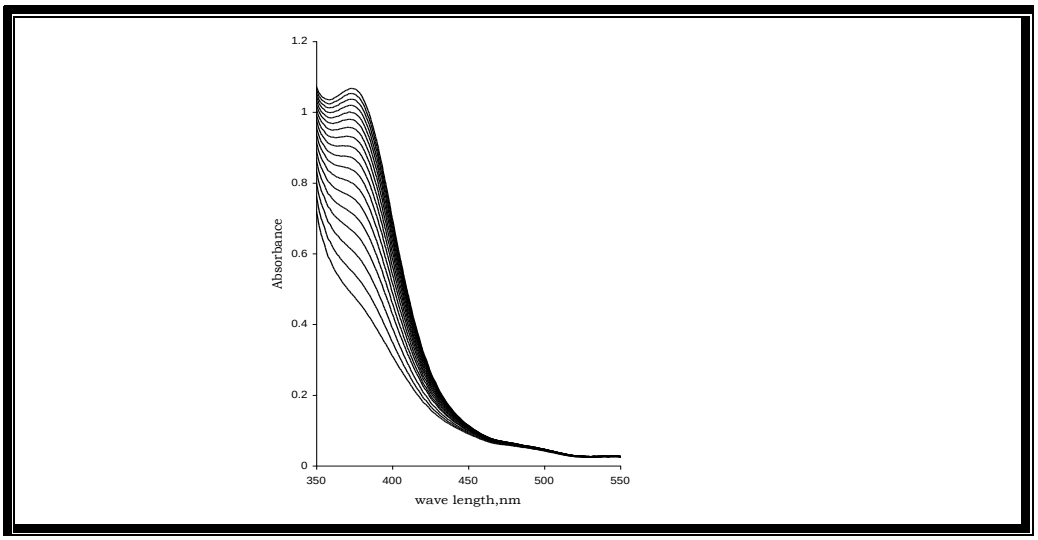

Figure 4.3 Visible spectra (0.1 min interval) for the reaction between [Rh(CH_3cupf)(CO)(P(*p*-$MeOC_6H_4)_3$)] and iodomethane in acetone at 25.0 °C, [Rh]= 1.7 $\times 10^{-4}$ M, [CH_3I]= 0.5 M

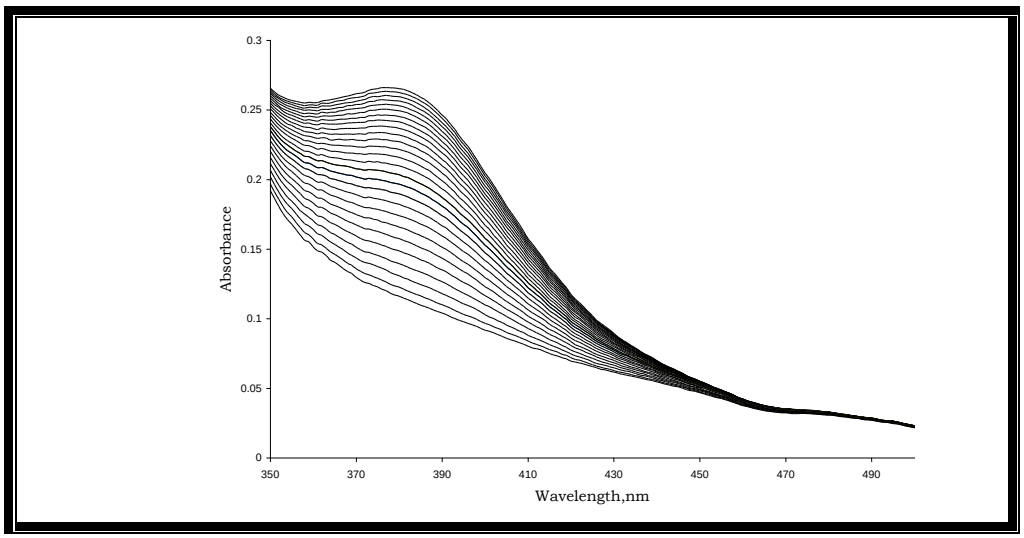

Figure 4.4 Visible spectra (0.5 min interval) for the reaction between [Rh(CH_3cupf)(CO)(P(*p*-$Tol)_3$] and iodomethane in acetone at 25.0 °C, [Rh]= 1.7 $\times 10^{-4}$ M, [CH_3I]= 0.5 M

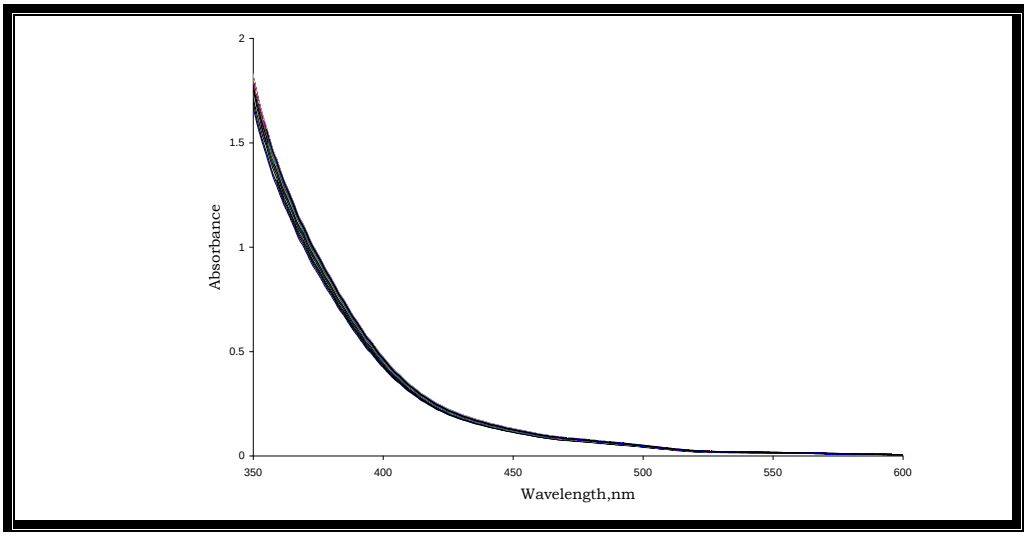

Figure 4.5 Visible spectra (2 min interval) for the reaction between [Rh(CH_3cupf)(CO)(PCy_3)] and iodomethane in acetone at 25.0 °C, [Rh]= 1.7 $\times 10^{-4}$ M, [CH_3I]= 0.5 M

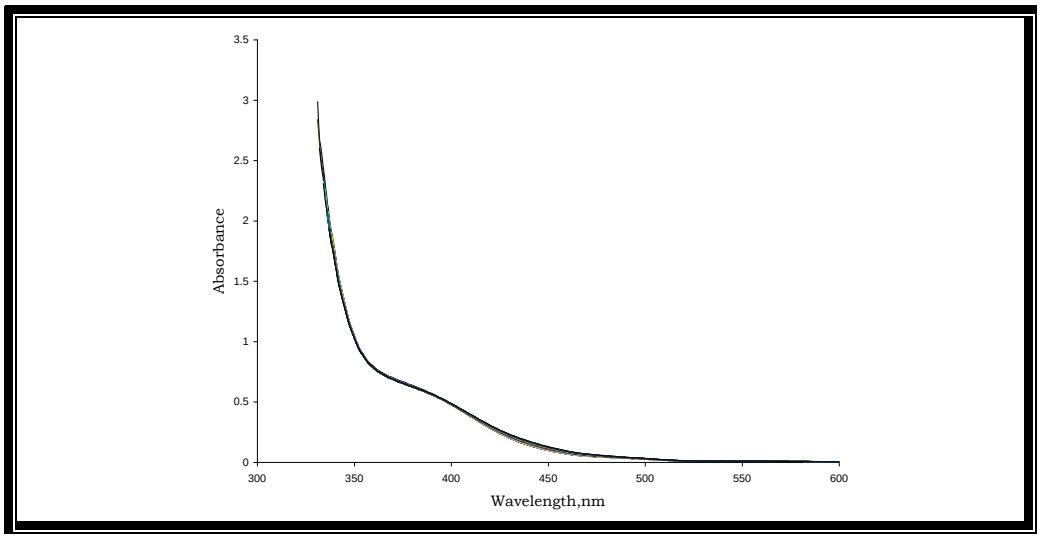

Figure 4.6 Visible spectra (2 min interval) for the reaction between [Rh(CH_3cupf)(CO)(P(*o*-Tol)$_3$)] and iodomethane in acetone at 25.0 °C, [Rh]= 1.7 $\times 10^{-4}$ M, [CH_3I]= 0.5 M

4.3.3 REACTION MECHANISM

The IR and UV/Visible spectra (**Figure 4.2** to **4.13**) as well as the product identification in **Chapter 3** clearly indicate that all the different Rh(I)-CH_3cupf complexes react with iodomethane. These results also point to the formation of the Rh(III)-alkyl product in the first reaction and the subsequent acyl formation in the second reaction.

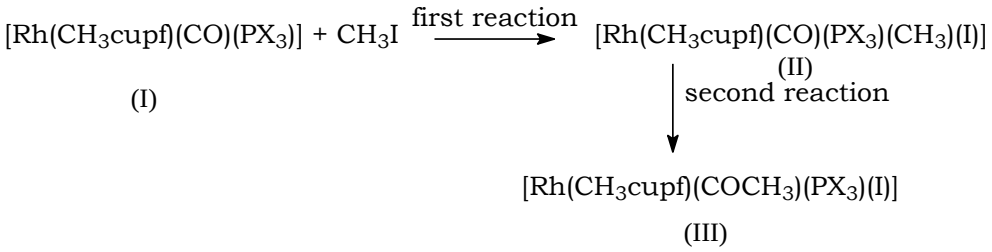

The Rh(I)-CO stretching frequency at about 1982 cm^{-1} (I) disappears with the simultaneous appearance of the Rh(III)-CO peak at about 2056 cm^{-1} (II). The peak formation at 1720 cm^{-1} is indicative of acyl formation (III). Another important aspect of all the IR spectra is the complete disappearance of the Rh(I)-CO peak which points to a large forward reaction (large equilibrium constant) with little or no reverse reaction.

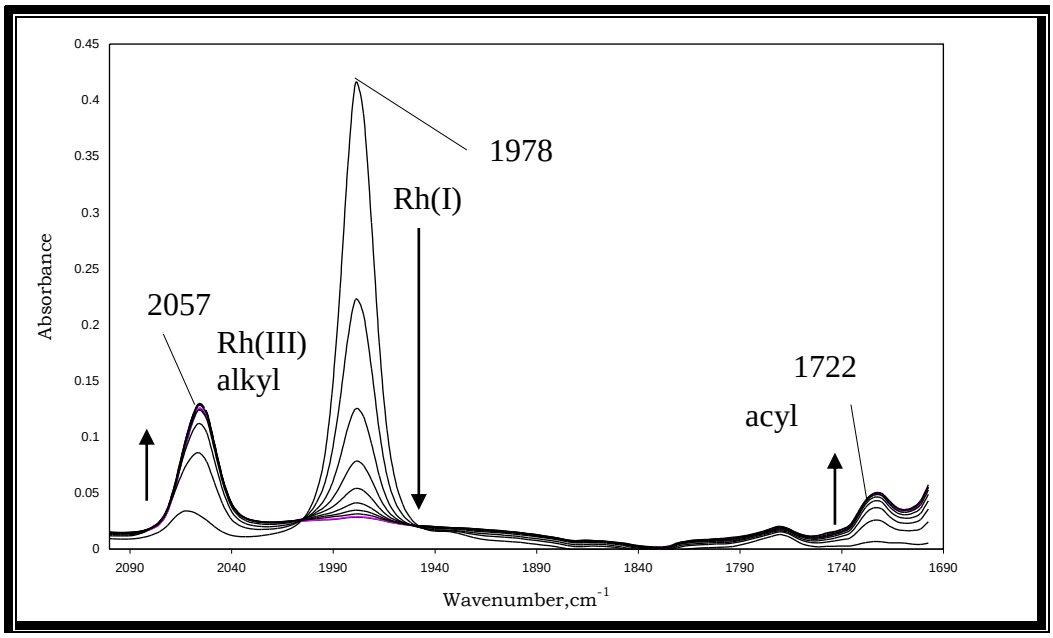

Figure 4.7 Consecutive IR scans (4 min intervals) for the oxidative addition of [Rh(CH_3cupf)(CO)(PPh_3)] with iodomethane in acetonitrile at 25.0 °C, [Rh] = 0.02 M, [CH_3I] = 0.2 M. Rh(I)-CO at 1978 cm^{-1}, Rh(III)-CO at 2057 cm^{-1} and Rh(III)-acyl at 1722 cm^{-1}

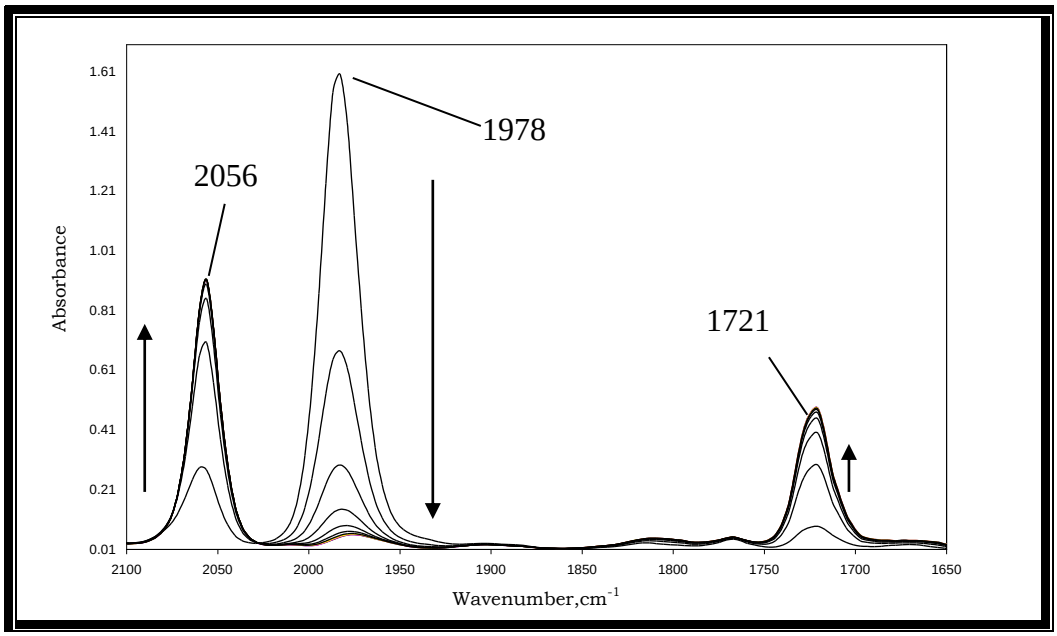

Figure 4.8 Consecutive IR scans (4 min intervals) for the oxidative addition of [Rh(CH_3cupf)(CO)(PPh_3)] with iodomethane in chloroform at 25.0 °C, [Rh] = 0.02 M, [CH_3I] = 0.2 M. Rh(I)-CO at 1978 cm^{-1}, Rh(III)-CO at 2056 cm^{-1} and Rh(III)-acyl at 1721 cm^{-1}

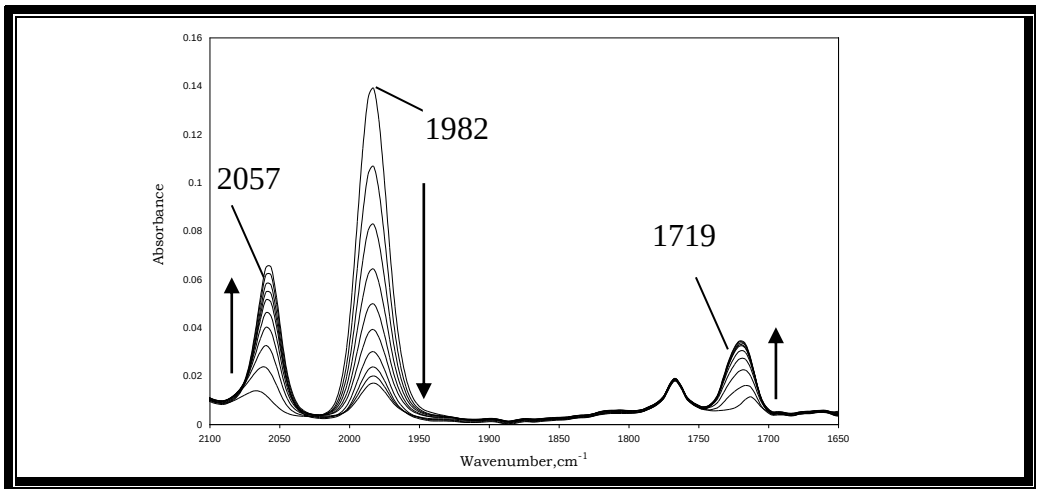

Figure 4.9 Consecutive IR scans (2 min intervals) for the oxidative addition [Rh(CH_3cupf)(CO)(PPh_3)] with iodomethane in chloroform at 25.0 °C, [Rh] = 0.02 M, [CH_3I] = 0.4 M. Rh(I)-CO at 1982 cm^{-1}, Rh(III)-CO at 2057 cm^{-1} and Rh(III)-acyl at 1719 cm^{-1}

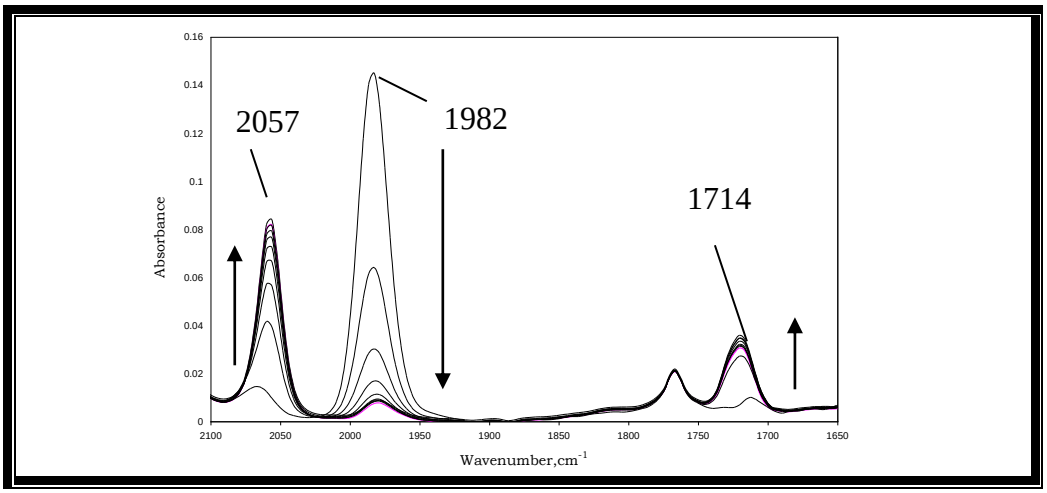

Figure 4.10 Consecutive IR scans (4 min intervals) for the oxidative addition of [Rh(CH_3cupf)(CO)(PPh_3)] with iodomethane in chloroform at 25.0 °C , [Rh] = 0.02 M, [CH_3I]=0.6 M. Rh(I)-CO at 1982 cm^{-1}, Rh(III)-CO at 2057 cm^{-1} and Rh(III)-acyl at 1714 cm^{-1}

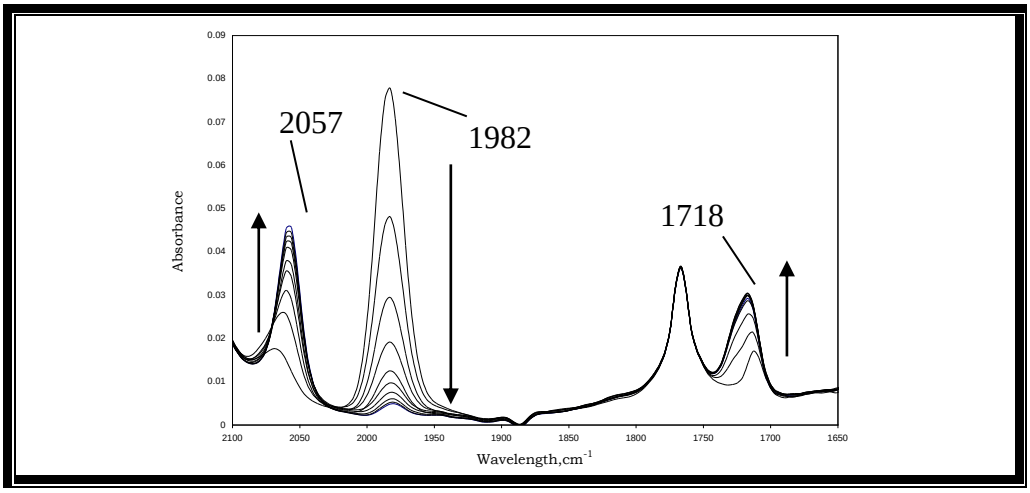

Figure 4.11 Consecutive IR scans (2 min intervals) for the oxidative addition of [Rh(CH_3cupf)(CO)(PPh_3)] with iodomethane in chloroform at 25.0 ºC, [Rh] = 0.02 M, [CH_3I] = 0.8 M. Rh(I)-CO at 1982 cm^{-1}, Rh(III)-CO at 2057 cm^{-1} and Rh(III)-acyl at 1718 cm^{-1}

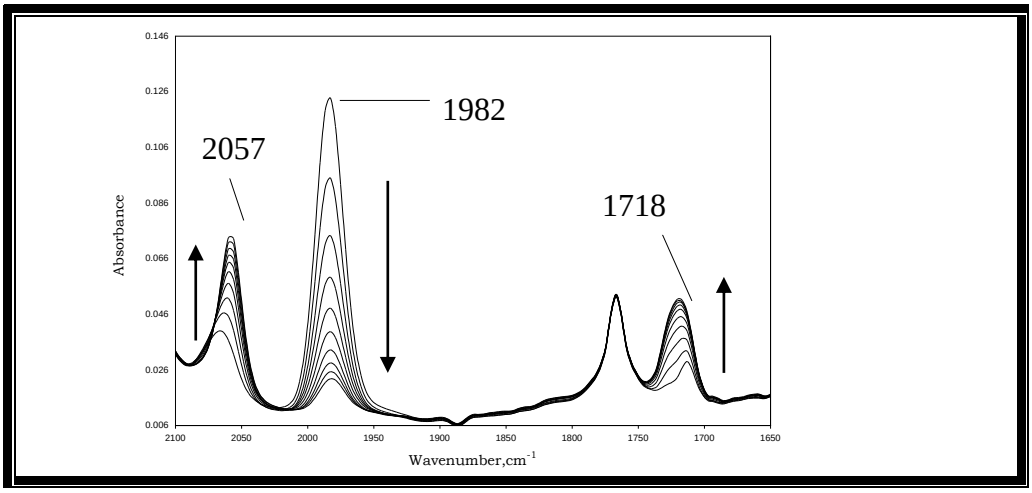

Figure 4.12 Consecutive IR scans (1 min intervals) for the oxidative addition of [Rh(CH_3cupf)(CO)(PPh_3)] with iodomethane in chloroform at 25 ºC, [Rh] = 0.02 M, [CH_3I] = 1.0 M. Rh(I)-CO at 1982 cm^{-1}, Rh(III)-CO at 2057 cm^{-1} and Rh(III)-acyl at 1718 cm^{-1}

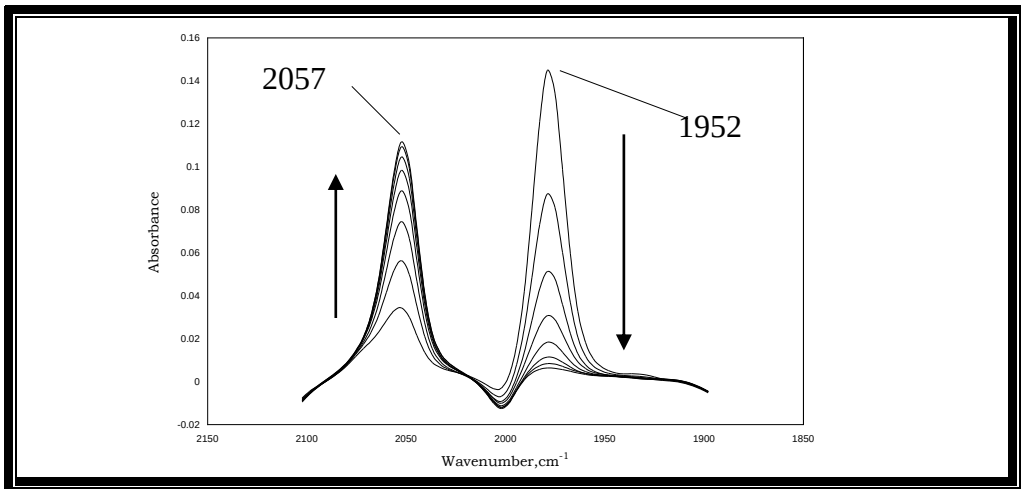

Figure 4.13 Consecutive IR scans (4 min intervals) for the oxidative addition of [Rh(CH_3cupf)(CO)(PPh_3)] with iodomethane in acetone at 25°C, [Rh] = 0.02 M, [CH_3I] = 0.2 M. Rh(I)-CO at 1952 cm^{-1}, Rh(III)-CO at 2057 cm^{-1}

The kinetic study of the reaction between [Rh(CH_3cupf)(CO)(PX_3)] and different [CH_3I] (**Figure 4.14** and **Figure 4.17**) showed a large intercept which could clearly not be attributed to the reverse reaction. This intercept can only be attributed to the involvement of solvent molecules in the overall reaction. Using all these informations the following reaction scheme can be proposed for the reaction between [Rh(CH_3cupf)(CO)(PX_3)] and iodomethane.

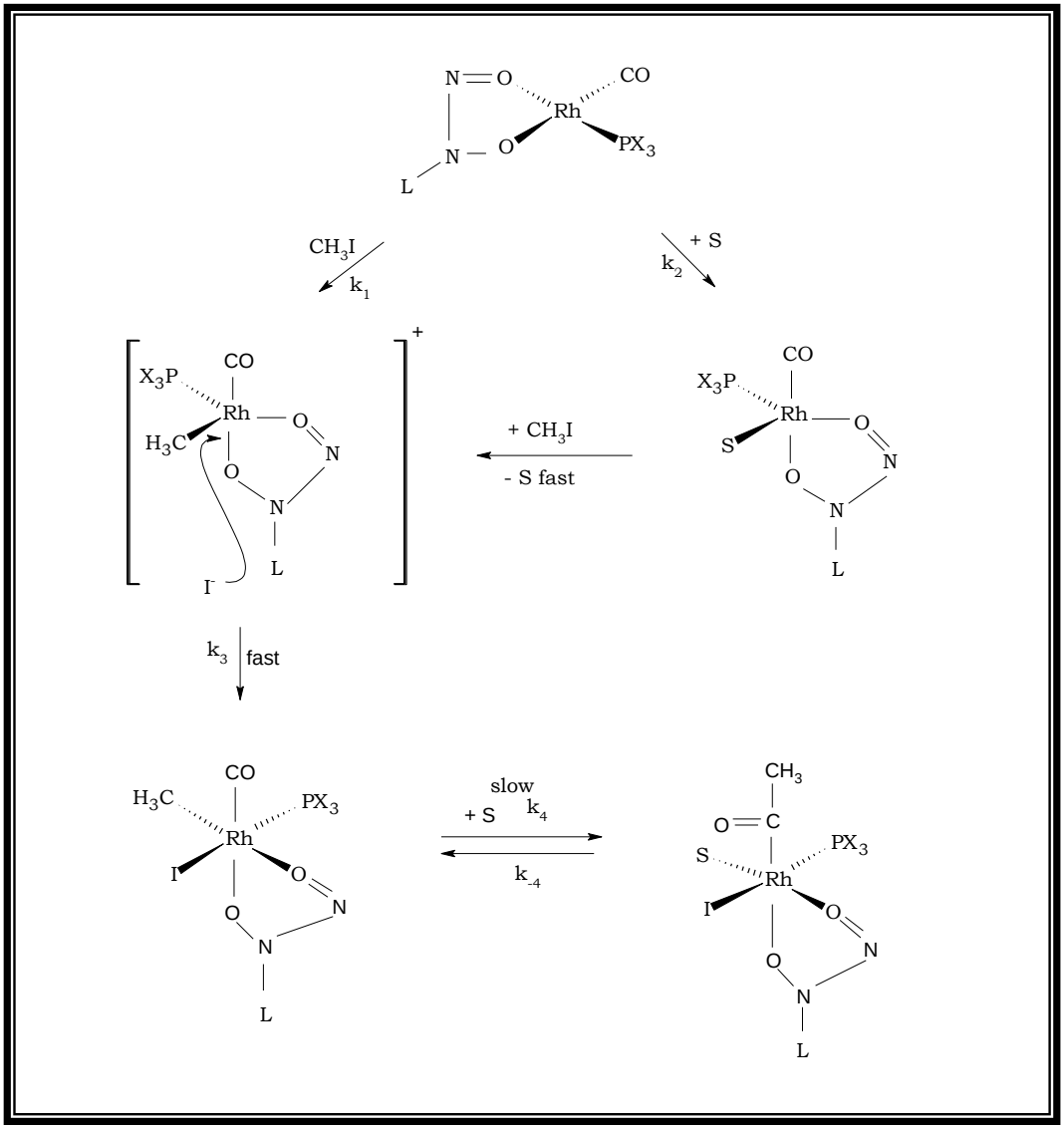

Scheme 4.4 Mechanistic scheme for oxidative addition of [Rh(CH3cupf)(CO)(PX3)] with iodomethane (where L = *m*-toluene)

This mechanism proposes two different pathways for the formation of the alkyl product. The first step involves the direct oxidative addition of CH_3I to the Rh(I) complex with the second parallel pathway involving the addition of the solvent molecule (S) to the

metal complex with a subsequent fast reaction with iodomethane. The next step in the proposed mechanism involves methyl migration to form the acyl product. The difference in Rh(I) and Rh(III) CO stretching frequencies allows for the complete study of all the reactions involved in this scheme.

4.3.4 RATE LAWS FOR THE OXIDATIVE ADDITION OF [Rh(CH_3cupf)(CO)(PX_3)] COMPLEXES WITH IODOMETHANE

The rate law for the formation of the alkyl product assuming that k_3 is fast, is given by **Eq 4.2**

$$-d[Rh(I)]/dt = (k_1[CH_3I] + k_2[S])[Rh(CH_3cupf)(CO)(PX_3)] \qquad \textbf{Eq.4.2}$$

Performing these reactions under pseudo-first-order conditions with $[Rh(CH_3cupf)(CO)(PX_3)] << [CH_3I]$, **Eq.4.2** simplifies to

$$k_{obs} = k_1[CH_3I] + k_2[S]$$
$$= k_1[CH_3I] + k_2' \qquad \textbf{Eq.4.3}$$

The rate law for the acyl formation (final step in the reaction **Scheme 4.4**) is given by **Eq.4.4**

$$\frac{d[Rh(CH_3cupf)(COCH_3)(PX_3)(I)(S)]}{dt} = k_4[Rh(CH_3cupf)(CO)(PX_3)(CH_3)(I)][S] + k_{-4}[Rh(CH_3cupf)(CO)(CH_3)(PX_3)(I)]$$

$$= (k_4[S] + k_{-4})[Rh(CH_3cupf)(CO)(PX_3)(CH_3)(I)]$$

Eq.4.4

Hence,

$$R = (k_4[S] + k_{-4})[Rh(CH_3cupf)(CO)(PX_3)(CH_3)(I)] \quad \textbf{Eq.4.5}$$

Integration of **Eq 4.5** yielded **Eq 4.6** with [S]>> [Rh(CH_3cupf)(CO)(PX_3)(CH_3)(I)]

$$k_{obs} = k_4[S] + k_{-4}$$
$$= k_4' + k_{-4} \quad \textbf{Eq.4.6}$$

Eq.4.6 predicts a rate constant which is independent of the iodomethane concentration with an intercept of k_{-4}.

4.3.5 KINETIC RESULTS

The linear dependence between the observed rate constant and the [CH_3I] at different temperatures is clearly illustrated in **Figure 4.14** and the values of k_1 and k_2' are reported in **Table 4.3**. The k_1 and k_2' values were also used to calculate the activation enthalpy ($\Delta H^{\#}$) and entropy ($\Delta S^{\#}$) using **Eq.4.1**. The results are illustrated in

Figure 4.15 while the calculated values for the activation parameters are reported in **Table 4.4**. **Table 4.5** lists the results obtained from kinetic measurements done on IR, with **Figure 4.16** a comparison between the IR and UV kinetic results.

Table 4.3 Temperature effect for the oxidative addition of [Rh(CH_3cupf)(CO)(PPh_3)] with CH_3I in acetone (UV/Visible)

Temperature/K	**$10^3k_1/M^{-1}s^{-1}$**	**$10^4k'_2/s^{-1}$**
290.5	0.73(1)	1.98(7)
298.0	1.33(4)	5.1(2)
302.1	1.52(1)	7.91(9)
313.3	3.45(1)	10.92(7)

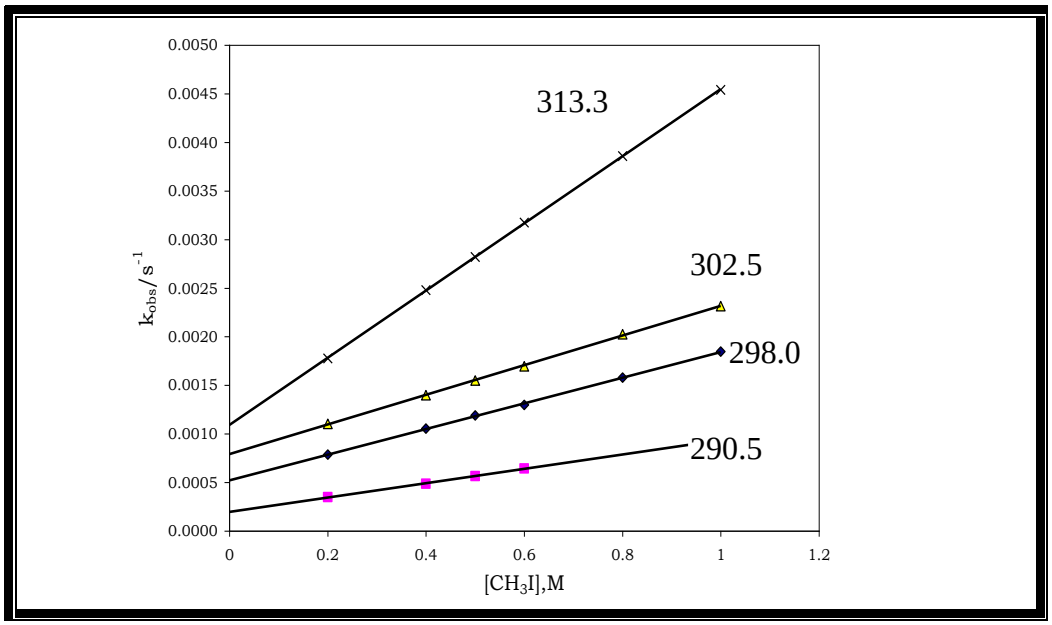

Figure 4.14 Kinetic results for the reaction between [Rh(CH_3cupf)(CH_3)(CO)(PPh_3)] and iodomethane in acetone, [Rh^{+1}]= 1.7×10^{-4} M(UV/Visible)
λ_{max} = 380 nm

Table 4.4 Activation parameters for the reaction between [Rh(CH_3cupf)(CO)(PPh_3)] and iodomethane in acetone

Reaction path	**$\Delta H^{\#}$/kJ mol^{-1}**	**$\Delta S^{\#}$/J K^{-1} mol^{-1}**
k_1	48(1)	-137(1)
k_2	52(5)	-154(40)

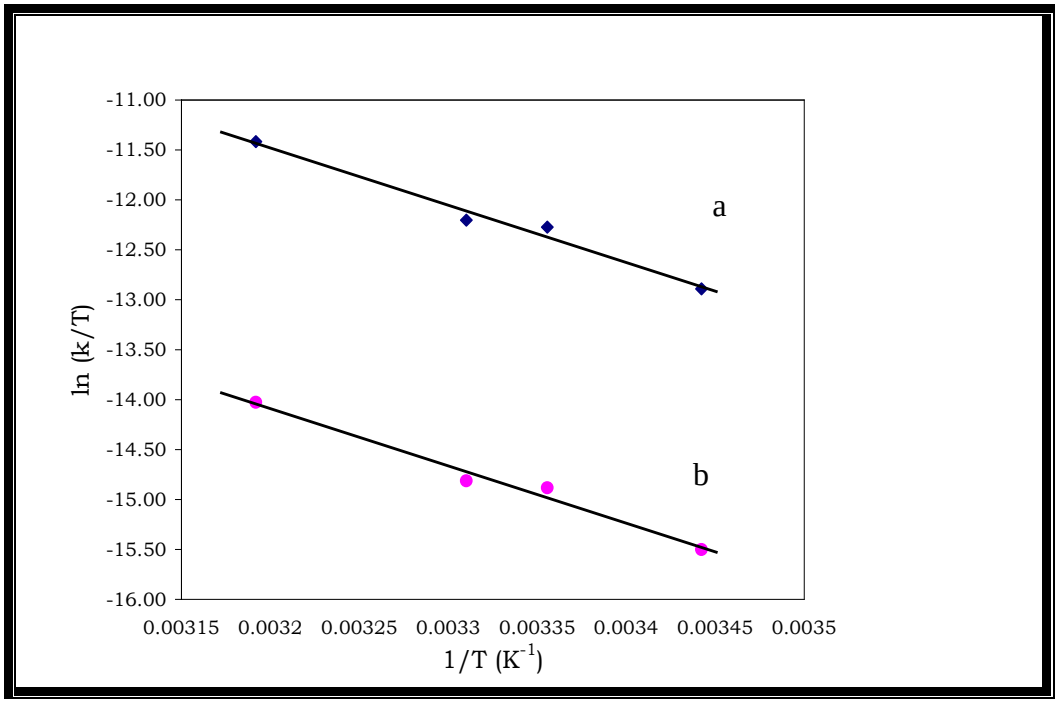

Figure 4.15 Plot of ln(k/T) versus 1/T in acetone for the reaction between [Rh(CH_3cupf)(CO)(PPh_3)] and iodomethane

a. $[Rh(CH_3cupf)(CO)(PPh_3)] + CH_3I \xrightarrow{k_1} [Rh(CH_3cupf)(CO)(PPh_3)(CH_3)]^+I^-$

b. $[Rh(CH_3cupf)(CO)(PPh_3)]\ S \xrightarrow{k_2} [Rh(CH_3cupf)(CO)(PPh_3)(S)]$

Table 4.5. IR kinetic results for the reaction between [Rh(CH_3cupf)(CO)(PPh_3)] and CH_3I in chloroform at 25.0 °C

[CH_3I]/M	**IR, $10^3k_{obs}/s^{-1}$**		
	Rh(I)	Rh(III)-alkyl	Rh(III)-acyl
0.2	1.23(1)	1.3(2)	0.4(1)
0.4	1.4(3)	1.36(6)	0.3(3)
0.6	1.7(3)	1.99(1)	0.4(3)
0.8	2.5(6)	2.4(2)	0.4(3)
1.0	5.12(9)	2.8(1)	0.5(1)

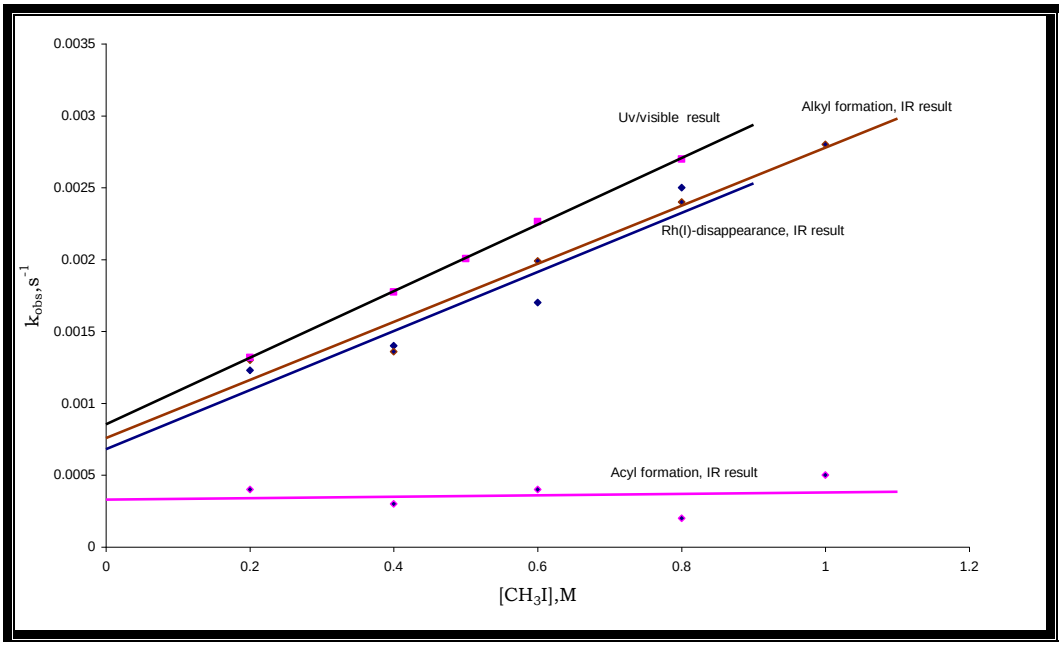

Figure 4.16 Comparison between IR and UV kinetic results for the reaction between [Rh(CH_3cupf)(CO)(CH_3)(PPh_3)] and iodomethane in chloroform at 25.0 °C

4.3.6 SOLVENT DEPENDENCE OF OXIDATIVE ADDITION

In an attempt to determine the influence of solvent in these reactions, a selection of solvents having different polarities (ε) and donocities (D) were also used in the study of the oxidative addition

between [Rh(CH_3cupf)(CO)(PPh_3)] and iodomethane. The results are reported in **Table 4.6**.

Table 4.6 Solvent effect for the oxidative addition of [Rh(CH_3cupf)(CO)(PPh_3)] with iodomethane at 25.0 °C using UV/Visible spectroscopy. ($k_2=k_2'/[S]$)

Solvent	ε	D	10^3k_1/ $M^{-1}s^{-1}$	$10^4k'_2$/ s^{-1}	10^5k_2/ $M^{-1}s^{-1}$	k_1/k_2
Benzene	2.3	0.1	0.101(2)	0.02(1)	0.0178	567
Ethyl acetate	6	17.1	0.658(7)	0.94(3)	0.919	71
Acetone	17	17	1.33(4)	5.1(2)	3.75	35
Chloroform	4.8	4	2.31(2)	8.5(1)	6.8	33
Methanol	32.6	19	3.94(5)	12.0(3)	4.86	81
Acetonitrile	38	29.8	5.18(6)	15.7(4)	8.2	63

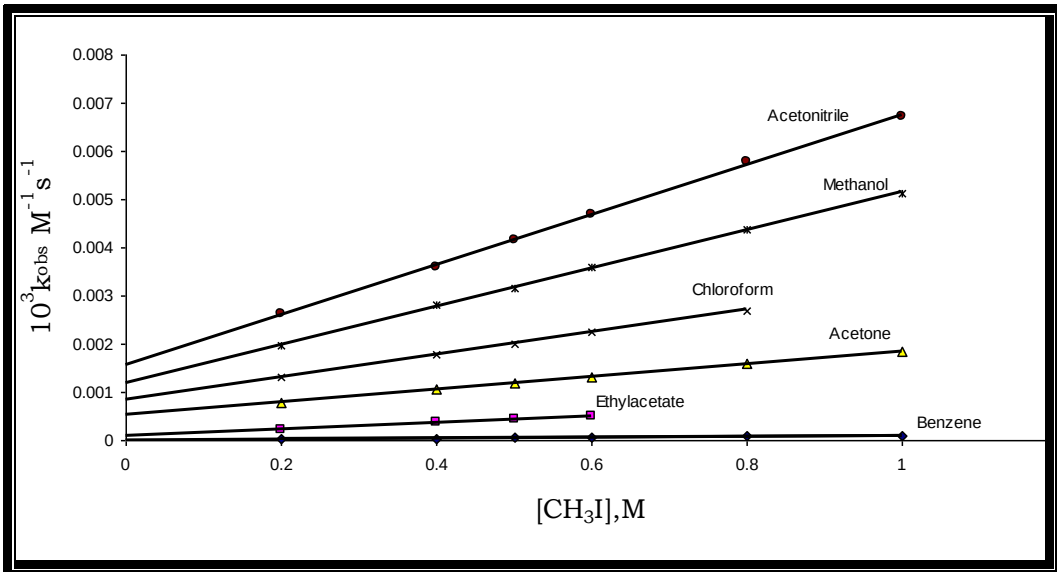

Figure 4.17 Solvent dependence for the oxidative addition reaction of [Rh(CH_3cupf)(CO)(PPh_3)] with iodomethane at 25.0 °C , $[Rh^{+1}]= 1.7\times10^{-4}$ M

Table 4.7 Solvent concentrations

Solvent	**Density/ g cm^{-1}**	**Molar Mass/ g mol^{-1}**	**Concentration/ mol dm^{-3}**
Benzene	0.877	78.11	11.23
Ethylacetate	0.901	88.11	10.23
Acetone	0.79	58.08	13.6
Chloroform	1.492	119.38	12.5
Methanol	0.791	32.04	24.7
Acetonitrile	0.786	41.05	19.14

4.3.7 THE INFLUENCE OF THE TERTIARY PHOSPHINE LIGAND

The influence of different tertiary phosphine ligands on the rate of oxidative addition was also studied. Kinetic results for the oxidative addition of [Rh(CH_3cupf)(CO)(PX_3)] complexes with iodomethane (where X = Ph, *p*-MeOph, *o*-Tol, *p*-Tol and Cy) are given in **Table 4.8**. The phosphines were chosen in such a way to investigate phosphines with different cone angles as well as different electron densities.

Table 4.8 Ligand effect for the oxidative addition of [Rh(CH_3cupf)(CO)(PX_3)] with iodomethane at 25.0°C using UV/Visible spectroscopy in acetone

PX_3	**pKa**	**ν(CO)/ cm^{-1}**	**Cone angle(°)**	**10^3k_1/ $M^{-1}s^{-1}$**	**10^4k_2'/s^{-1}**
PPh_3	2.73	1982	145	1.33(4)	5.1(2)
P(*p*-Tol)$_3$	3.84	1970	145	2.30(7)	3.5(3)
P(*p*-$MeOC_6H_4$)$_3$	4.57	1964	145	7.05(7)	7.89(4)
PCy_3	9.65	1954	170	3.35(4)	5.2(2)
P(*o*-Tol)$_3$	3.08	1965	194	0.615(5)	2.55(3)

4.4 DISCUSSION

The IR spectrum of the reaction mixture of [Rh(CH_3cupf)(CO)(PX_3)] and CH_3I clearly indicated the disappearance of the Rh(I) peaks at approximately 1980 cm^{-1}, the appearance of the Rh(III)-alkyl peak at about 2050 cm^{-1} and the formation of Rh(III)-acyl peak at about 1720 cm^{-1}. An important feature of these spectra is the complete disappearance of the Rh(I) peak indicating the absence of any reverse reaction or the existence of an equilibrium between the Rh(I) and Rh(III)-alkyl complex. The final spectra in all cases contained both the Rh(III)-alkyl and Rh(III)-acyl peaks suggesting an equilibrium between these two species.

The kinetic study of the disappearance and formation of these different complexes in the IR region (**Table 4.9**) clearly indicates the rate of Rh(I) disappearance (2.0(2) × 10^{-3} $M^{-1}s^{-1}$) and the rate of Rh(III) alkyl formation (2.1(5) × 10^{-3} $M^{-1}s^{-1}$) is within experimental error the same. The rate for the formation of the Rh(III)-acyl

product is approximately a factor 13 slower than the above mentioned reactions.

Table 4.9 IR and UV/Visible kinetic results for the oxidative addition of [Rh(CH_3cupf)(CO)(PPh_3)] with iodomethane at 25.0 °C

Complex	**k_1/$M^{-1}s^{-1}$**	**Intercept/s^{-1}**
Rh(I)-Rh(III) alkyl conversion, UV/Visible results	0.00231(3)	0.00085(1)
Alkyl formation, IR	0.0021(5)	0.0008(2)
Rh(I) disappearance, IR	0.0020(2)	0.0007(3)
Acyl formation, IR	0.00015(9)	0.00031(6)

The UV/Visible spectra on the other hand only showed one reaction in the wavelength range that was used. All these spectra showed a steady absorption increase at about 400 nm. The kinetic results for the reaction between [Rh(CH_3cupf)(CO)(PX_3)] with iodomethane in chloroform (same conditions as those of the IR study) gave a rate constant of 2.31(3) × 10^{-3} $M^{-1}s^{-1}$, which corresponds very favourably with the rate constants for Rh(I) disappearance and Rh(III)-alkyl formation (**Table 4.9**). It is difficult to assign the UV/Visible spectrum change to either the Rh(I) disappearance or Rh(III)-alkyl formation due to the fact that the two rate constants are actually the same. The absence of a second reaction in the UV/Visible area can be attributed to a very small extinction coefficient for the acyl product.

The UV/Visible kinetic study for a whole temperature range (**Figure 4.14**) as well as the IR kinetic study gave straight lines

with relatively large intercepts as predicted by **Eq.4.3**. The fact that the IR spectrum clearly indicates the absence of an equilibrium for the Rh(I) and Rh(III)-alkyl reaction leads to the interpretation of the intercept as indicative of a solvent assisted pathway. The kinetics of the same reaction in different solvents (**Figure 4.17**) clearly pointed to a difference in rate (slope) as well as solvent pathway intervention (intercept), with the largest contribution by acetonitrile.

The rate of Rh(III)-acyl formation was also found to be [CH_3I] independent (**Figure 4.16**) with an average rate constant of $1.5(9) \times 10\ M^{-1}s^{-1}$.

From these discussions it is clear that there is a fairly good correlation between the mechanism and the subsequent rate laws for this system and the experimental results that were obtained in this study. This suggests that the model presented in **Scheme 4.4** is a fair reflection of the reaction that was experimentally investigated.

A possible reaction mechanism consistent with the experimental results is shown in **Scheme 4.4**. It includes the reactant, [Rh(CH_3cupf)(CO)(PPh_3)], [Rh(CH_3cupf)(CO)(CH_3)(I)(PPh_3)] and the final acyl product. The k_1 path implies a nucleophilic attack on CH_3I giving the 5-coordinate intermediate for which the degree of ion separation will be solvent dependent. During the Rh-CH_3 bond formation, the CH_3 ligand will tend, based on similar assumptions for square planar substitution reactions (Purcell and Kotz,

1977:700), to move towards the least strongly bound ligand (nitroso oxygen) and away from the most strongly bound ligand (PPh_3). Once the Rh-C bond is established, the phosphorus atoms can facilitate the simultaneous C-I bond breaking. The same effect will also facilitate the fast nucleophilic attack of I^- between the Rh-C and Rh-O bonds thus leading to the proposed *cis*-addition product (Basson *et al.*, 1987:31).

The rate of the oxidative addition of [Rh(CH_3cupf)(CO)(PPh_3)] with iodomethane is slightly faster than of that of the corresponding [Rh(cupf)(CO)(PX_3)] complex (**Table 4.10**), but still appreciably slower than the [Rh(acac)(CO)(PPh_3)] complex containing a six-membered bidentate ligand. The electronic effect of the addition of a methyl group to the cupferron backbone in the current structure is relatively small. From these results it appears that the methyl group donates electron density to the bidentate ligand. This in turn increases the electron density on the Rh centre which renders the metal complex to be a better Lewis base. The final result is better interaction between the metal d-orbital and the vacant π-orbital of the methyl iodide and finally an increase in the oxidative addition rate (bond breaking of the CH_3—I bond).

The data in **Table 4.10** indicates that in general, for the same donor atoms L and L', an increase in the rate of oxidative addition with an increase in size of the chelating ring is observed. The increase in the rate for the donor atoms of bidentate ligands is found to be in the order O,O < O,S < O,N < N,S while no meaningful correlation was found for the rate of acylation. For instance, in case of the [Rh(cupf)(CO)(PPh_3)] and

[Rh(CH_3cupf)(CO)(PPh_3)] complexes, the acyl complex is not an intermediate as in the case of the β-diketone complexes but is slowly formed from the alkyl complexes.

Table 4.10 Kinetic data for the oxidative addition of selected [Rh(LL'-BID)(CO)(PX_3)] complexes with iodomethane in chloroform at 25.0 °C (Damoense, 2000:5)

L-L'-BID	**L**	**L'**	**Ring size**	**Rate constants**	
				alkyl/$M^{-1}s^{-1}$	**acyl/s^{-1}**
cupf	O	O	5	0.0050(1)	0.0012(1)
CH_3cupf	O	O	5	0.00231(2)	0.00015(9)
acac	O	O	6	0.0065(4)	0.0016(1)
sacac	O	S	6		>0.01
hpt	O	S	5	0.0083	0.01
macsm	N	S	6	0.034(1)	0.0078(4)

Rate constants for the oxidative addition of [Rh(Sacac)(CO)(PPh_3)] with iodomethane in different solvents showed that the rates are independent of the donocity of the solvent as in the case for the oxidative addition reactions of [Rh(CH_3cupf)(CO)(PPh_3)] and [Rh(cupf)(CO)(PPh_3)] with iodomethane. A solvent assisted path was however observed for the two Rh(I)-cupferrate complexes.

A quite significant solvent effect is evident from the values for k_1, which shows an increasing trend with increased solvent polarity (**Figure 4.18**), and the chloroform case being the only exception. The marked solvent dependence of k_1 strongly suggests a mechanism in which a polar transition state is stabilised by more

polar solvents and can be taken as evidence that the function of the solvent is to ease the charge separation during the rearrangement and formation of the 5-coordinate intermediate. This idea is also supported from the large entropy of activation for acetone medium (**Table 4.4**). The relative small $\Delta H^{\#}$ values, accompanied by large negative $\Delta S^{\#}$ values, indicate an associative mechanism including bond formation and/or partial charge creation (electrostriction) during the formation of the transition state.

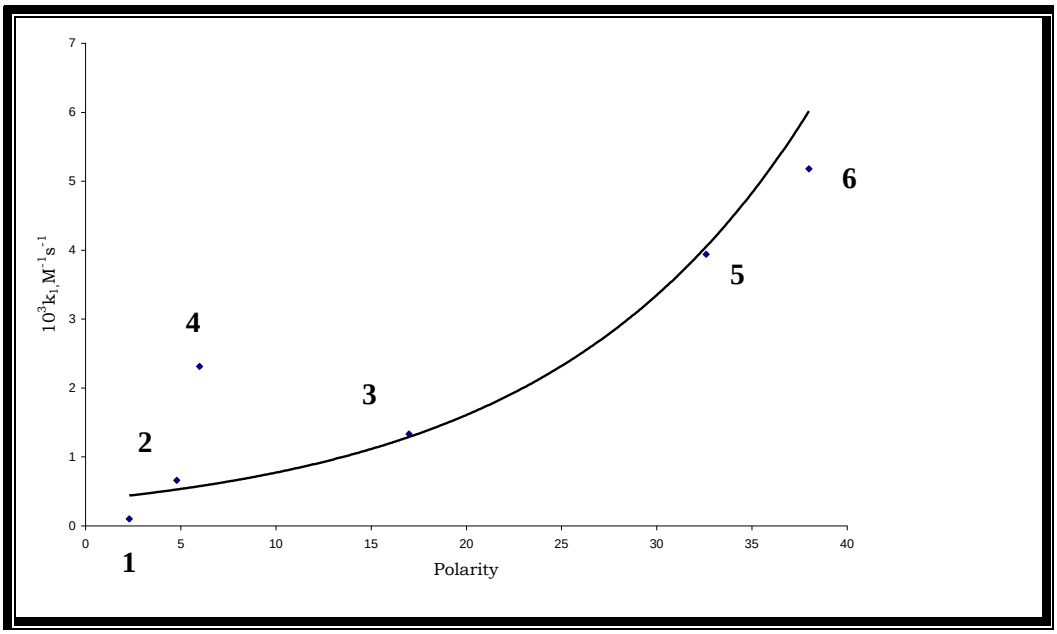

Figure 4.18. Solvent effect on the oxidative addition of [Rh(CH_3cupf)(CO)(PPh_3)] with iodomethane where 1 = Benzene, 2 = Ethyl acetate, 3 = Acetone, 4 = Chloroform, 5 = Methanol and 6 = Acetonitrile. Data taken from **Table 4.6**

Van Eldik *et al.* (1991:2207) conducted a combined solvent, temperature and pressure dependence study on the oxidative addition of [Rh(Sacac)(CO)(PPh_3)] and [Rh(cupf)(CO)(PPh_3)] with iodomethane. Kinetic data for the [Rh(Sacac)(CO)(PPh_3)] complex exhibited no significant dependence on the solvent and were interpreted in terms of a concerted three-center transition state (I, **Figure 4.19**). The [Rh(cupf)(CO)(PPh_3)] complex on the other hand, showed a significant solvent effect in most polar solvents. This observation was interpreted in terms of a linear transition state with participation of an ion-pair intermediate (II, **Figure 4.19**).

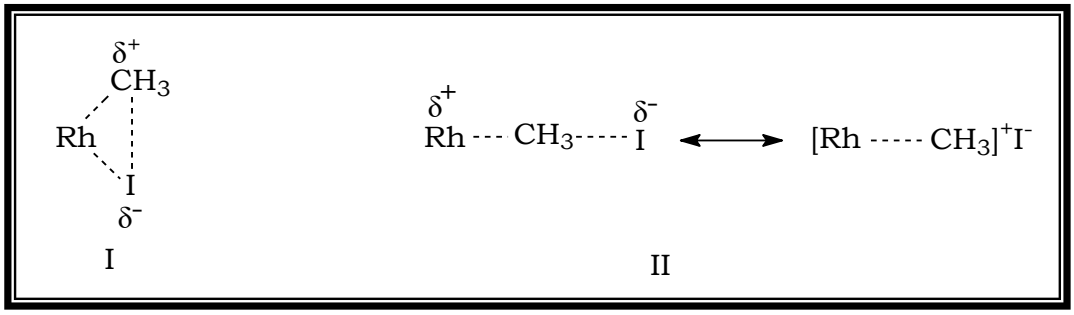

Figure 4.19 Postulated transition states for the oxidative addition of Rh(I) center with iodomethane

In order to make a more realistic comparison between k_1 and k_2' values, the latter was divided by the solvent concentrations to obtain the second order constants, k_2. The ratio k_1/k_2 is thus a measure of competition between CH_3I and solvent dependent pathways. In case of acetonitrile, the k_2 path becomes more pronounced when compared to k_1 if compared with, for example benzene (**Table 4.6**). On the other hand, for ethyl acetate and acetone, having nearly the same donocity, the ratio increases almost two fold. The proposed rate determining k_2 path is exactly

the same as that for the solvent dependent path of square planar substitution reactions. The rate of oxidative addition (k_1-path) changes with a factor of about 51 as the polarity of the solvent increases from benzene to acetonitrile. Highly polar solvents favour the solvent route (k_2-path) since a factor 785 increase was found for the k_2-path while only a factor of 51 was noticed for the k_1-path.

The existence of a solvent stabilised intermediate for the k_2 path is justified in terms of the ability of [Rh(cupf)(CO)(PPh_3)] to add an extra π-bonding ligand (PPh_3) as well as the reactivity of this complex towards solvents alone (Basson *et al.*, 1987:31). The same tendency can be expected for [Rh(CH_3cupf)(CO)(PPh_3)]. Secondly, the solvent assisted path can be viewed as an oxidative addition catalysis phenomenon similar to the solvent effects in the migratory insertion of CO into transition-metal alkyl bonds (**Eq 4.13**).

$$LnM(CO)R + L' \longrightarrow LnL'MC(=O)R$$

Eq.4.13

Research has indicated that the formation of a 5-coordinated intermediate acyl product is the key to the solvent's role in these insertion reactions (Webb *et al.*, 1986:345). Similarly, it could be visualised that a fast dissociative trapping of the solvent-stabilised intermediate by CH_3I takes place during its conversion to the ionic intermediate of the k_1 path. This solvent-stabilised intermediate is

also expected to be much more reactive towards CH_3I (Basson *et al.*, 1987:31). The results of solvent effects in this study show that it is the major factor responsible for enhancement of oxidative addition rates, which is believed to be another example of a solvent catalysed pathway.

The increase in the σ-donating ability of tertiary phosphines by the introduction of electron donating substituents must always be considered in conjuction with the effect that electron donating groups will have on the π-back bonding capabilities of the phosphine. This is especially true when tertiary phosphines are used as ligands in transition metal complexes, since their electron donor-acceptor capabilities determine the electron density on the metal and this will have an effect on other possible ligands such as CO. When a transition metal complex undergoes oxidative addition, the metal acts as a nucleophile. Any influence of a ligand that will increase the electron density on the central metal, will lead to an increase in the rate of oxidative addition, assuming all other influences, factors and parameters remain constant. The oxidative addition of [Rh(CH_3cupf)(CO)(PX_3)] (where X= Ph, *p*-$MeOC_6H_4$, *p*-Tol, *o*-Tol and Cy) with iodomethane illustrates the steric and electronic effect of tertiary phosphines on the rate of oxidative addition.

According to **Table 4.7** the first three phosphines are isosteric with a common cone angle of 145º and therefore have the same steric demand on the rate expected. However, electronically there is an increase in their σ-donating ability as predicted by their respective

Brönsted pK_a values (McAuliffe, 1987:989). The second-order rate constants for the oxidative addition (k_1) show a corresponding increase from PPh_3 to P(*p*-MeO-Ph)$_3$. This is in agreement with the higher nucleophlicity of the respective Rh(I) complexes. In accordance, the k_1 path shows a 5 fold increase from PPh_3 to P(*p*-$MeOC_6H_4)_3$ which is an expected trend for a nucleophilic attack at the sp^3 carbon of iodomethane. The result $k_1(PCy_3) > k_1$(P(*o*-Tolyl)$_3$) is in agreement with the electronic effect. The fact that both values are less than that of P(*p*-$MeOC_6H_4)_3$ indicates that the steric effect is also operative. However, upon considering the pK_a value of PCy_3 (9.65), it is anticipated that k_1 should be larger compared to P(*p*-$MeOC_6H_4$). Since the cone angle of PCy_3 is 170˚ and it is known to have a much larger steric demand compared to PPh_3, P(*p*-Tol)$_3$ and P(*p*-$MeOC_6H_4)_3$, the electronic effect is overshadowed by the steric component resulting in a k_1 value of only 0.00335(4). This is approximately a two fold decrease when compared to P(*p*-MeOPh)$_3$.

Oxidative Addition of [Rh(CH_3cupf)(CO)(PX_3)] Complexes with Iodomethane

Oxidative Addition of [Rh(CH_3cupf)(CO)(PX_3)] Complexes with Iodomethane

CHAPTER 5

EVALUATION OF THE STUDY

The relevance and success of the this study are briefly discussed **Section 5.1** in terms of the presented aims as outlined in **Chapter 1**, while some future aspects are discussed in **Section 5.2**

5.1 SCIENTIFIC RELEVANCE

The overall aim of this study was to extend the range of O,O bidentate ligands bonded to the square planar Rh(I) complex by introducing electron donating groups to the cupferrate ligand and determine their effect on the oxidative addition reactions of these complexes.

In the first part of the study we succeeded in synthesising the CH_3cupf ligand by applying an alternative method to those found in literature. This ligand was also successfully bonded to the Rh(I) centre and a number of new Rh(I)-CH_3cupf complexes, namely [Rh(CH_3cupf)(CO)(PPh_3)], [Rh(CH_3cupf)(CO)(P(*p*-$MeOPh_3$)], [Rh(CH_3cupf)(CO)(P(*p*-$Tol)_3$)], [Rh(CH_3cupf)(CO)(P(*o*-$Tol)_3$)] and [Rh(CH_3cupf)(CO)(PCy_3)] were synthesised. The new CH_3cupf ligand as well as all the complexes were characterised by means of IR and NMR techniques.

The oxidative addition of CH_3I to these square planar Rh(I)-CH_3cupf complexes proceeded *via* the mechanism which is shown in **Scheme 5.1**.

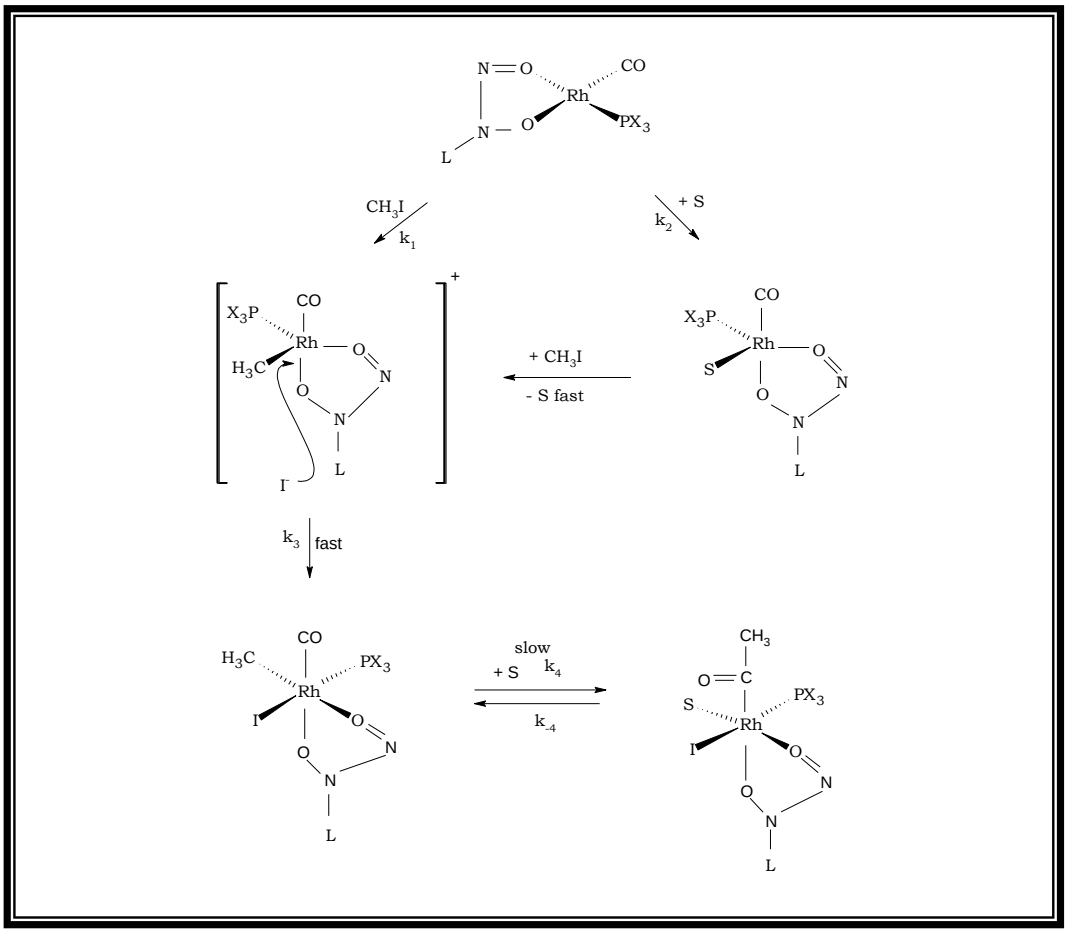

Scheme 5.1 Mechanistic scheme for the oxidative addition of [Rh(CH_3cupf)(CO)(PX_3)] with iodomethane (where L = *m*-toluene)

IR data clearly indicated the disappearance of the Rh(I)-carbonyl peak with appearance of the Rh(III)-alkyl peak as well as the formation of the Rh(III)-acyl peak. The kinetic results indicated that the rate of Rh(I) disappearance and the Rh(III)-alkyl formation

are the same within experimental error while the acyl formation is substantially slower and [CH_3I] independent. The above mechanism also propose a solvent assisted pathway. The rate constant for the reaction between [Rh(CH_3cupf)(CO)(PX_3)] and iodomethane clearly indicate an activation centre resulting from the CH_3 group bonded to the cupferrate ligand when compared to the cupferrate ligand it self.

The kinetic results for the different triphosphine ligands showed that the phosphine ligand with the largest electron donating ability, namely [Rh(CH_3cupf)(CO)(P(*p*-MeOPh)$_3$)] (pK_a = 4.57), has the largest activation towards oxidative addition while the smallest activation is caused by [Rh(CH_3cupf)(CO)(PPh_3)] (pK_a = 2.73). The solvent variation clearly indicated that acetonitrile with largest polarity (ε = 38) caused a much higher activation towards oxidative addition when compared to benzene with the least polarity (ε = 2.3)

From these results it is clear that most of the different goals that were set in **Chapter 1** were successfully achieved. It is also believed that this study contributes significantly to the scientific knowledge that already exists on this type of chemical systems.

5.2 FUTURE RESEARCH

The oxidative addition of [Rh(CH_3cupf)(CO)(PX_3)] with iodomethane proceeded more rapidly compared to the [Rh(cupf)(CO)(PX_3)] complex. Although the mechanism established above represents a

solvent assisted pathway, a high pressure study of this reaction step would provide valuable information about the transition state as well as the intrinsic mechanism which is followed during the reaction.

Further manipulation of the electron density on the Rh(I) centre may be accomplished by the introduction of other cupferron derivatives such as $-ClCH_3$, $-FCH_3$, $-EtCH_3$ etc. It would be interesting to observe by crystallographic means the influence of donor atoms on the Rh-P bond distance in the *trans*-L-Rh-P moiety. A ^{13}C and ^{31}P-NMR study may further provide useful information regarding the different isomers of the $[Rh(CH_3cupf)(CO)(PX_3)]$ complex present in solution.

The investigation could be extended to include a larger solvent range while PX_3 ligands could be replaced by AsX_3 and SbX_3 to include the effect of arsine and stibine ligands on the rate and mechanism of oxidative addition.

Finally, the effect of the metal centre can be incorporated in a study where Ir(I) and even similar charged complexes containing Pt and Pd as the centre metal may be attempted in the future.

REFERENCES

ADKINS, H. and KRSEK, G., 1984. *J. Am. Chem. Soc.*, 70:383.

ALEXANDRU, T., ROBERT, E., MELANIE, J. and WILLIAM, A., 1998. *Organic Preparations and Procedures Int.,* 4:439.

ANDERSON, G.K. and CROSS, R.J., 1984. *Acc. Chem. Res.*, 17:67.

ANDREA, D., ZHANG, W. and WITTBRODT. J., 2000. *Bioinorganic and medicinal chemistry*. Detriot:University of Wayne. p.405.

ATWOOD, J.D., 1985 *Inorganic and organometallic reaction mechanisms.* California:Brooks/Cole Publishing Company. p.113.

BASSON, S.S., LEIPOLDT, J.G. and NEL, J.T., 1984. *Inorg. Chim. Acta.*, 84:167.

BASSON, S.S., LEIPOLDT, J.G., ROODT, A. and VENTER, **J.A**., 1986. *Inorg. Chim. Acta.*, 118:L45.

BASSON, S.S., LEIPOLDT, J.G., ROODT, A. and VENTER, J.A., 1987. *Inorg. Chim. Acta.*, 128:31.

BASSON, S.S., LEIPOLDT, J.G., ROODT, A., VENTER, J.A. and VAN DER WALT, T.J., 1986. *Inorg. Chim. Acta.*, 119:35.

BASSON, S.S., LEIPOLDT, J.G., SCHLEBUSH, J.J.J. and GROBLER, E.C., 1982. *Inorg. Chim. Acta.*, 62:113.

BERTY, J. and MARKO, L., 1953. *Acta Chim. Acad. Sci. Hung.*, 3:177.

BIRD, C.W., 1967. *Transition metal intermediates in organic synthesis*. London:Logos. p.345.

BLAKE, D.M. and KUBOTA, M., 1970. *Inorg. Chem.*, 9:989.

BONDER, G.M., MAY, M.P. and McKINNEY, L.E., 1980. *Inorg. Chem.*, 19:1971.

BOWSER, J.R., *Inorganic chemistry*. 1993. California: Brooks/Cole publishing company. p.549.

BUTLER, I.S. and HARROD, J.F., 1989. *Inorganic chemistry principles and applications*. California:Benjamin/Cummings Publishing Company. p.630.

BUTLER, I.S., BASOLO, F. and PEARSON, R.G., 1967. *Inorg. Chem.*, 6:2074.

CALDERAZZO, F. and COTTON, F.A., 1962. *Inorg. Chem.*, 1:30.

CHATT, J. and UNDERHILL, A.E., 1963. *J. Chem. Soc.*, 2088.

CHATT, J. and VENANZI, L.M., 1956. *Nature*. 177:852.

COLLMAN, J.P. and HEGEDUS, L.S., 1980. *Principles and Application of Organotransition Metal Chemistry*. California:University Science Books. p.345.

COLLMAN, J.P. and MACLAURY, M.R., 1974. *J. Am. Chem. Soc.*, 96:3019.

COLLMAN, J.P. and SEARS, C.T., 1968. *Inorg. Chem.*, 7:27.

COLLMAN, J.P., HEGEDUS, L.S., NORTON, J.R. and FINKE, R.G., 1987. *Principles and Applications of Organotransition Metal Chemistry*. California:University Science Books. p.279.

CORNILS, B. and HERMANN, W.A., 2000. *Applied homogeneous catalysis with organometallic compounds*. New York:Wiley-VCH. p.198.

CORNILS, B., HERMANN, W.A. and RAUSCH, M., 1994. *Angew. Chem. Int. Ed. Engl.*, 33:2144.

COTTON, F.A., WHIPPLE, R.O and WILKINSON, G., 1953. *J. Am. Chem. Soc.*, 75:3586.

CRAIG, P.J. and GREEN, M.J., 1968. *J. Chem. Soc.*, A:1978.

CRAMER, R., 1962. *Inorg.Chem.*, 1:722.

CROSS, R.J., 1985. *Chem. Soc. Rev.*, 14:197.

DAMOENSE, L.J., PURCELL, W. and ROODT, A., 1995. *Rhodium Express*. 14:6.

DAMOENSE, LJ., 2000. Fundamental aspects of selected rhodium complexes in homogeneous catalytic acetic acid production. Ph.D Thesis, University of Free State.

DEUTSCH, P.P. and EISENBERG, R., 1988. *Chem. Rev.*, 88:1147.

DICKSON, R.S., 1983. *Organometallic Chemistry of rhodium and iridium*. New York:Academic Press. p.45.

DICKSON, R.S., 1985. *Homogeneous catalysis with compounds* of *rhodium and iridium*. Dordrecht: Reidel Publishing Company. p.1.

DOUGLAS, B., MCDANIEL, D.H. and ALEXANDER, J.J., 1983. *Concepts and models of inorganic chemistry* (2nd ed.). New York: John Wiley & Sons Inc. p.405.

FESSAHAYE, K. 2004. *Unpublished results*. University of Free State.

FISCHER, E.O., ZAHN, U. and BAUMGARTNER, F., 1959. *Z. Naturforsch. Teilb.*, 14:133.

GARLASCHELLI, L., MARCHINNA, M., IAPALUCCI, M.C. and LONGONI, G., 1989. *J. Organomet. Chem.*, 378:457.

GIRALDI, T., SAVA, G., BERTOLI, G., MESTRONI, G. and ZASSINOVICH, G., 1977. *Cancer Res.*, 37:2662.

GOSWAMI, K. and SINGH, M.M., 1980. *Transition Met. Chem.*, 5:83.

GRIFFIN, T.R., COOK, D.B., HAYES, A., PEARSON, T.M., MONTIC, D. and MORRIS, G.E., 1995. *J. Am. Chem. Soc.*, 118:3029.

GRIFFITH, W.P., 1967. *The chemistry of rarer platinium metals* (6th ed). New York: Wiley-Interscience. p.589.

GUERRA, M.K., 1994. *Acetic acid and acetic anhydride*. California:SRI International, Menlon Park No.37B. p368.

HART-DAVIS, A.J. and GRAHAM, W.A.G., 1970. *Inorg. Chem.*, 9:2658.

HAYNES, A., MANN, B.E., GULLIVIE, D.J., MORRIS, G.E. and MAITIS, P.M., 1991. *J. Am. Chem. Soc.*, 113:8567.

HAYNES, A., MANN, B.E., MORRIS, G.E. and MAITLIS, P.M., 1993. *J. Am. Chem. Soc.*, 115:4093.

HIEBER, W. and HEUSINGER, H., 1956. *Angew. Chem.*, 68:678.

HERMANN, W.A. and CORNILS. B., 1997. *Angew. Chem. Int. Ed. Engl.*, 36:1048.

HICKEY, C.E. and MAITLIS, P.M., 1984. *J. Chem. Soc. Chem. Commun.*, 1609.

HIEBER, W. and LAGALLY, H., 1943. *Z. Anorg. Allg. Chem.*, 251:96.

HUGES, R.P., 1982. *Comprehensive Organometallic Chemistry*. Oxford: Pergamon Publishing Company. p.277.

IGNARRO, L. and MURAD, F., 1995. *Advanced in Pharmacology*. 34:36.

KANO, K. and ANSELME, J.P., 1993. *Tetrahedron.*, 49:9453.

LANAM, R.D and ZYSK, E.D, 1982. Platinum-Group Metals. (In GRAYSON, m., ed. Kirk-Othmer *Encyclopedia of Chemical Technology*. New York:John Wiley & Sons). p228-253.

LAPLANCA, S.R and IBERS, J.A., 1966. *Inorg. Chem.*, 5:405.

LEIPOLDT, J.G., BASSON, S.S. and NEL, J.T., 1983. *Inorg. Chim. Acta.*, 74:85.

LEIPOLDT, J.G., BASSON, S.S. and POTGIETER, J.H., 1986. *Inorg. Chim. Acta.*, 117:L3.

LEIPOLDT, J.G., LAMPRECHT, G.J. and VAN ZYL, G.J., 1984. *Inorg. Chim. Acta.*, 96:L31.

LIVINGSTONE, S.E., 1973. *Comprehensive Inorganic Chemistry*. Oxford: Pergamon Publishing Company. p.1233.

MANCHOT, W. and KONIG, J., 1925. *Chem. Ber.*, 58B:2173.

McAULIFFE, C.A. and WILKINSON, G., 1987. *Comprehensive Coordination Chemistry*. New York:Pergamon Press. p.989.

MONCADA, S. PALMER., R.M.J. and HIGGS, E.A., 1991. *Pharmacol. Rev.*, 3:109.

MULLER, A.J., 2000. *The Characterization And Kinetic Study of Rhodium(I) and Iridium(I) Traizole Complexes*. Bloemfontien:University of Free State. (Dissertation-M.Sc.).

NORMAN, E.H., 2004. *History of the Origin of Chemical Elements and Their Discoverers*. New York:Brookhaven National Laboratory. p.1.

NYHOLM, R.S. and VRIEZE, K., 1965. *J. Chem. Soc.*, 5337.

OLIVIER, K.L. and BOOTH, F.B., 1970. *Hydrocarbon Process* (4th ed). New York:Plenium Publishers. p.245.

PARSHALL, G.W. and ITTEL, S.D., 1992. *Homogeneous Catalysis*. New York:Wiley. p.346.

PEARSON, J.M., HAYNES, A., MORRIS, G.E., SUNLEY, G.J. and MAITIS, P.M. 1995. *J. Chem. Soc. Chem. Comm.*, 45:1045.

PURCELL, K.F. and KOTZ, J.C., 1977. *Inorganic Chemistry*. Philadelphia:Saunders College Publishing. p.700.

PURCELL, K.F. and KOTZ, J.C., 1980. *Introduction to Inorganic Chemistry*. Philadelphia:Saunders College Publishing. p.392.

REICHARDT, C., 1979. *Solvent Effects in Organic Chemistry*. NewYork:Verlag-Chemie. p.186.

RICHARDSON, J.T., 1989. *Principles of Catalyst Development*. New York:Plenium Press. p.217.

ROELEN, O., 1977. *ChED Chem. Exp. Didakt.*, 3:119.

ROODT, A. and STEYN, J. J. J., 2000. *Res. Dev. Inorg. Chem.*, 2:1.

RUSINA, A., 1965. *Nature*. 206:295.

SAAVEDRA, J.E., DUNAMAS, T.M., FLIPPEN, J.L. and KEEFER, L.K., 1992. *J. Org. Chem.*, 57:6134.

SANSHIRO, K., 1997. *Synthesis of Organometallic Compounds: a Practical Guide* (3rd ed). Chichester:Wiley Publishing Company. p.2.

SERPONE, N. and JAMIESON, M.A., 1987. *Comprehensive Coordination Chemistry*. Oxford: Pergamon. p.1097.

SCIENTIST FOR WINDOWS, 1990. Least Square Parameter Estimation, Version 4.00, Micromath.

STEYNBERG, E.C., LAMPRECHT, G.J. and LEIPOLDT, J.G., 1987. *Inorg. Chim. Acta.*, 133:33.

STILLE, J.K. and Lau, K.S.Y., 1977. *Acc. Chem. Res.*, 10:434.

THOMPSON, W.H. and SEARS, C.T. 1977. *Inorg. Chem.*, 16:769.

TOLMAN, C.A. 1970**.**, *J. Am. Chem. Soc.*, 92:2953.

TOLMAN, C.A., 1977. *Chem. Rev.*, 77:313.

TRECIAK, A.M. and ZIOLKOWSKI, J.J., 1985. *Inorg. Chim. Acta.*, 96:15.

UGO, R., PASINI, A., FUSI, A. and CENINI, S., 1972. *J. Am. Chem. Soc.,* 94*:*7364.

VALLARINO, L., 1957. *J. Chem. Soc.*, 2287.

VAN ASWEGEN, K.G., LEIPOLDT, J.G., POTGIETER, I.M., LAMPRECHT, G.J, ROODT, A. and VAN ZYL, G.J., 1991. *Transition Met. Chem.*, 16:396.

VAN ELDIK, R., LEIPOLDT, JG. and VENTER, J.A., 1991. *Inorg. Chem.*, 30:2207.

VAN ZYL, G.J., LAMPRECHT, G.J. and LEIPOLDT, J.G., 1985. *Inorg. Chim. Acta.*, 102:L1.

VAN ZYL, G.J., LAMPRECHT, G.J. LEIPOLDT, J.G. and SWADDLE, T.W., 1988. *Inorg. Chim. Acta.*, 143:223.

VASKA, L., 1968. *Acc. Chem. Res.,* 1:136.

VASKA. L. and DILUZIO, J.W., 1961. *J. Am. Chem. Soc.*, 83:2784.

VENTER, J.A., LEIPOLDT, J.G. and VAN ELDIK, R., 1991. *Inorg. Chem.*, 30:2107.

VINCENT, S.R., 1995. *Nitric Oxide in the Nervous System*. New York:Acadamic Press. p.193.

VOGEL, A.I., 1989. *Vogel's Textbook Of Quantitative Chemical Analysis* (5th ed.). New York:John Wiley & Sons Inc. p.955.

WEBB, S.L., GIANDOMEICO, C.M. and HALPERN, J., 1986. *J. Am. Chem. Soc.*, 108:345.

WILKINSON, G., 1987. *Comprehensive Coordination Chemistry*: *the synthesis, reactions, properties and applications*. Oxford:Pergamon Press. p.458.

WILLIAMS, R.J.P., 1996. *Chem. Soc. Rev.*, 25:77.

ADDENDUM A

A. THEORETICAL PRINCIPLES

In this section, the relevant rate expressions and kinetic principles as well as activation parameters are briefly discussed.

A.1 BASIC CONCEPTS

The interpretation of kinetic data is largely based on an empirical finding called the Law of Mass Action, which states that in diluted solutions the rate of a one-step reaction is proportional to the powers of their stoichiometric coefficients and independent of other concentrations and reactions. Thus for a bimolecular reaction:

$$A + B \xrightarrow{k_1} C$$

Eq.A.1

the rate of the reaction can be written as :

$$R = k_1[A]^a[B]^b$$ **Eq.A.2**

with k_1 being a proportionality constant that relates the rate of change of the reagent concentrations while a and b are called the

order of the reaction with respect to A an B respectively. The values of a and b can be determined experimentally by using pseudo-first order conditions where [B] >> [A], hence **Eq.A.2** reduces to:

$$R = k_{obs}[A]^a \qquad \textbf{Eq.A.3}$$

With the observed pseudo-first order rate constant being:

$$k_{obs} = k_1[B]^b \qquad \textbf{Eq.A.4}$$

Pseudo-first order conditions (with [B] at least 10 times in excess of [A]) is used to obtain the rate constant by determining k_{obs} at different concentrations of B. In the case of **Eq.A.1** being an equilibrium with k_{-1} the reverse rate constant, it can be shown that:

$$k_{obs} = k_1[B] + k_{-1} \qquad \textbf{Eq.A.5}$$

Where k_1 and k_{-1} can be determined from the slope and intercept of a linear plot of this equation.

Integration of **Eq.A.2** between time = 0 and t respectively gives the following equation (expressed in terms of C in **Eq.A.1**):

$$[C]_t = [C]_o e^{-k_1 t} \qquad \textbf{Eq.A.6}$$

Using the Beer-Lambert law, $A = \varepsilon cl$, with ε and l as constants, the absorbance is directly proportional to concentration, which leads to:

$$[C]_o \alpha A_o - A_\infty \qquad \textbf{Eq.A.7}$$

$$[C]_t \alpha A_t - A_\infty \qquad \textbf{Eq.A.8}$$

with A_o = absorption at time zero

A_t = absorption at time t

A_∞ = absorption at time infinity.

Incorporating **Eq.A.7** and **Eq.A.8** into **Eq.A.6** and manipulating it, the following equation results:

$$A_t = A_\infty - (A_\infty - A_o)e^{-k_{obs}t} \qquad \textbf{Eq.A.9}$$

Infinity is the time at which the reaction is complete for all practical reasons and k_{obs} can then be determined by a least square fit utilizing absorbance *vs* time for the first order reaction.

A.2 ACTIVATION ENTHALPY AND ENTROPY

The transition theory states that the activated complex or transition state is in equilibrium with the reagent before the reaction takes place and that the rate is given by the decomposition rate (k) of the activated complex to yield the products:

$$A + B \overset{K^{\#}}{\rightleftharpoons} (AB) \xrightarrow{k} C$$

Eq.A.10

The rate of which is given by:

$$k = \frac{k_B T}{h} K^{\#}$$

Eq.A.11

where k_B = Boltzmann's and h = Planck's constants.

From basic dynamics it follows that:

$$K^{\#} = e^{\frac{\Delta G^{0\#}}{RT}}$$

Eq.A.12

with $\Delta G^{\circ\#}$ = standard free energy change and R = universal gas constant. Substituting **Eq.A.11** into **Eq.A.12** and the fact that $\Delta G^{o}=\Delta H^{o}- T\Delta S^{o}$, yields the following:

$$k = \frac{Tk_B}{h} e^{\left[\frac{\Delta S^{\#}}{R}\right]\left[\frac{\Delta H^{\#}}{R}\right]}$$

Eq.A.13

Eq.4.13 is generally written in a logarithmic form as follows:

$$\ln\left(\frac{k}{T}\right) = \ln\left(\frac{k_b}{h}\right) + \left(\frac{\Delta S\#}{R}\right) - \left(\frac{\Delta H^{\#}}{RT}\right)$$

Eq.A.14

The graph of ln k/T *vs* 1/T will have a slope of $-\Delta H^{\#}/R$ with the y-intercept giving $\ln(k_B/h) + \Delta S^{\#}/R$

Addendum A

ADDENDUM B

B. SUPPLEMENTARY KINETIC ASPECTS

B.1 KINETIC DATA

Table B.1: Observed pseudo-first order constants for the oxidative addition of [Rh(CH_3cupf)(CO)(PPh_3)] with iodomethane in different solvents at 25.0 °C

Solvent	**[CH_3I]/M**	**$10^3k_{obs}/s^{-1}$**
Benzene	0.2	0.02435(4)
	0.4	0.04292(6)
	0.5	0.05311(1)
	0.6	0.06438(3)
	0.8	0.08179(4)
	1.0	0.10613(6)
Ethylacetate	0.2	0.225012(1)
	0.4	0.3602(3)
	0.5	0.424(6)
	0.6	0.488(3)
Acetone	0.2	0.786(2)
	0.4	1.055(6)
	0.5	1.119(2)
	0.6	1.297(4)
	0.8	1.578(3)
	1.0	1.846(3)
Chloroform	0.2	1.31817(1)
	0.4	1.77327(2)
	0.5	2.00529(3)
	0.6	2.26275(1)
	0.8	2.69817(2)
Methanol	0.2	1.96(2)
	0.4	2.827(2)
	0.5	3.147(3)

	0.6	3.586(4)
	0.8	4.37(1)
	1.0	5.125(4)
Acetonitrile	0.2	2.639(2)
	0.4	3.602(3)
	0.5	4.157(3)
	0.6	4.688(1)
	0.8	5.785(4)
	1.0	6.729(3)

Table B.2: Kinetic results for the oxidative addition of [Rh(CH_3cupf)(CO)(PPh_3)] with iodomethane in acetone at four different temperatures.

Temperature	**[CH_3I]/M**	**10^3k_{obs}/ s^{-1}**	**10^3k_1/ $M^{-1}s^{-1}$**	**$10^4k'_2$/ s^{-1}**	**10^5k_2/ $M^{-1}s^{-1}$**
290.5	0.2	0.348(4)	0.73(1)	1.97(7)	1.45
	0.4	0.487(2)			
	0.5	0.566(3)			
	0.6	0.643(3)			
298.0	0.2	0.7861(2)	1.32(1)	5.22(9)	3.84
	0.4	1.054(6)			
	0.5	1.190(2)			
	0.6	1.297(4)			
	0.8	1.578(3)			
	1.0	1.845(3)			
302.5	0.2	1.103(1)	1.52(1)	7.91(9)	5.82
	0.4	1.398(2)			
	0.5	1.550(1)			
	0.6	1.694(5)			
	0.8	2.024(6)			
	1.0	2.314(2)			
313.3	0.2	1.775(4)	3.45(1)	10.92(7)	8.03
	0.4	2.48(4)			
	0.5	2.82(3)			
	0.6	3.174(5)			
	0.8	3.86(2)			
	1.0	4.54(2)			

Table B.3 Observed pseudo-first order constant for the oxidative addition of [Rh(CH_3cupf)(CO)(PR_3)] with iodomethane in acetone at 25.0 °C.

Ligand	**[CH_3I]/M**	**k_{obs}/s^{-1}**
PPh_3	0.2	0.7861(2)
	0.4	1.054(6)
	0.5	1.119(2)
	0.6	1.297(4)
	0.8	1.578(3)
	1.0	1.845(3)
P(*p*-Tolyl)$_3$	0.2	0.0008(1)
	0.4	0.0013(7)
	0.6	0.0017(2)
	0.8	0.0022(4)
P(*p*-MeOPh)$_3$	0.2	0.0022(1)
	0.4	0.0036(2)
	0.5	0.0043(5)
	0.8	0.0065(1)
	1.0	0.0078(7)
PCy_3	0.2	0.0012(2)
	0.4	0.0019(3)
	0.5	0.0022(2)
	0.6	0.0025(9)
	0.8	0.0032(4)
	1.0	0.0039(6)
P(*o*-Tolyl)$_3$	0.2	0.00038(6)
	0.4	0.0005(2)
	0.5	0.00056(7)
	0.6	0.00063(1)
	0.8	0.00075(4)
	1.0	0.00087(2)

SUMMARY

A number of dicarbonylrhodium complexes of the type [Rh(CH_3cupf)$(CO)_2$] as well as their substituted monocarbonyl products [Rh(CH_3cupf)(CO)(PX_3)] (where X = Ph, *p*-MeOph, *p*-Tol, *o*-Tol and Cy) have been prepared and identified by IR and NMR techniques. The square planar substitution of the carbonyls in these dicarbonylrhodium complexes by different tertiary phosphine ligands have also been identified using UV/Visible and IR spectroscopic techniques. One of the aims of this study was to determine the mechanism for the oxidative addition of [Rh(CH_3cupf)(CO)(PX_3)] (X = Ph, *p*-MeOPh, *p*-Tol, *o*-Tol and Cy) with iodomethane and to investigate the effect of temperature and solvent, as well as the steric and electronic effect of the phosphine ligands on this reaction.

The [Rh(CH_3cupf)(CO)(PPh_3)] complex is expected to have a similar geometric configuration as that of [Rh(cupf)(CO)(PX_3)]. Extrapolation of this structural data predicted that the [Rh(CH_3cupf)(CO)(PPh_3)] complex also contain the CO group *trans* to the nitroso group. It can be concluded that the electronic properties of the cupferrate ligand overshadows the steric effect of the different phosphine ligands.

The different Rh(I)-CH_3cupf complexes underwent oxidative addition with iodomethane to form the corresponding Rh(III)-alkyl species followed by the slower formation of Rh(III)-acyl species

according to the **scheme** below. All the Rh(I) and Rh(III) species were characterised by infrared spectroscopy.

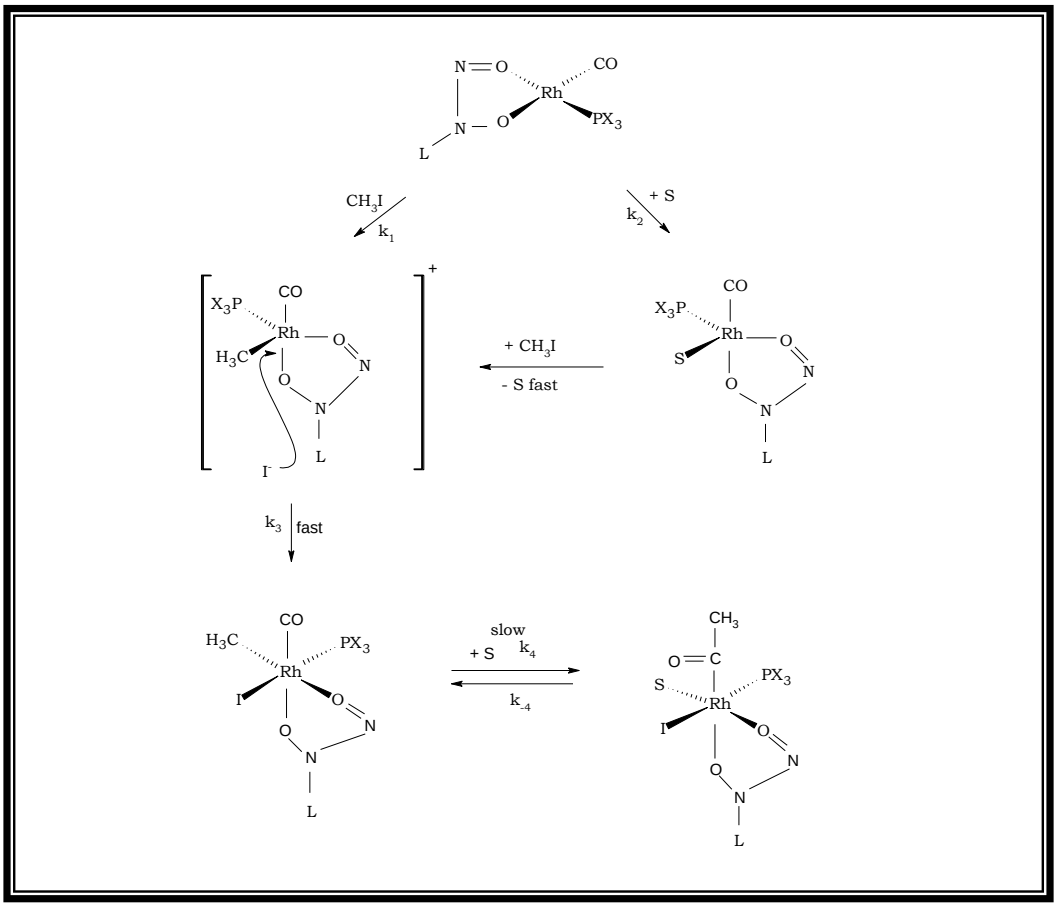

The rate constant for the oxidative addition of [Rh(CH_3cupf)(CO)(PX_3)] with iodomethane increased with increasing polarity of solvents. At 25.0 °C, this reaction proceeds at a rate of $k_1 = 3.94(5) \times 10^{-3}$ $M^{-1}s^{-1}$ in the highly polar methanol and at a rate of $k_1 = 1.33(4) \times 10^{-3}$ $M^{-1}s^{-1}$ in less polar acetone, compared to the least polar benzene with a rate of $k_1 = 0.101(2) \times 10^{-3}$ $M^{-1}s^{-1}$. Activation parameters ($\Delta H^{\#}$ and $\Delta S^{\#}$) were determined for the temperature dependence of k_1 in acetone. A large negative $\Delta S^{\#}$ value ($\Delta S^{\#} = -137(1)$ $JK^{-1}mol^{-1}$) and a positive $\Delta H^{\#}$ ($\Delta H^{\#} = 48(1)$ $kJmol^{-1}$) were obtained which clearly point to an associative

mechanism. Considering the experimental results, the formation of a linear, polar transition state with subsequent formation of an ion-pair intermediate is postulated for the intrinsic mechanism. The rate of formation of the Rh(III) acyl species was found to be independent of iodomethane concentrations.

The rate constant of the oxidative addition was also affected by electronic and steric manipulations. The electronic effect was achieved by interchanging, for example, PPh_3 with $P(p\text{-}MeOC_6H_4)_3$ which resulted in a more than fivefold increase in magnitude for the rate of oxidative addition. An elevenfold decrease in the k_1 value for $P(o\text{-}Tol)_3$, when compared to $P(p\text{-}MeOC_6H_4)_3$, showed the impact of the steric effect.

OPSOMMING

'n Aantal dikarbonielrodiumkomplekse, [Rh(CH_3cupf)$(CO)_2$], sowel as hulle gesubstitueerde monokarbonielprodukte [Rh(CH_3cupf)-(CO)(PX_3)] (waar X = Ph, *p*-MeOph, *p*-Tol, *o*-Tol en Cy) is berei en geïdentifiseer met behulp van IR and KMR tegnieke. Die vierkantig-planêre substitusie van die karboniele in hierdie dikarbonielrodiumkomplekse deur verskillende tersiêre fosfienligande is ook geïdentifiseer deur gebruikmaking van UV/Sigbare en IR spektroskopiese metodes. Een van die doelwitte van hierdie studie was om die meganisme van die oksidatiewe addisie van [Rh(CH_3cupf)$(CO)(PX_3)$] (X = Ph, *p*-MeOPh, *p*-Tol, *o*-Tol and Cy) met jodometaan te bepaal en om die invloed van temperatuur en oplosmiddel, asook die steriese- en elektroniese effek van die fosfienligande op hierdie reaksie te ondersoek.

Die [Rh(CH_3cupf)$(CO)(PPh_3)$] kompleks behoort dieselfde geometriese konfigurasie as [Rh(cupf)$(CO)(PX_3)$] te hê. Ekstrapolering van hierdie struktuurdata lei tot die voorspelling dat die [Rh(CH_3cupf)$(CO)(PPh_3)$] kompleks ook die CO groep *trans* ten opsigte van die nitrosogroep bevat. Daar kan tot die slotsom gekom word dat die elektroniese eienskappe van die cupferraatligand die steriese effek van die fosfienligande ooskadu.

Die verskillende Rh(I)-CH_3cupf komplekse ondergaan oksidatiewe addisie met jodometaan om die ooreenstemmende Rh(III)-alkielspesies te vorm, gevolg deur die stadiger vorming van die

Rh(III)-asielspesies volgens die **skema** hieronder. Al die Rh(I) en Rh(III) spesies is gekarakteriseer met behulp van infrarooi spektroskopie.

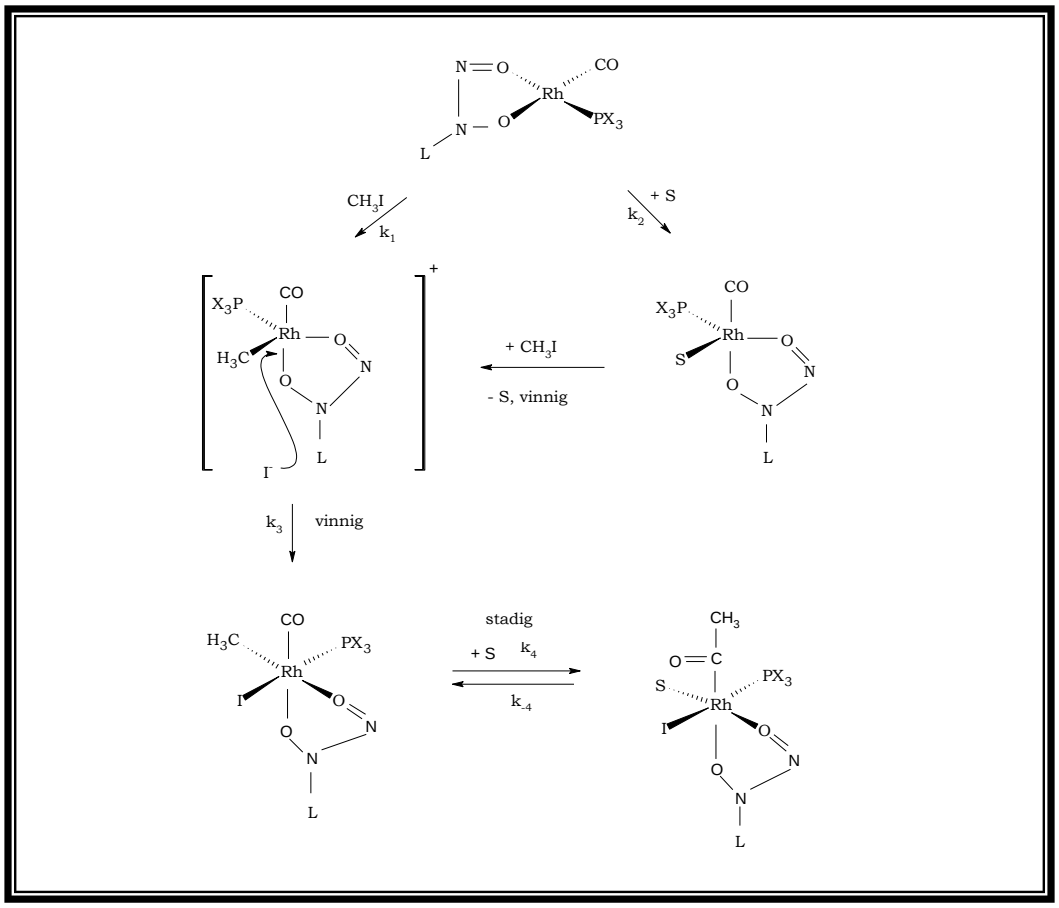

Die tempokonstante vir die oksidatiewe addisie van [Rh(CH3cupf)(CO)(PX3)] met jodometaan neem toe met toenemende polariteit van die oplosmiddels. Hierdie reaksie verloop by 25.0 °C in die hoogs polêre metanol om 'n tempokonstante van k_1 = 3.94(5) × 10^{-3} $M^{-1}s^{-1}$ te lewer, met k_1 = 1.33(4) × 10^{-3} $M^{-1}s^{-1}$ in die minder polêre asetoon en k_1 = 0.101(2) × 10^{-3} $M^{-1}s^{-1}$ in die mins polêre benseen. Aktiveringsparameters ($\Delta H^{\#}$ and $\Delta S^{\#}$) is bepaal vir die temperatuurafhanklikheid van k_1 in asetoon. 'n Groot negatiewe $\Delta S^{\#}$ waarde ($\Delta S^{\#}$ = -137(1) $JK^{-1}mol^{-1}$) en positiewe $\Delta H^{\#}$ ($\Delta H^{\#}$ = 48(1)

kJmol^{-1}) is verkry wat op 'n assosiatiewe meganisme dui. Met inagneming van die eksperimentele resultate kan die vorming van 'n lineêre, polêre oorgangstoestand met die daaropvolgende vorming van 'n ioonpaar intermediêr as intrinsieke meganisme gepostuleer word. Die tempo van vorming van die Rh(III)-asielspesie is as onafhanklik van die jodometaan-konsentrasie bevind.

Die tempokonstante van die oksidatiewe addisiereaksie was ook afhanklik van elektroniese en steriese manipulasies van die rodiumkomplekse. Die veranderinge in die elektroniese effek is verkry met fosfieligandwisseling, deur byvoorbeeld PPh_3 met P(*p*-$MeOC_6H_4)_3$ te vervang wat gelei het tot 'n vyfvoud toename in die tempo van oksidatiewe addisie. 'n Elfvoudige afname in die k_1 waarde vir P(*o*-Tol)$_3$ in vergelyking met P(*p*-$MeOC_6H_4)_3$ toon die dramatiese uitwerking van die steriese effek van fosfienligande.

Summary